

Improving the Turbulence Coupling between High Resolution Numerical Weather Prediction Models and Lagrangian Particle Dispersion Models

THÈSE N° 4827 (2010)

PRÉSENTÉE LE 26 NOVEMBRE 2010

À LA FACULTÉ ENVIRONNEMENT NATUREL, ARCHITECTURAL ET CONSTRUIT
LABORATOIRE DE MÉCANIQUE DES FLUIDES DE L'ENVIRONNEMENT
PROGRAMME DOCTORAL EN ENVIRONNEMENT

ÉCOLE POLYTECHNIQUE FÉDÉRALE DE LAUSANNE

POUR L'OBTENTION DU GRADE DE DOCTEUR ÈS SCIENCES

PAR

Balazs SZINTAI

acceptée sur proposition du jury:

Prof. F. Golay, président du jury
Prof. M. Parlange, directeur de thèse
Dr P. Kaufmann, rapporteur
Prof. F. Porte Agel, rapporteur
Prof. M. Rotach, rapporteur



ÉCOLE POLYTECHNIQUE
FÉDÉRALE DE LAUSANNE

Suisse
2010

Abstract

For the modelling of the transport and diffusion of atmospheric pollutants during accidental releases, sophisticated emergency response systems are used. These modelling systems usually consist of three main parts. The atmospheric flow conditions can be simulated with a numerical weather prediction (NWP) model. The evolution of the pollutant cloud is described with a dispersion model of variable complexity. The NWP and the dispersion models have to be coupled with a so-called meteorological pre-processor. This means that all the necessary – in most cases turbulence related – variables which are not available from the standard output of the NWP model have to be diagnosed. The main difficulty of the turbulence coupling is that these subgrid scale variables of NWP models are not routinely verified and thus little is known concerning their quality and impact on dispersion processes. The general aim of the present work is to better understand and improve this coupling mechanism. For this purpose all the three main components of the emergency response system of MeteoSwiss are carefully evaluated and possible improvement strategies are suggested.

In the first part, the NWP component of the system, namely the COSMO model, is investigated focusing on the model performance in the Planetary Boundary Layer (PBL). Three case studies, representing both unstable and stable situations, are analyzed and the COSMO simulations are validated with turbulence measurements and Large Eddy Simulation (LES) data. It is shown that the COSMO model is able to reproduce the main evolution of the boundary layer in dry convective situations with the operational parameter setting. However, it is found that the COSMO model tends to simulate a too moist and too cold PBL with shallower PBL heights than observed. During stable conditions the operational parameter setting has to be significantly modified (e.g., the minimum diffusion coefficient) to obtain a good model performance. The turbulence scheme of COSMO, which carries a prognostic equation for Turbulent Kinetic Energy (TKE), is studied in detail to understand the shortcomings of the simulations. The turbulent transport term (third order moment) in the TKE equation is found to be significantly underestimated by the COSMO model during unstable situations. This results in inaccurate TKE profiles and hence missing entrainment fluxes at the top of the PBL. A solution to increase the TKE transport in the PBL is proposed in the present work and evaluated during a three-month continuous period. While improving the TKE profile substantially, the modification is demonstrated to not impair other model output characteristics.

The second component of the emergency response system, namely the meteorological pre-processor, is also validated on case studies and a continuous period. The main objective of this analysis is to compare the currently operational coupling approach, which is based on the direct usage of the prognostic TKE from the COSMO model, to a classical approach based on similarity theory considerations, thereby using turbulence measurements on the one hand and LES data on the other hand. To be able to use similarity theory approaches for the determination of turbulence characteristics, the PBL height has first to be diagnosed from the NWP model. In the present study, several approaches for the determination of PBL height have been implemented and validated with radio sounding measurements. Based on the verification results and the operational convenience, the method based on the bulk Richardson number method has been chosen for the diagnosis of the PBL height. Validation results of post-diagnosed turbulence characteristics show that during convective situations, the similarity approach tends to overestimate the turbulence intensity, while the approach based on the direct usage of TKE yields more accurate results. For stable conditions the different approaches are closer to each other and both give reasonable predictions. It is found that the main drawback of the direct approach is the isotropic assumption in the horizontal direction. A new hybrid method is proposed which uses similarity considerations for the partitioning of horizontal TKE between along-wind and cross-wind directions.

In the last part, pollutant dispersion in complex terrain is studied using a new scaling approach for TKE that is suited for steep and narrow Alpine valleys. This scaling approach is introduced in the interface between COSMO and a Lagrangian particle dispersion model (LPDM), and its results are compared to those of a classical similarity theory approach and to the operational coupling type, which uses the TKE from the COSMO model directly. For the validation of the modelling system, the TRANSALP-89 tracer experiment is used, which was conducted in highly complex terrain in southern Switzerland. The ability of the COSMO model to simulate the valley-wind system is assessed with several meteorological surface stations. The dispersion simulation is evaluated with the measurements from 25 surface samplers. The sensitivity of the modelling system towards the soil moisture, horizontal grid resolution, and boundary layer height determination is investigated. It is shown that if the flow field is correctly reproduced, the new scaling approach improves the tracer concentration simulation compared to the classical coupling methods.

Keywords: numerical weather prediction, meteorological pre-processor, Lagrangian particle dispersion model, turbulence, complex topography, PBL height

Résumé

En cas de rejet accidentel de polluants dans l'atmosphère, des systèmes d'alarme sophistiqués sont déployés pour modéliser le transport et la diffusion des polluants. Ces systèmes de modélisation sont généralement constitués de trois composants principaux. Les conditions atmosphériques sont simulées à l'aide d'un modèle numérique de prévision météorologique. L'évolution du nuage de polluants est, quant à elle, décrite par un modèle de dispersion dont la complexité varie considérablement d'un système à l'autre. Le modèle de prévision météorologique et le modèle de dispersion sont couplés à l'aide d'un outil appelé préprocesseur. Toutes les variables nécessitées par le modèle de dispersion et qui ne sont pas disponibles dans les sorties standard du modèle météorologique – généralement les variables liées à la turbulence – sont diagnostiquées grâce à cet outil. Le fait que les grandeurs turbulentes – dont la dimension est inférieure à la taille de la grille du modèle météorologique – ne soient pas vérifiées systématiquement constitue l'une des principales incertitudes dans la modélisation des processus de dispersion et représentent, par conséquent, un point crucial du couplage. Le principal objectif de ce travail est la connaissance approfondie ainsi que l'amélioration du mécanisme de couplage. À cette fin, les trois principaux composants du système d'alarme de MeteoSuisse sont soigneusement évalués et des stratégies d'amélioration sont proposées.

Dans la première partie de ce travail, le modèle météorologique utilisé par MeteoSuisse, COSMO, et plus particulièrement sa capacité à représenter la couche limite, est exploré en détail. Trois études de cas, correspondant à des conditions atmosphériques stables et instables, sont analysées et les simulations COSMO sont validées en utilisant des mesures de turbulence et des résultats de Large Eddy Simulation (LES). Nous pouvons démontrer que le modèle COSMO, dans sa configuration opérationnelle, est capable de reproduire l'évolution générale de la couche limite dans le cas de situations convectives sèches. Le modèle COSMO a cependant tendance à simuler des couches limites trop humides et trop froides, avec une épaisseur réduite par rapport aux observations. En présence de conditions stables, la configuration opérationnelle doit être modifiée de façon significative (coefficient de diffusion minimum p.ex.) afin d'obtenir une représentation adéquate de la couche limite. Le schéma de turbulence de COSMO, qui conduit une équation pronostique pour l'énergie cinétique turbulente (TKE), est étudié en détail pour comprendre les déficits du modèle. Il apparaît que le terme de transport turbulent (moment du troisième ordre) dans l'équation de

la TKE est significativement sous-estimé par le modèle COSMO durant les épisodes instables. Il en résulte des profils de TKE imprécis et, conséquemment, un déficit de flux d'entraînement au sommet de la couche limite. Une solution pour augmenter le transport de TKE au sein de la couche limite est proposée et évaluée sur une période continue de trois mois. Les profils de TKE sont significativement améliorés et les autres sorties du modèle ne sont pas affectées par cette modification.

Dans un deuxième temps, le préprocesseur météorologique – constituant le deuxième composant du système d'alarme - est également validé pour des cas d'étude et sur une période continue. Le principal objectif de cette analyse est la comparaison entre l'approche de couplage utilisée actuellement de façon opérationnelle, basée sur l'usage direct de la TKE pronostique fournie par le modèle COSMO, et une approche classique basée sur la théorie de similitude. Dans les approches conventionnelles, des mesures de turbulence ainsi que des résultats de LES sont utilisées à des fins de vérification. Afin de pouvoir utiliser des approches basées sur la théorie de similitude pour caractériser la turbulence, la hauteur de la couche limite doit être diagnostiquée par le modèle météorologique. Dans cette étude, de nombreuses méthodes de détermination de la hauteur de couche limite ont été implémentées et validées à l'aide de radiosondages. En se basant sur les résultats de la vérification et sur la praticabilité des méthodes en mode opérationnel, la méthode dite « bulk Richardson number » a été choisie pour le diagnostic de la hauteur de couche limite. La validation des caractéristiques de la turbulence diagnostiquées a posteriori montre que les approches basées sur la théorie de similitude ont tendance à surestimer l'intensité de la turbulence durant des épisodes convectifs. L'approche basée sur l'utilisation directe de la TKE fournit des résultats plus précis. Dans des conditions stables, les différentes approches convergent vers des résultats relativement similaires et raisonnables. Le principal inconvénient de l'approche directe est l'hypothèse d'isotropie de la turbulence dans la direction horizontale. Une nouvelle méthode hybride est proposée, qui se fonde sur des considérations de similitude pour le partitionnement de la TKE horizontale dans les directions parallèle au vent et perpendiculaire au vent.

La troisième partie est dédiée à l'étude de la dispersion de polluants en terrain complexe par le biais d'une nouvelle approche d'analyse dimensionnelle (scaling) pour la TKE adaptée au cas de vallées alpines raides et étroites. Cette nouvelle approche de scaling est introduite à l'interface entre COSMO et un modèle lagrangien de dispersion de particules (LPDM). Les résultats obtenus sont comparés aux résultats d'une approche classique basée sur la théorie de similitude ainsi qu'au type de couplage opérationnel, utilisant la TKE du modèle COSMO de façon directe. Pour la validation du système de modélisation, les résultats de l'expérience de traceurs TRANSALP-89, conduit sur le terrain complexe situé dans la partie Sud de la Suisse, sont utilisés. La capacité du modèle COSMO de simuler le système de vent de vallée est évaluée grâce à de nombreuses stations météorologiques au sol. La simulation de

la dispersion est validée à l'aide de mesures provenant de 25 échantillonneurs d'air disposés à la surface du sol. La sensibilité du système de modélisation à l'humidité du sol, à la résolution de la grille horizontale ainsi qu'à la détermination de la hauteur de couche limite est examinée. Nous pouvons montrer que, si les champs de vent sont simulés correctement, la nouvelle approche de scaling permet une simulation plus exacte des concentrations de traceurs comparée aux méthodes de couplage traditionnelles.

Mots-clés: prévision numérique du temps, préprocesseur météorologique, modèle lagrangien de dispersion des particules, turbulence, topographie complexe, hauteur de couche limite

Acknowledgement

This study was carried out in the framework of the COST 728 Action and financed by the State Secretariat for Education and Research, SER through grant C05.0138, which support is gratefully acknowledged.

Contents

Abstract	iii
Résumé	v
1 Introduction	1
1.1 Current problems in the coupling of NWP and dispersion models	1
1.2 The emergency response system of MeteoSwiss	5
1.3 Aims and structure of the thesis	7
2 Evaluation of the COSMO model's turbulent diffusion scheme	9
2.1 Introduction.....	9
2.2 Performance of the COSMO-SC model during an ideal convective case.....	13
2.2.1 Simulation results.....	13
2.3 Simulation of a real convective case with the three-dimensional COSMO model	16
2.3.1 Description of the LITFASS-2003 measurement campaign	16
2.3.2 New Large Eddy Simulations for the LITFASS-2003 campaign.....	18
2.3.3 Details of the COSMO simulations.....	19
2.3.4 General performance of the COSMO model in simulating the PBL evolution.....	22
2.3.5 Sensitivity to horizontal diffusion.....	30
2.3.6 Analysis of the TKE budget	35
2.3.7 Verification of a longer period	41
2.4 Simulation of a real, stable boundary layer with COSMO-SC	46
2.4.1 Description of the GABLS3 experiment.....	46
2.4.2 Simulation of the SBL evolution	48
2.5 Summary and conclusions	52
3 Deriving turbulence characteristics from the COSMO model for dispersion applications	55
3.1 Introduction.....	55
3.1.1 Direct usage of TKE	55
3.1.2 Similarity theory approach	56
3.1.3 Parameterizations of ADPIC.....	60
3.2 PBL height determination from the COSMO model.....	61

3.2.1	Methodology	61
3.2.2	PBL height validation against radio soundings	63
3.3	Evaluation of diagnosed turbulence characteristics	71
3.3.1	Ideal convective case	72
3.3.2	LITFASS-2003 convective case.....	72
3.3.3	GABLS3 stable case	74
3.3.4	The CN-Met measurement campaign	75
3.4	Conclusions and outlook.....	84
4	Simulation of pollutant transport in complex terrain with a NWP – particle dispersion model combination	89
4.1	Introduction	89
4.2	The TRANSALP-89 campaign.....	91
4.3	The modelling system.....	92
4.3.1	The COSMO model.....	92
4.3.2	The Lagrangian Particle Dispersion Model.....	93
4.3.3	Turbulence coupling between COSMO and LPDM	95
4.4	Evaluation of model results.....	100
4.4.1	COSMO simulation.....	100
4.4.2	Verification of the tracer dispersion.....	102
4.5	Sensitivity experiments	105
4.5.1	Initial soil moisture.....	105
4.5.2	PBL height determination	112
4.5.3	Horizontal resolution.....	113
4.6	Conclusions	115
5	Conclusions and outlook	119
5.1	Conclusions	119
5.2	Outlook.....	122
	Bibliography.....	124
	List of acronyms and abbreviations	136
	List of symbols	138
	Acknowledgements	141
	Curriculum Vitae	142

1 Introduction

For the assessment of air quality, two sources of information are at the disposal of decision makers. First, in situ or remote sensing measurements can be used for the determination of the concentration of air pollutants. Secondly, air quality or dispersion models can also be applied which can complement the measurements. The modelling approach can provide several advantages, e.g., it allows the assessment of the full three-dimensional distribution of air pollutants and it can also be used for the prediction of air quality.

Models applied for the transport and diffusion of air pollutants in emergency situations show great variability, ranging from the simplest Gaussian plume models based on in situ meteorological measurements to the most sophisticated Lagrangian particle dispersion models (LPDMs) driven by numerical weather prediction (NWP) models. All these modelling systems have two main components. First, detailed information is required from the atmospheric conditions, where the dispersion process takes place. This can be obtained, e.g., by the use of observations or by complex NWP models. Secondly, a dispersion model is needed to consider all the processes related to transport and diffusion of air pollutants. In most cases the meteorological measurements or the driving models do not provide all the variables that are required by the dispersion model, and consequently, an interface or meteorological pre-processor has to be used between these two models which derives all the necessary – in most cases turbulence related – parameters. The aim of the present work is to validate the above described three components of an emergency response system and to improve the turbulence coupling between NWP models and LPDMs. In particular, the emergency response system of MeteoSwiss is used for the validation studies, which consists of the COSMO (COntortium for Small-scale MOdelling) numerical weather prediction model and an LPDM.

1.1 Current problems in the coupling of NWP and dispersion models

One of the main issues in connection with the coupling of NWP and air quality models is the difference between the so-called off-line and online coupled systems. In the case of off-line coupling, the air-quality model is run after the integration of the NWP model, using its output fields which have a frequency on the order of an hour. Off-line coupling is used with both

Eulerian and Lagrangian air-quality models. For the on-line coupling approach, the NWP and the air-quality models are run at the same time, and the air-quality model is able to use the meteorological fields at each time step. On-line coupling is mostly used in the case of Eulerian chemical transport models, and has the distinct advantage that it can also consider feedback mechanisms (e.g., aerosol effect on cloud formation) between the two models.

One of the main goals of the COST 728 Action (*“Enhancing mesoscale meteorological modelling capabilities for air pollution and dispersion applications”*), which gave the framework of the present work, was to compile a state-of-the-art model inventory of integrated systems used for air quality and dispersion modelling in Europe (Baklanov et al., 2007). The modelling landscape of Europe is rather diverse in this respect, which is reflected by the fact, that the inventory describes more than 25 systems used at 40 institutions in 16 countries. The majority of the presented systems are based on mesoscale meteorological models available at the national weather services or in weather forecasting consortia (i.e., HIRLAM, COSMO, ALADIN) and on international free community models developed by universities (i.e., MM5, WRF, MC2, RAMS, see model descriptions in Baklanov et al., 2007).

In most cases the above mentioned meteorological models are coupled off-line with the dispersion or air quality counterpart of the system. The latter model components show greater variability than the meteorological models. In the case of Lagrangian models we can find simple puff models (CALPUFF) as well as highly sophisticated Lagrangian particle dispersion models (FLEXPART, LPDM). The applied Eulerian models differ from each other in the number of described chemical species and processes, as well as the numerical schemes (CAMx, CHIMERE, CMAQ).

Next to the off-line coupled systems there are a growing number of on-line systems utilized for air quality modelling in Europe (BOLCHEM, COSMO-ART, ENVIRO-HIRLAM, WRF-Chem). Main research areas in connection with on-line systems are tropospheric ozone reactions as well as direct and indirect aerosol effects (e.g., Riemer et al., 2003, Korsholm, 2009).

In the present work the scientific challenges in connection with off-line coupled systems are discussed. For the integration of many Lagrangian particle dispersion models – next to the grid scale wind speed and direction – two different turbulence related subgrid scale variables are needed: the standard deviation of wind fluctuations and the Lagrangian integral timescales in the three coordinate directions. As these variables are not explicitly present in the turbulence schemes of NWP models (or even if present, usually not written into the standard output files), these have to be post-diagnosed from the standard output fields, like wind, temperature and Turbulent Kinetic Energy (TKE). In present day integrated systems two main approaches are used for this. In the case of the classical approach, these variables are diagnosed using similarity theory considerations. The alternative method is to directly use the prognostic TKE of the NWP model if available. The main advantage of the similarity

theory approach is that the vertical profiles of wind and temperature and the surface turbulent fluxes, which are the input variables of the meteorological pre-processor, are more frequently validated and thus give more reliable predictions. However, the consistency between the NWP model and the pre-processor is not ensured using this approach. The direct usage of TKE is a more consistent solution, but TKE is not verified regularly at national weather services. One of the aims of the present work is to investigate the quality of the predicted turbulence values of the COSMO model with respect to dispersion modelling applications.

As a consequence of the increasing computing power, today's NWP and dispersion models are run with even higher horizontal resolutions. With horizontal mesh sizes on the order of 1 km in operational systems, these models become capable of the application in very complex terrain such as the Swiss Alps. However, the increase of the horizontal resolution in these models should only be realized with the simultaneous adaptation of the model dynamics and physics. These motivations are already present in some of the ongoing projects of the COSMO consortium. On one hand, the Priority Project CDC (Conservative Dynamical Core) aims at the implementation of a new dynamical core which gives adequate performance even in the presence of very steep model orography. On the other hand, the Priority Project UTCS (Towards Unified Turbulence-Shallow Convection Scheme) aims at the description of turbulent and shallow convection processes in a common framework, which is another important step towards the kilometre scale modelling (Mironov, 2008). Next to the NWP model, the meteorological pre-processor of an emergency response system should also be adapted to the complex topography. In the case of the direct coupling approach this step is done implicitly. However, the similarity theory considerations should be modified to account for the special turbulence characteristics in steep and narrow Alpine valleys. These investigations are also part of the present work.

There are other important aspects in connection with the coupling of NWP and dispersion models which are beyond the scope of the present work. Still they are shortly discussed in the following. First, the impact of different urban parametrizations on the dispersion process should be mentioned. Currently, in the most operational NWP models surface exchange processes are described in urban areas with the same approach as in rural environment, and cities are only represented with modified surface external parameters (namely larger albedo and roughness length). However, it has been shown, that this approach is not fully capable of capturing the proper structure of turbulence over a city (Martilli et al., 2003). As a large part of the population lives in cities and the sources of air pollutants are very often associated with urban areas, the impact of an urban parameterization on the dispersion process is of great importance (Rotach, 1999, 2001; Baklanov et al., 2006).

Another phenomenon is worth mentioning when investigating the turbulence coupling in dispersion modelling systems: Plume meandering, being one of the most interesting and

controversial phenomena in the stable boundary layer (SBL). The term refers to non turbulent motions in the SBL (also called sub-mesoscale motions) with time scales on the order of one hour and length scales between 10^2 and 10^4 m (Belusic and Mahrt, 2008). The explanation for the existence of these submeso motions is not clear at the moment. Possible causes could be gravity waves, microfronts, drainage flows and thermally induced subgrid scale circulations (Mahrt, 2007). The impact of meandering is most pronounced during low-wind conditions and its omission from the model equations usually results in an overestimation of the measured concentrations (Gupta et al., 1997; Vickers et al., 2008). The most difficult property of flow meandering is that no scaling or similarity properties of this phenomena has been found so far (Vickers and Mahrt, 2007). Consequently, the current parameterizations of plume meandering based on similarity considerations in state-of-the-art dispersion models (e.g. Hanna, 1990; Maryon, 1998) are not likely to describe these motions adequately. Therefore, it seems more promising to follow the direct approach, and try to use the predicted wind fields of the driving high-resolution NWP model at a very high coupling frequency. Belusic and Güttler (2010) performed numerical experiments for a stable case with the WRF-Chem model and found that with a horizontal resolution of 333 m it is possible to qualitatively simulate the meandering motions. Today's finest-resolution operational NWP models are run with 2 km mesh sizes, therefore it is not expected that these models are able to resolve the meandering motions explicitly. Consequently, the parameterization of submeso motions should be included in the turbulence scheme of the NWP model. In the case of the COSMO model a first attempt was made in this direction, as the effect of thermally induced subgrid scale circulations was included in the prognostic equation of TKE (Raschendorfer, 2007a). However, the detailed validation of this "circulation term" is beyond the scope of the present study.

As the last relevant challenge of the turbulence coupling in integrated systems, the impact of the variability of subgrid scale surface properties on the surface turbulent fluxes should be mentioned. The basic idea of this approach is that with the mesh sizes of operational NWP (and climate) models, which are on the order of 5-10 km, it is not possible to correctly account for the variability of surface properties (e.g., roughness length or plant cover), which is usually on the order of 1 km or less in Europe. To resolve this problem, the surface-vegetation-atmosphere transfer (SVAT) schemes of these models are run on a higher resolution than the hosting NWP model and the averaged impact of these finer surface fluxes are computed on the overlying atmospheric layer. Two main approaches are applied in state-of-the-art NWP models. The tile approach (Avisar and Pielke, 1989) divides an NWP grid box to several land cover types and computes surface fluxes for each of these types, which are not located geographically (e.g., all the forest patches are aggregated to one type). The mosaic approach (Seth et al., 1994) is a modification of the tile approach where the geographical locations of the different patches are also taken into account. As

shown by, e.g., Mölders and Raabe (1996) and Ament and Simmer (2006) the application of the tile or mosaic approaches can have a significant impact on the surface fluxes and thus on the vertical profiles predicted by a NWP model. Consequently, the impact on dispersion simulations is also assumed to be significant in certain situations. However, to the author's knowledge no corresponding studies have been performed so far.

1.2 The emergency response system of MeteoSwiss

At MeteoSwiss an integrated modelling system is used to simulate the dispersion of radioactive material in emergency situations. For the prediction of the atmospheric flow, the COSMO numerical weather prediction model is used. The COSMO model is coupled off-line with the Lagrangian Particle Dispersion Model (LPDM). In the following the main features of these models will be presented, with special attention to the turbulence coupling between the models.

The COSMO model is a limited-area numerical weather prediction model (Doms and Schaettler, 2002) which was originally developed at the German Weather Service (DWD). The model is now further developed in the framework of the COSMO consortium. At MeteoSwiss the COSMO model is run operationally at two horizontal resolutions. COSMO-7 has a horizontal resolution of 6.6 km and is integrated out to 72 hours twice a day on a European domain, with lateral boundary conditions from the IFS model of ECMWF (European Centre for Medium-Range Weather Forecasts). COSMO-2, which is nested in COSMO-7, has a 2.2 km horizontal resolution and provides 24 hour forecasts eight times a day for a smaller domain covering the Alps (Figure 1.1).

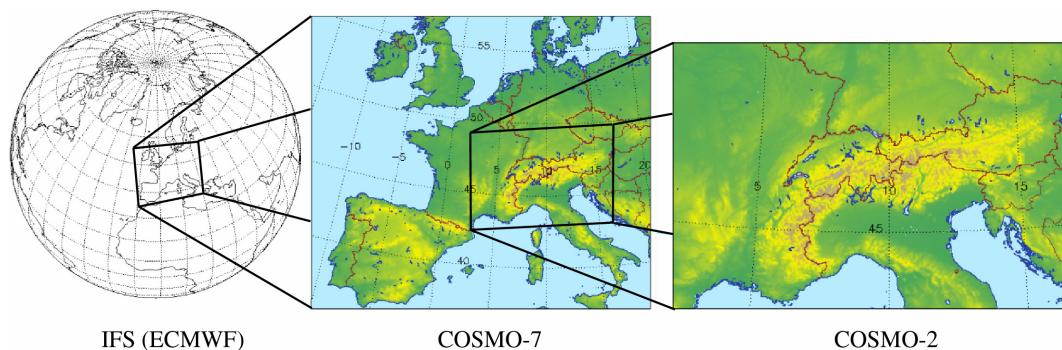


Figure 1.1: Nesting of the two versions of the COSMO model run operationally at MeteoSwiss.

During the integration of the COSMO model the non-hydrostatic hydro-thermodynamical system of equations is solved on an Arakawa-C/Lorenz grid (Arakawa and Lamb, 1977), which is based on a rotated geographical coordinate system. In the vertical a stretched

terrain following coordinate system is used (Gall-Chen and Sommerville, 1975). COSMO-7 and COSMO-2 have identical vertical coordinates with 60 vertical levels, the lowest level being at 10 m and the highest level over 23 km. The model carries prognostic equations for pressure perturbation, wind components, temperature, specific humidity, cloud liquid water, cloud ice, graupel, rain, snow and turbulent kinetic energy. The set of equations is solved with a two time level integration scheme with third order upwind and fifth order horizontal advection formulation (Wicker and Skamarock, 2002). In the horizontal direction a fourth-order numerical filter can be used optionally to remove small scale disturbances from the solution.

The COSMO model uses a data assimilation system based on the nudging scheme. In the fine resolution version (COSMO-2) also radar reflectivity is assimilated with the use of the latent heat nudging approach (Leuenberger and Rossa, 2007). Windprofiler measurements are also assimilated in COSMO-2 with the aim of getting better wind forecasts in the PBL.

Subgrid scale processes like radiation, cloud microphysics, convection, surface-atmosphere interaction and turbulence, which are not explicitly resolved by the model, are parameterized. At low horizontal resolutions radiation is computed on horizontal surfaces after Ritter and Geleyn (1992), while for high-resolution applications in complex terrain a new topographic radiation correction is implemented (Müller and Scherrer, 2005, Buzzi, 2008). The parameterization of cloud microphysics carries prognostic equations for cloud liquid water, cloud ice, graupel, rain and snow (Reinhardt and Seifert, 2006). For deep convection a mass-flux scheme after Tiedke (1989) is applied in COSMO-7. In COSMO-2 deep convection is supposed to be resolved explicitly and thus a simpler shallow convection scheme is used. Atmospheric turbulence is parameterized with a 1.5 order closure at the hierarchy level 2.5 in the Mellor and Yamada (1982) notation. This scheme is active on all model levels and carries a prognostic equation for TKE. Surface-atmosphere interactions are also parameterized in the framework of the TKE scheme (Raschendorfer, 2007a). Soil and vegetation processes are simulated with a coupled multi-layer soil model (Schrodin and Heise, 2001). In the recent years a single-column model of COSMO (COSMO-SC) has also been available for research purposes (Raschendorfer, 2007b).

The model used at MeteoSwiss for the calculation of pollutant dispersion in an emergency situation is the 'Lagrangian Particle Dispersion Model' (LPDM), which was developed by Glaab (1996) at the German Weather Service (DWD). In the case of a particle dispersion model the pollutant cloud is simulated by a large number (more than 100.000) of individual particles. For the trajectory calculation of each particle the Langevin equation after Legg and Raupach (1982) is integrated. Parameterization of deep convection, dry and wet deposition is included in LPDM. Output concentrations are calculated on arbitrary three-dimensional grids, by counting the number of particles in each grid cell.

1.3 Aims and structure of the thesis

The aim of the thesis is to understand and improve the coupling of numerical weather prediction and Lagrangian particle dispersion models in state-of-the-art emergency response systems in complex terrain. Following the structure of these systems, the work has three main goals:

- 1) Evaluate the COSMO numerical weather prediction model in the Planetary Boundary Layer (PBL), with special attention to the turbulence characteristics which are applied in dispersion models. Suggest possible improvement strategies in connection with the turbulence scheme of the COSMO model.
- 2) Review and validate different possibilities for off-line diagnosis of turbulence characteristics serving as input variables for dispersion models.
- 3) Introduce and validate a new coupling approach for emergency response systems in very complex terrain such as the Swiss Alps.

The thesis is organized in three chapters to cover the above described goals.

In *Chapter 2* the COSMO model is evaluated on three selected case studies. Both the single column and the full three-dimensional model are used in the simulations. For the validation, turbulence measurements and Large Eddy Simulation (LES) data is used. The suggested improvements of the turbulence scheme of COSMO are presented on a real-world dry convective case from the LITFASS-2003 measurement campaign (Beyrich and Mengelkamp, 2006). For this case study simulations with 1 km horizontal resolution are also made and the model performance in the PBL is investigated in detail. It is shown that the simulated model fields are very sensitive to the applied horizontal diffusion. Both 'numerical' and 'physical' schemes are tested for horizontal diffusion, which are already implemented in the COSMO code. Next to these schemes, the turbulence closure of Smagorinsky (1963) is also implemented and evaluated. Based on the findings of a component testing the problematic term in the TKE equation is identified and a solution to improve model performance is suggested.

Different approaches to post-diagnose turbulence characteristics for dispersion models are reviewed and evaluated in *Chapter 3*. The two main approaches are the method based on similarity theory and the direct usage of the prognostic TKE from the COSMO model. The similarity theory approach requires the PBL height as input variable. As PBL height is not a standard output field of the COSMO model, first, this characteristic has to be implemented in the COSMO model. Seven different approaches are implemented for the diagnosis of PBL heights from NWP model fields. PBL height predictions are validated with radio sounding

measurements for ideal cases and a one-month continuous period. For the evaluation of post-diagnosed turbulence characteristics the same case studies are used as in Chapter 2.

In *Chapter 4* the emergency response system of MeteoSwiss is validated on the TRANSALP-89 tracer experiment in very complex terrain. First, the ability of the COSMO model to simulate the valley wind system in the Southern Alps is investigated. Secondly, the tracer cloud is simulated with LPDM and the sensitivity of concentration predictions towards the different coupling approaches is investigated. A new scaling approach by Weigel et al. (2007) suited for steep and narrow Alpine valleys is implemented in the coupling interface of LPDM to better describe the special turbulence characteristics in Alpine valleys.

The main findings are summarized at the end of each chapter, however, in *Chapter 5* the results are synthesized, general conclusions are drawn and these are compared to other scientific results. Possible further directions of research in connection with the turbulence coupling in emergency response systems are also given.

2 Evaluation of the COSMO model's turbulent diffusion scheme

2.1 Introduction

In this Chapter, the ability of the COSMO model in simulating the evolution of the Planetary Boundary Layer is investigated. The performance of an operational NWP model in the PBL is of great importance for several reasons. First, the area of interest for most NWP applications is located near the surface where people live. Let us think of, e.g., 2 metre temperature forecasts for the general public or for the energy sector. Secondly, in today's emergency response systems dispersion models are very often coupled to operational NWP models to predict the transport and diffusion of pollutants (Baklanov et al., 2007). For this application, next to the grid scale NWP model variables (wind or atmospheric stability), the predicted subgrid scale turbulence characteristics also play an important role. Grid-scale variables of operational NWP models are verified routinely at national weather services, which is not the case for subgrid scale characteristics. Consequently, the aim of this Chapter is to evaluate the predicted grid- and subgrid-scale variables of the COSMO model at the same time.

In the PBL, momentum, heat and tracers are transferred by turbulent motions. The maximum length scale of these motions is on the order of the PBL depth, which varies between several 10 metres in very stable situations to a couple of kilometres in highly unstable cases. In operational NWP models with mesh sizes greater than 1-2 km, these turbulent motions cannot be resolved explicitly, thus a parameterization scheme has to be used to account for the averaged impact of these motions to the grid scale variables.

In the COSMO model the parameterization of subgrid scale turbulence follows the ensemble mean approach, the main assumption of which is to handle the grid scale variables as the mean over all possible realisations of the flow for the given conditions. The separation of mean and turbulent part of the prognostic quantities is made with Reynolds decomposition, e.g., for a variable ϕ this can be written as:

$$\phi = \Phi + \phi', \quad (2.1)$$

where Φ is the grid scale and ϕ' is the subgrid scale part of the given quantity. The governing equations for the mean (grid scale) variables of the turbulent flow can be obtained

by applying Reynolds decomposition and averaging to the general conservation equations (momentum, energy and mass). However, this results in the appearance of second order moments (variances and covariances) in the equations. With further decomposition and averaging it is possible to derive budget equations for the second order moments, which on the other hand will contain third order moments. This chain of equations is known as the closure problem and its solutions are the different turbulence closures or parameterizations.

In the COSMO model subgrid scale turbulence is parameterized with a 1.5-order closure (Raschendorfer, 2007a, 2001) based on the Level 2.5 scheme of Mellor and Yamada (1982). A detailed description of the scheme can also be found in Buzzi (2008) and Buzzi et al. 2010, in the following only the main features of the scheme are discussed. The derivation of the scheme starts with the budget equations of the second order moments ($\overline{u'_i u'_j}$, $\overline{u'_i \theta'}$ and $\overline{\theta'^2}$, where u'_i and θ' refer to velocity and temperature fluctuations, respectively). The system of these partial differential equations is simplified by introducing the turbulent velocity scale, $q = \sqrt{\overline{u_i'^2}}$, the master length scale λ and the following assumptions:

- Local equilibrium is applied to all second order moments, thus local tendencies and advection terms are neglected, except for the velocity fluctuations.
- The Rotta-hypothesis (Rotta, 1951a, 1951b) is used to parameterize the return-to-isotropy term.
- The pressure correlation term is handled as part of the turbulent transport.
- Dissipation rates are parameterized according to Kolmogorov (1941).
- The diffusion of $\overline{\theta'^2}$ is neglected.
- The master length scale of turbulence is parameterized following Blackadar (1962), independently of the atmospheric stability.

With these assumptions the original second order equations reduce to ten algebraic equations for the second order moments and a prognostic equation for the Turbulent Kinetic Energy (TKE or $e = \frac{1}{2} \overline{u_i'^2}$), formulated in q .

The turbulence scheme of COSMO is a moist scheme, which means that it considers subgrid scale phase changes of water. To avoid additional source terms in the equations the scheme is formulated in terms of the liquid water potential temperature (Θ_l) and total water content (Q_w), which are conservative variables for moist-adiabatic processes. The coefficients for these variables (A_{Θ_l} and A_{Q_w}) are determined by a subgrid scale cloud scheme after Sommeria and Deardorff (1976).

Turbulent fluxes of momentum, heat and moisture in a 1.5-order closure framework can be written as:

$$\overline{u'w'} = -K_M \frac{\partial U}{\partial z} \quad (2.2)$$

$$\overline{\theta_l'w'} = -K_H \frac{\partial \Theta_l}{\partial z} \quad (2.3)$$

$$\overline{q_w'w'} = -K_H \frac{\partial Q_w}{\partial z} \quad (2.4)$$

$$K_M = q\lambda S_M \quad (2.5)$$

$$K_H = q\lambda S_H, \quad (2.6)$$

where K_M and K_H are the turbulent diffusion coefficients of momentum and heat, respectively. S_M and S_H are stability functions which are related to q and λ , and their exact formula can be derived from the above mentioned ten algebraic equations. It can be seen that this scheme is a local scheme, because it generates turbulent fluxes only locally, where gradients of mean variables are present.

The arising third order moment in the TKE (or q^2) equation (turbulent transport of TKE) is parameterized with a simple down-gradient approach, which means that the TKE flux is proportional to the gradient of TKE. This approach could have its drawbacks in strongly convective situations when the turbulent transport of mean variables as well as that of TKE is dominated by non-local effects. This issue is further discussed in the following sections.

One particular extension of the COSMO model's turbulence scheme as compared to the Mellor and Yamada Level 2.5 closure is the inclusion of the effect of thermally induced subgrid scale circulations. This term is a positive definite source term in the TKE equation and is only important in very stable situations, when this term inhibits TKE to approach zero. Without this term, the vanishing TKE would lead to a decoupling of the atmosphere from the underlying surface.

After all the above mentioned assumptions and extensions the TKE equation in the COSMO model has the following form:

$$\begin{aligned} \frac{\partial q^2}{\partial t} = & -2K_H \frac{g}{\Theta_v} \left[A_{\Theta_l} \frac{\partial \Theta_l}{\partial z} + A_{Q_w} \frac{\partial Q_w}{\partial z} \right] + K_M \left[\left(\frac{\partial U}{\partial z} \right)^2 + \left(\frac{\partial V}{\partial z} \right)^2 \right] - \\ & - \frac{1}{\rho} \frac{\partial}{\partial z} \left[\alpha \bar{\rho} \lambda q \frac{\partial q^2}{\partial z} \right] - 2 \frac{q^3}{B_1 \lambda} + \frac{1}{\rho} \frac{\partial}{\partial z} \left[2L_{pat} \bar{\rho} \left(\frac{\lambda g}{q \Theta_v} \right) K_H \left(A_{\Theta_l} \frac{\partial \Theta_l}{\partial z} + A_{Q_w} \frac{\partial Q_w}{\partial z} \right)^2 \right], \end{aligned} \quad (2.7)$$

where $\bar{\rho}$ is the density of moist air, α is the coefficient for the turbulent transport of TKE and L_{pat} is a constant characterizing the surface inhomogeneities in the circulation term. The term on the left hand side of the equation is the local tendency of the TKE. Terms on the right hand side refer to the buoyancy and shear production/destruction, the turbulent transport of TKE, the dissipation rate and the subgrid scale circulations, respectively.

There are two details in connection with the implementation of the scheme which has to be noted. First, there is a constant lower limit defined for the turbulent diffusion coefficients, to avoid numerical instabilities in stable situations. In the current operational COSMO configuration at MeteoSwiss this limit is set to $1 \text{ m}^2/\text{s}$, which proved to be a rather high value. Buzzi (2008) and Buzzi et al. (2010) showed that the model performance in stable situations can be improved if the limiting value is reduced. However, to avoid numerical instabilities, a vertical filter function has to be applied to the wind gradients in this case. Secondly, it is worth to mention the numerical solution of the TKE equation. On the one hand, the grid scale variables are integrated by the numerical core of COSMO, which applies the implicit Runge-Kutta scheme. On the other hand, the turbulent transport term in the TKE equation is handled inside the turbulence scheme and solved explicitly. This could lead to instabilities when using very fine vertical level distributions. As will be shown in the next section, this problem can be solved by the implementation of a semi-implicit solver for the TKE transport.

In the following sections the performance of the COSMO model's turbulence scheme is investigated in different situations. First, an idealized convective case is studied and COSMO is compared only to LES data. Secondly, a real-world convective case from the LITFASS-2003 measurement campaign is investigated, presenting comparisons with both measurements and LES. Finally, the performance of COSMO is studied on the GABLS3 stable case. This part of the PhD work was done in the framework of the COSMO Priority Project UTCS (Towards Unified Turbulence-Shallow Convection Scheme), which aims at the further development of the turbulence scheme. The contribution of the present research to the UTCS project was to perform a component testing of the current turbulence scheme. This means that the budget terms in the TKE equation are analyzed separately, problematic terms are identified and a possible solution is proposed to improve the model performance.

2.2 Performance of the COSMO-SC model during an ideal convective case¹

To understand the behaviour of the turbulence scheme of the COSMO model in detail, several case studies were investigated. First, an ideal convective case described in Mironov et al. (2000) was studied. The setting for this simulation was a horizontally homogeneous and flat terrain with constant heating rate at the bottom. In the simulation no phase changes were considered (dry case) and wind shear was neglected. For this case a LES dataset was available from Dmitrii Mironov (DWD), containing all the TKE budget terms that were important for the evaluation. Figure 2.1 shows the scaled TKE budget terms from the LES run after the steady state was achieved.

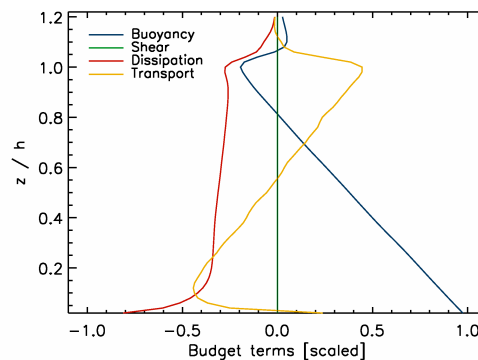


Figure 2.1: Scaled TKE budget terms from the Large Eddy Simulation of the ideal convective case. TKE terms as in the legend in the inlet.

2.2.1 Simulation results

The above described case was simulated with the single column version of the COSMO model (Raschendorfer, 2007b). In the single column simulation the operational 60 vertical levels were used with the first level at 10 m height, and the time step for the integration was 72 s. The results (Figure 2.2) show that the turbulent transport of TKE is much too weak in the COSMO model as compared to the LES results. Consequently, TKE values at the top of the planetary boundary layer are low and the negative buoyancy flux in the entrainment zone is almost completely missing.

Due to the stretched vertical level distribution, the model layers are relatively thick (around 100 m) near the top of the PBL. In the next step it was investigated, whether an increased resolution in the PBL would result in a better description of the transport term. To achieve this, a 10 m equidistant level distribution was tested with the same integration time

¹ This Section is based on the following proceedings paper:

Szintai, B., and O. Fuhrer, 2008: Component testing of the COSMO model's turbulent diffusion scheme. COSMO Newsletter No. 9., 37-41.

step (72 s). The result of this simulation (Figure 2.3) is astonishing at first sight, because the transport term completely vanishes, causing a sharp decrease of TKE at the PBL top.

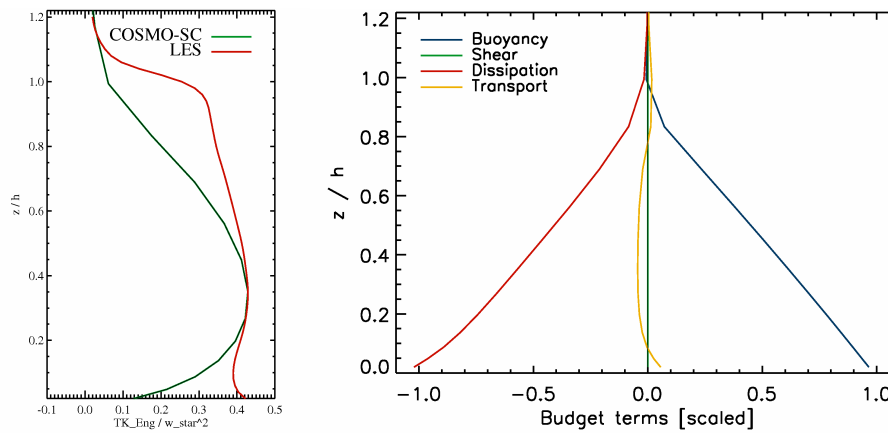


Figure 2.2: Scaled profiles of TKE (left) and the TKE budget terms (right) from the COSMO-SC simulation with the operational level distribution and $dt=72$ s.

The cause for this strange behaviour is a numerical limiter in the explicit scheme of the transport term. This numerical limiter is active, if the selected time step is too large for the given vertical level distribution.

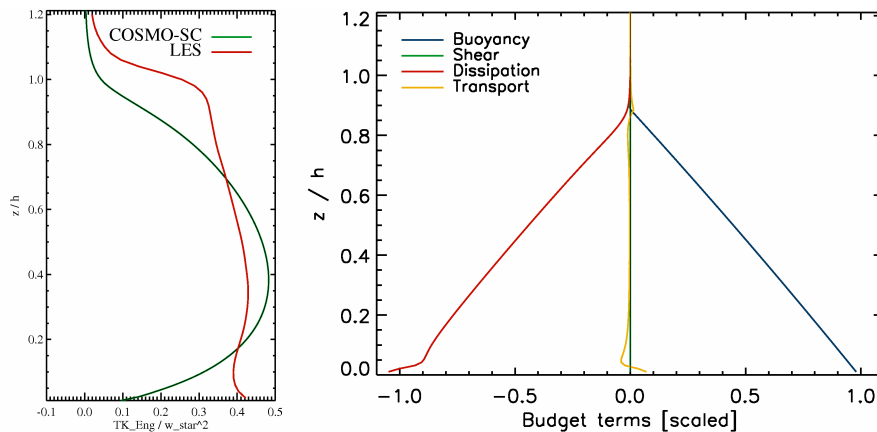


Figure 2.3: Scaled profiles of TKE (left) and the TKE budget terms (right) from the COSMO-SC simulation with 10 m equidistant level distribution and $dt=72$ s.

To achieve a physically consistent solution without any numerical limitations, first, the numerical limiter in the transport term should be deactivated. This was realized in two different ways. First, an appropriately small time step was chosen, and secondly, a semi-implicit formulation of the transport term was utilised. Figure 2.4 shows the result of the first approach. To achieve a stable integration without the numerical limiter, a significantly smaller time step of 3.6 s had to be used for 10 m equidistant levels. It has to be noted, that the solution was independent of the vertical resolution, if the correct time step was used in each case (e.g., $dt=7.2$ s for 20 m equidistant levels).

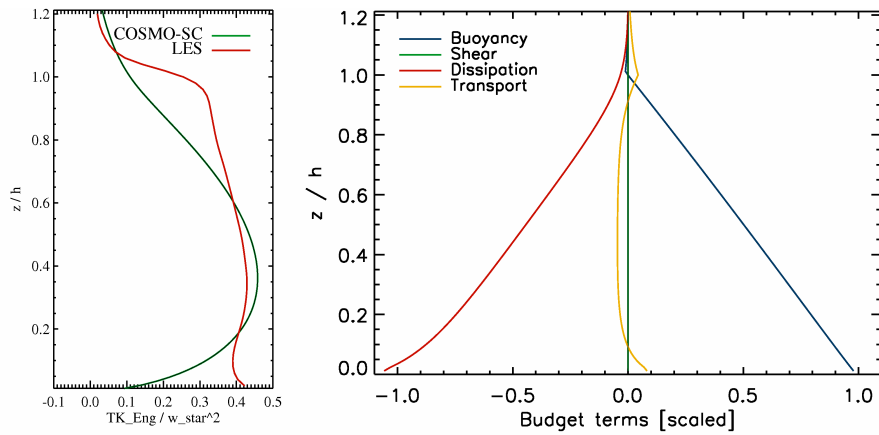


Figure 2.4: Scaled profiles of TKE (left) and the TKE budget terms (right) from the COSMO-SC simulation with 10 m equidistant level distribution and $dt=3.6$ s.

In the case of the second approach a semi-implicit formulation was implemented for the transport term, which allowed the use of large time steps even for very high (even 1 m) vertical resolution. Due to the semi-implicit approach the solution was independent of the vertical resolution and timestep (Figure 2.5).

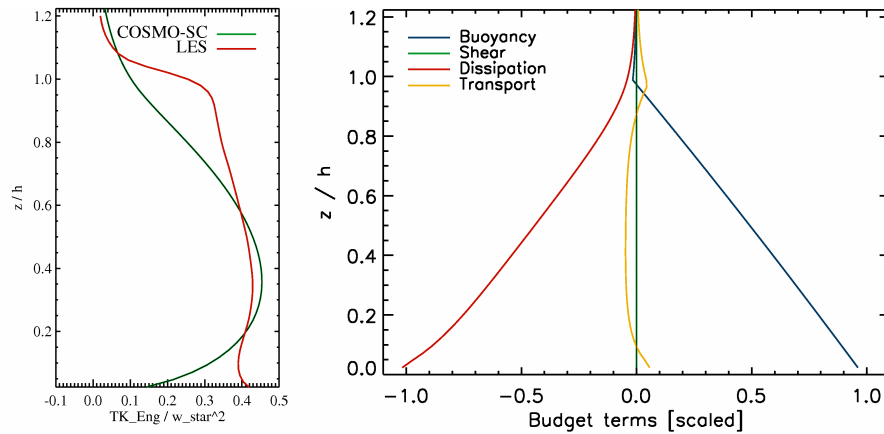


Figure 2.5: Scaled profiles of TKE (left) and the TKE budget terms (right) from the COSMO simulation with semi-implicit formulation for the transport term (20 m equidistant level distribution with $dt=72$ s).

The run with semi-implicit TKE diffusion still shows serious deficiencies compared to the LES profiles. The TKE transport term is too weak and it causes a wrong TKE profile. As the TKE budget in COSMO is balanced per definition, the wrong TKE profile causes a wrong dissipation profile. Due to the TKE underestimation at the top of the PBL the entrainment heat flux is significantly underestimated in COSMO.

2.3 Simulation of a real convective case with the three-dimensional COSMO model

After the investigation of an ideal case described in the previous section, it is important to study a real convective case as well, to see, whether the previously drawn conclusions also apply during real-world conditions. It is also important to compare the COSMO simulations not only with LES data, but also to atmospheric observations, like radio sounding, surface measurements and turbulence datasets.

For this study, a specific day from the LITFASS-2003 measurement campaign was chosen. The COSMO simulation covers a whole diurnal cycle, consequently, not only the steady-state convective boundary layer can be studied, but the evolution of the PBL characteristics can be investigated, too. The simulation domain can be considered flat to a close approximation, however, surface conditions are characterized by strong horizontal heterogeneity, and thus there is a possibility to investigate the role of surface heterogeneity in the evolution of the PBL.

The structure of this section is the following. First, the measurement campaign is introduced and the main conclusions drawn from previous modelling studies are mentioned. After that, the main features of the COSMO simulation are described. For the chosen convective case Large Eddy Simulations were also performed at EFLUM-EPFL. Some details about these LES runs are given. Following this, the sensitivity of the COSMO simulation towards the model resolution and the horizontal diffusion parameterization is investigated. Finally, the TKE budget terms of COSMO are analysed. Based on this budget analysis, a new parameterization of the TKE transport term is proposed and the impact of the new approach to the simulation of the PBL evolution is described.

2.3.1 Description of the LITFASS-2003 measurement campaign

The LITFASS-2003 (Lindenberg Inhomogeneous Terrain - Fluxes between Atmosphere and Surface: a Long-term Study) measurement campaign was realized in the framework of the EVA_GRIPS (Evaporation at Grid / Pixel Scale) project in the area of Lindenberg, Germany (the so-called LITFASS-domain, Figure 2.6). The main goal of the EVA_GRIPS project was to determine the area-averaged evaporation over a heterogeneous land surface at the scale of a grid box of a regional atmospheric circulation model and / or at the scale of a pixel of a satellite picture both from measurements and model simulations (Beyrich and Mengelkamp, 2006).

To achieve this goal a large set of measurement systems were deployed near the main measurement site of the German Weather Service, which included:

- Micrometeorological stations on all the land cover types measuring the turbulent exchange processes between the land surface and the PBL.
- A 99 m high tower near Falkenberg, measuring both mean and turbulence characteristics.
- Different remote sensing instruments (sodar, windprofiler, Lidar, scintillometer).
- Airborne turbulence measurements in the PBL made by the Helipod sonde carried by a helicopter.

These observations were supported by comprehensive modelling work, which included the application of meso-scale NWP/climate models (Ament and Simmer, 2006) and LES (Uhlenbrock, 2006). The main conclusions drawn from the NWP modelling experiments were the following:

- External parameters in the soil-vegetation-atmosphere scheme are key parameters for correctly simulating the exchange processes at the surface.
- It is very important to achieve a reliable initial analysis in the soil model. This can be done by a measurement driven soil moisture analysis.
- The representation of subgrid scale surface variability (e.g., with the tile or mosaic approach) can substantially improve the simulation in a heterogeneous domain.

Large Eddy Simulations in connection with the LITFASS-2003 campaign were focusing on the phenomenon of meso-scale circulations over heterogeneous surface (e.g., lake effects). It was found that on radiation days with weak geostrophic forcing these meso-scale circulations can account for a considerable part of the turbulence intensity.

The above mentioned meso-scale NWP experiments were mostly dealing with surface-atmosphere exchange processes. The work presented in this section investigates model performance in the middle and upper part of the PBL. Thus this study is concentrating on the atmospheric turbulence scheme of the COSMO model.

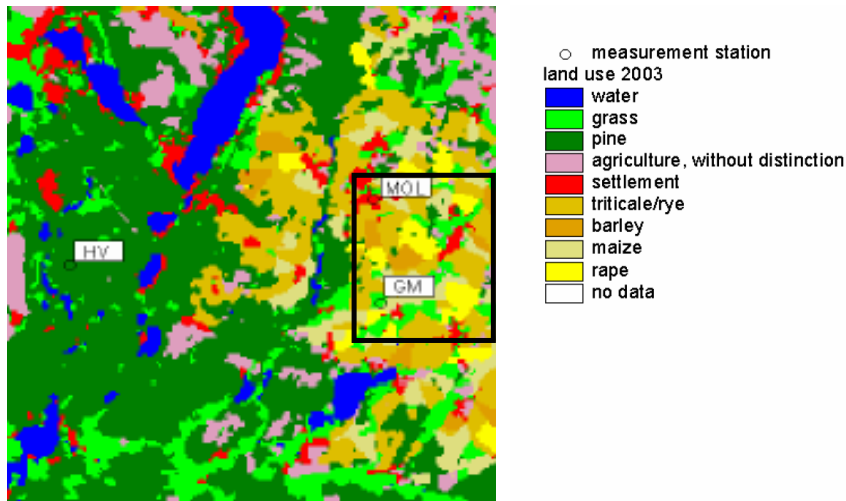


Figure 2.6: Land cover classes (at 100 m resolution) over the LITFASS-domain (20 km × 20 km). “GM” indicates the boundary layer site of DWD with the 100 m tower, “MOL” indicates the Lindenberg Observatory, where the radio sounding ascents were made. The “Falkenberg area” used for the evaluation of surface variables is indicated by the black rectangle. (This figure was prepared by C. Heret, TU Dresden, and J. Uhlenbrock, University of Hannover).

For the modelling exercise the 30 May 2003 was selected as a case study. This day is characterized by low geostrophic forcing and cloudfree conditions. As there were no clouds observed, both the LES and NWP modelling could be realized by applying dry turbulence schemes, which simplified the analysis of the results. Another aspect by the selection of the case was that the 30 May was one of the “golden days” of the LITFASS-2003 campaign, when all the measuring devices were working properly. This day was previously simulated with both the COSMO model (Ament and Simmer, 2006) and with LES (Uhlenbrock, 2006), giving a good dataset for the present COSMO runs to compare with.

2.3.2 New Large Eddy Simulations for the LITFASS-2003 campaign

During the investigation of the COSMO model’s turbulence scheme it was essential to have high quality LES runs with all the necessary turbulence characteristics written to the model output that are needed for the validation of the COSMO model. These characteristics should include not only TKE, which was present also in the previous LES datasets, but all the TKE budget terms. For this reason, new Large Eddy Simulations had to be made for the selected case study. These simulations were realized in the Laboratory of Environmental Fluid Mechanics and Hydrology (EFLUM) at the Swiss Federal Institute of Technology, Lausanne (EPFL).

The LES code that was used has its origins in the work of Albertson and Parlange (1999), and was further developed by Porté-Agel et al. (2000) and Bou-Zeid et al. (2005).

Recently, this LES code was successfully applied for the simulation of the diurnal cycle of the atmospheric boundary layer (Kumar et al., 2006). The model solves the filtered Navier-Stokes equations and applies a sophisticated Lagrangian scale-dependent dynamic subgrid scale model. Considering the numerics of the model, a spectral representation is used in the horizontal direction, while in the vertical the finite differences method is applied. The lateral boundary conditions are periodic and at the upper model boundary a stress-free lid is used. At the surface the model is forced with measured surface temperature and the heat exchange between the surface and the atmosphere is calculated using Monin-Obukhov similarity.

For the LITFASS-2003 case the afternoon hours were simulated between 1200 and 1900 UTC, using a three-hour spin-up time (so the actual simulation was started at 0900 UTC). The simulation domain was 6 by 6 km in the horizontal and 3 km in the vertical using 64^3 grid points. Consequently, the horizontal and vertical mesh size of the LES was 94 and 47 m, respectively, and a 0.1 s time step was used. For the comparison with the COSMO turbulence characteristics, an averaging on the whole LES domain was made. Next to these profiles, three-dimensional snapshots of the turbulent flow were also studied.

2.3.3 Details of the COSMO simulations

In the present study the COSMO model version 4.0 (MeteoSwiss local version 4.0.13) was used to simulate the diurnal cycle of 30 May 2003, with 2.2 and 1 km horizontal resolution (referred to as COSMO-2 and COSMO-1 in the following). COSMO-2 was run with the operational 60 vertical levels, while COSMO-1 was tested with both the operational level distribution and a higher vertical resolution of 74 levels. The configuration of the numerics and the physical parameterizations of COSMO-2 were similar to the operational setting (see Section 1.2). The configuration of COSMO-1 was mostly similar to COSMO-2, however, COSMO-1 was run with a three-dimensional turbulence parameterization assuming isotropic turbulence. COSMO-2 was run on the same $365 \text{ km} \times 365 \text{ km}$ model domain as COSMO-1 centred over the LITFASS-domain (Figure 2.7).

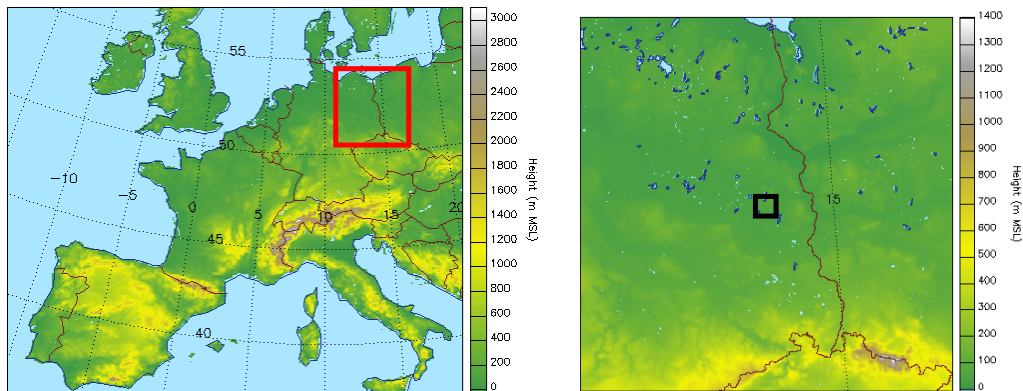


Figure 2.7: Model domains and orography of the driving COSMO-7 model (left) and COSMO-1 (right). The COSMO-1 domain is indicated with a red rectangle, the LITFASS-domain is shown by a black rectangle.

The simulation started on 0000 UTC on 30 May 2003 and the model was integrated for 24 hours. As the synoptic situation on the selected day was characterized by an anticyclone, it is assumed that the atmospheric properties in the area of interest will be determined mainly by local effects and not by the large-scale forcing. Consequently, it is of major importance to start the model simulation from as good initial conditions as possible. To achieve this, the following three aspects had to be considered:

- Accurate external parameters
- Soil analysis
- Atmospheric initial- and boundary conditions

As the operational external parameters (especially soil type and root depth) are not adequate in the LITFASS area (Gerd Vogel, DWD, personal communication), a new set of parameters were used for the COSMO simulations. This new dataset with 1 km horizontal resolution was prepared in the framework of the ‘LITFASS-Lokal-Model’ project (Herzog et al., 2002) and was made available for the present study by Felix Ament (University of Hamburg). In the new soil dataset the dominating type in the LITFASS area is sandy loam and sand, which is more realistic than the dominating type of the operational model, which is loam. In the operational dataset the root depth is only a function of latitude and height, while in the new dataset the vegetation type of each grid point is taken into account for this parameter, thus giving a more realistic spatial distribution (Figure 2.8).

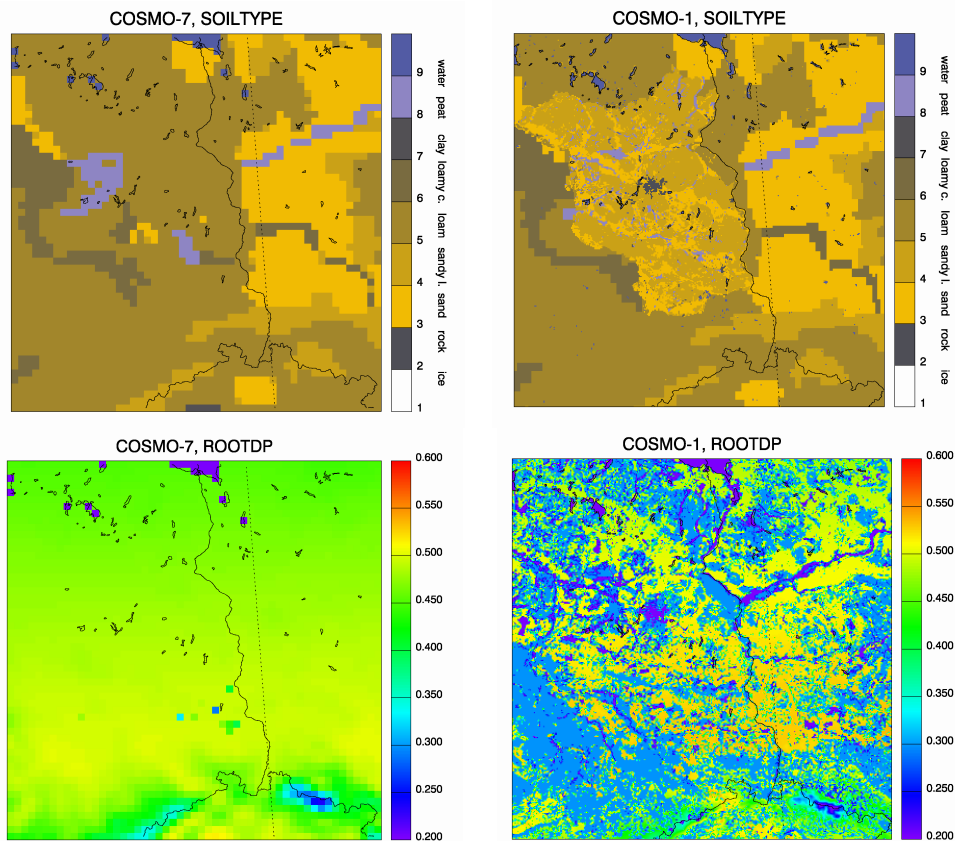


Figure 2.8: External parameters of the operational COSMO model at 7 km horizontal resolution (left) and from the modified dataset at 1 km resolution (right), on the COSMO-1 model-domain. Displayed are the soil type (upper row) and the root depth (lower row; in metres) for 30 May 2003.

The next step in achieving an accurate initial state of the model was to produce a good soil analysis using the new 1 km external dataset. A measurement driven soil analysis was already prepared in the work of Ament (2006). However, that study used the two-layer soil model of COSMO. Currently, an eight-layer soil model is operationally used at MeteoSwiss, thus the soil analysis for the present study was produced with this new soil model. For this, the standalone version of the soil module TERRA was used. The integration was started on 1 May 2003 at 0000 UTC and the soil model was run until 30 May 2003 0000 UTC. For forcing TERRA-standalone, the operational analysis of COSMO-7 was used, which provided wind, temperature and precipitation as boundary conditions for the model. As a result, an equilibrium soil analysis was achieved which agrees well with soil moisture and temperature measurements (see details in Section 2.3.4). Longer integration times (three and five months) for TERRA-standalone were also tested, however, these resulted in a very similar soil analysis to the one-month run.

Both the initial atmospheric analysis and the boundary conditions were derived from the operational analysis cycle of COSMO-7 from 2003. In this cycle the radio soundings of the area of interest (especially Lindenberg) were assimilated which assures an accurate wind and temperature profile for the initialization of COSMO. The application of COSMO-7

analyses as boundary conditions enables to circumvent the uncertainty of the driving global model to some extent. As in 2003 the operational COSMO-7 used only 45 vertical levels, the atmospheric fields had to be interpolated onto the vertical grid of COSMO-2 and COSMO-1, which consists of 60 or 74 levels. It has to be noted, that both COSMO-2 and COSMO-1 were driven with the same boundary conditions, and thus no intermediate step was applied between the 7 km and the 1 km horizontal resolution. This could lead to some disturbances close to the model boundary, however, as the model domain is rather large as compared to the area of interest (LITFASS-domain) these boundary effects are damped before they would reach the inner part of the domain.

2.3.4 General performance of the COSMO model in simulating the PBL evolution

In this section the COSMO simulation is analysed focusing on the model performance in the boundary layer. For the model evaluation, different in-situ measurements (surface micrometeorological stations, radio soundings, tower measurements) and Large Eddy Simulation data is used. In the following, simulation results of COSMO-1 (with 60 vertical levels) are presented, as for most of the parameters COSMO-2 gives similar results. Main differences between COSMO-2 and COSMO-1 are discussed at the end of this section.

Initial profiles

As discussed in the previous section, the initial conditions for the soil model were produced with a one-month TERRA-standalone run forced by COSMO-7 analyses. Figure 2.9 compares the initial soil temperature and moisture profiles of COSMO with measurements at micrometeorological stations. In the comparison of measured and modelled soil profiles two main land cover types – farmland and forest – were distinguished. In the case of the initial soil temperature for farmland it can be seen that the COSMO profile is accurate below 20 cm depth, but underestimated in the upper layer. For the forest type the situation is opposite. The upper layer temperature is well captured by the model, while the temperature of the deeper layers is overestimated. On farmland the mean profile of soil moisture is well reproduced, although the horizontal variance of measurements is seriously underestimated by the model. For the forest type the soil moisture is overestimated at all depths.

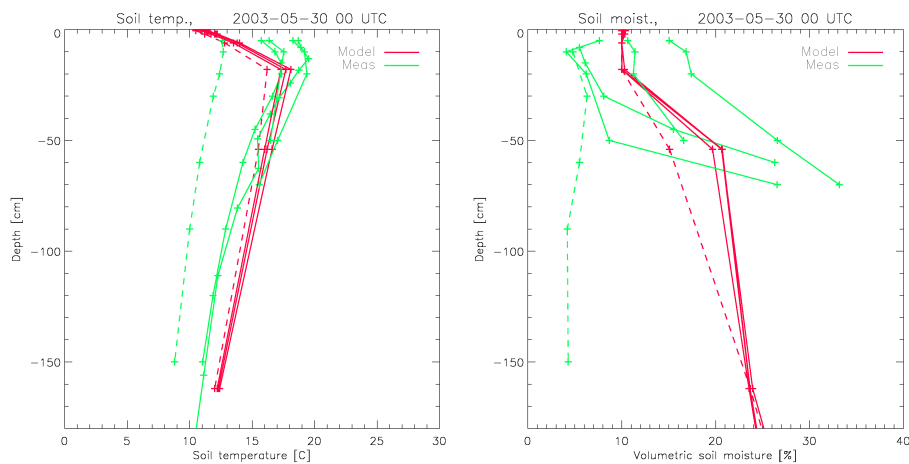


Figure 2.9: Initial soil temperature (left) and moisture (right) profiles of COSMO (red) compared with measurements (green). Different farmland stations are indicated with solid lines, the forest station with dashed lines.

The initial atmospheric profiles were interpolated from the operational COSMO-7 analysis. Figure 2.10 shows profiles of potential temperature, wind direction and speed and specific humidity for 30 May 2003 0000 UTC compared to the radio sounding measurements. The initial profiles of COSMO compare quite well with the radio sounding measurements. In the potential temperature profile, both the 200 m high surface inversion and the approximately 1000 m high residual layer are well represented. In the wind speed profile a nocturnal jet can be identified above the surface inversion.

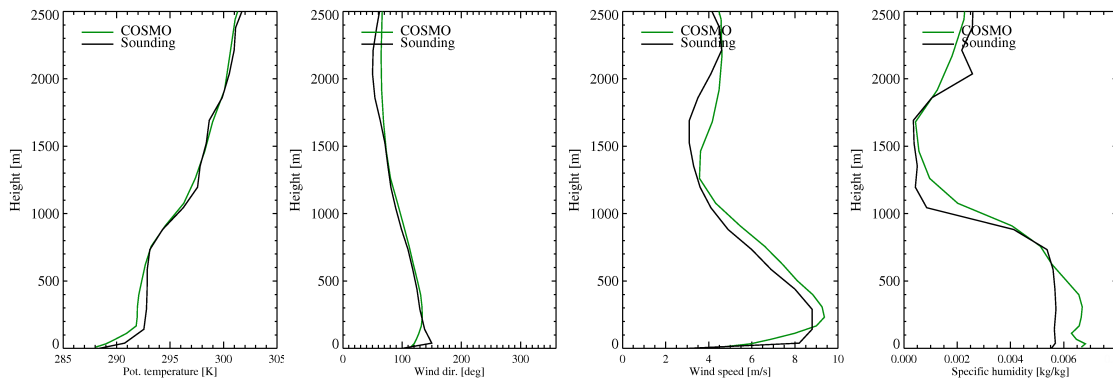


Figure 2.10: Initial atmospheric profiles of COSMO (green line) on 30 May 2003 at 0000 UTC compared to the radio sounding measurements (black line). From left to right: potential temperature, wind direction, wind speed and specific humidity. Height is indicated in metres above ground level.

Both the maximum and the intensity of the jet are slightly overestimated by COSMO. Specific humidity near the surface is slightly higher in the model than in the radio sounding profile, however, this might be traced back to the dry bias of the sounding instrument (this problem

will be further investigated later). Generally, it can be concluded that both the soil and the atmospheric profiles in the COSMO model are correct for the initial time of the simulation.

Surface forcing

Next to adequate initial conditions it is also very important that in the COSMO simulation the surface forcing is reproduced correctly. Only with correctly simulated surface forcing is it possible to investigate the performance of the turbulence scheme and compare the predicted turbulence values with field measurements. First, the daily cycle of the main radiative forcing term – net radiation – is investigated. Secondly, the partitioning of net radiation into surface sensible and latent heat flux is studied.

The analysis of these parameters is restricted to an approximately 7 by 8 km domain around the Falkenberg measurement site (cf. Figure 2.6). This domain (further referred to as the “Falkenberg area”) and the used measurements exclude the forest and the water land cover type. This restriction was made, because later on the tower measurements of Falkenberg and the radio soundings of Lindenberg will be applied to evaluate COSMO, and both of these sites have only farmland and grassland in the upwind direction.

Net radiation (Q) is calculated as the sum of the net shortwave and net longwave radiation:

$$Q = SW_{down} - SW_{up} + LW_{down} - LW_{up}, \quad (2.8)$$

where SW_{down} is the shortwave downwelling, SW_{up} is the shortwave upwelling, LW_{down} is the longwave downwelling, LW_{up} is the longwave upwelling radiation. Figure 2.11 shows the measured and modelled net radiation for the “Falkenberg area”. It can be noted, that for the investigated cloud free day the net radiation is simulated very well by the COSMO model. Daytime net radiation is nearly perfect, night time net radiation is somewhat underestimated by the model. This good performance is in line with previous verification results of the net radiation of the COSMO model (Buzzi, 2008), which indicate a generally adequate model performance during cloud free conditions.

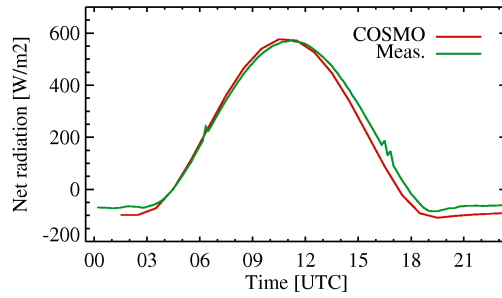


Figure 2.11: Surface net radiation time series of COSMO (red) compared to measurements (green) for 30 May 2003 over the “Falkenberg area”.

On the surface the incoming net radiation is distributed between surface sensible (H_0) and latent heat flux (λE_0) and ground heat flux (G_0):

$$Q = H_0 + \lambda E_0 + G_0. \quad (2.9)$$

Melting and sublimation effects (at least for the LITFASS-2003 case) can be neglected with good approximation, thus the above equation should be closed for the measured components. However, several studies on the subject (e.g., Foken and Oncley, 1995; Laubach and Teichmann, 1999; Beyrich et al., 2002) show that the energy balance is not closed in the observations, and the right hand side of Equation 2.2 is smaller than the net radiation. Reasons for this non-closure effect are summarized in Culf et al. (2004), who attribute the presence of a residuum to advection and storage terms. Ament (2006) points out that the positive definite property of the residuum may be caused by the fact, that the different sensors of sonic anemometers are not mounted on the exactly same location. Mauder et al. (2006) estimated the residuum for the LITFASS-2003 measurements as 25% of Q , consequently, this value is added in the following as an uncertainty range for both the surface sensible and latent heat flux measurements.

The following investigating will focus on the surface sensible and latent heat flux, as these are the main forcing variables for the upper atmospheric levels of the COSMO model. Figure 2.12 shows time series of measured and modelled surface fluxes for the “Falkenberg area”. Surface sensible heat flux is overestimated by COSMO, even if the modelled values still lie on the edge of the uncertainty range of the measurements. Latent heat flux is considerably underestimated, which may indicate a wrong Bowen ratio in the model. Also, the time of the daily maximum occurs too late for both variables in the model.

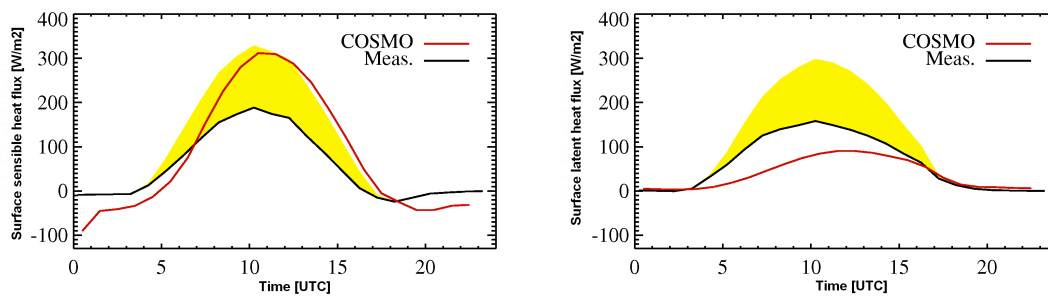


Figure 2.12: Time series of surface sensible (left) and latent (right) heat fluxes of the COSMO model (red) compared to measurements (black) over the “Falkenberg area”. The yellow shading indicates the uncertainty range of measurements due to the non-closure of the surface energy balance (see text).

Several sensitivity tests with modified soil moisture were made to study the inadequate partitioning of surface fluxes. These sensitivity runs attributed the wrong flux partitioning only partially to possibly wrong soil moisture, thus it is likely that other uncertainties in the model (e.g., parameterisation of heat conductivity or stomatal resistance) also play a role in this problem. As soil characteristics are extremely varying over the LITFASS-domain, the representativeness of single micrometeorological stations for a 1 km model grid may also be questionable. Consequently, in the following the model run with the unmodified soil moisture is investigated, keeping in mind that the surface sensible heat flux in the model may be overestimated.

Evolution of the Boundary Layer

As a consequence of the cloud free conditions on 30 May 2003 the PBL over the LITFASS-domain shows an ideal diurnal evolution. On such an ideal radiation day, profiles of potential temperature and humidity are the key variables to describe the boundary layer processes, thus in the following the analysis is restricted to these variables. Figure 2.13 compares profiles of the COSMO model with radio soundings and profiles measured by the Helipod sonde (Bange et al., 2006). Radio soundings were made four times a day during the LITFASS-2003 campaign, while the Helipod profile was available only for 1030 UTC on 30 May. Former authors (e.g., Uhlenbrock, 2006) pointed out a possible cold and dry bias of the applied radio sounding instrument, thus the COSMO profile of 1100 UTC should be compared to the Helipod measurements.

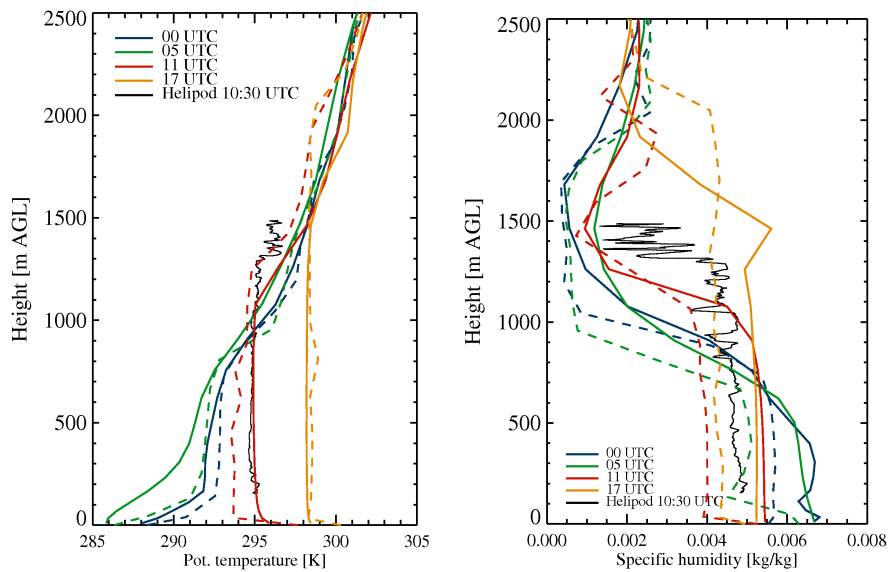


Figure 2.13: COSMO profiles (thick solid lines) of potential temperature (left) and specific humidity (right) compared to radio sounding measurements (thick dashed lines) and Helipod data (thin black line) on 30 May 2010.

The evolution of the potential temperature profile reveals a rapid nighttime cooling between 0000 and 0500 UTC. At 0500 UTC COSMO is considerably cooler in the near-surface layer (below 500 m AGL) as the radio sounding. This effect can most likely be attributed to the minimal diffusion coefficient applied in the turbulence scheme of COSMO, which results in overestimated turbulent transfer during nighttime and thus the erosion of the near-surface inversion. Daytime temperature and humidity profiles of both the measurements and COSMO show a well-mixed PBL. At 1100 UTC the temperature profile of COSMO is in good agreement with the Helipod measurement in the middle of the PBL, but the height of the boundary layer (capping temperature inversion) is underestimated by the model. At the same time the thickness of the entrainment zone is overestimated by the model, what later will be attributed to a too coarse vertical resolution at the PBL top (see Section 2.3.6). Generally, it can be concluded that COSMO simulates a too shallow and too moist boundary layer, which is surprising if we consider that the surface sensible heat flux is overestimated and the latent heat flux is underestimated by the model (cf. Figure 2.12). A possible explanation for this model behaviour is presented in Section 2.3.6.

Coherent structures in the PBL

In the following, the effect of surface heterogeneity on the COSMO simulation is investigated. It is expected that the largest impact could be observed in the PBL, which is directly affected

by the surface forcing. The study is restricted to daytime conditions, as the performance of COSMO during a stable case study is analysed separately.

Figure 2.14 shows two-dimensional horizontal plots of grid scale vertical wind at level 50 (approximately 800 m AGL) in COSMO-1 for two different simulations. First, the standard COSMO-1 run is presented with realistic, heterogeneous surface conditions. Second, a sensitivity run is shown, where all the surface parameters (land-sea mask, soil type, soil temperature and moisture) in the initial condition were set homogeneously to one single value on the whole model domain. For this, the COSMO-1 analysis values of the grid point nearest to the Falkenberg tower were used.

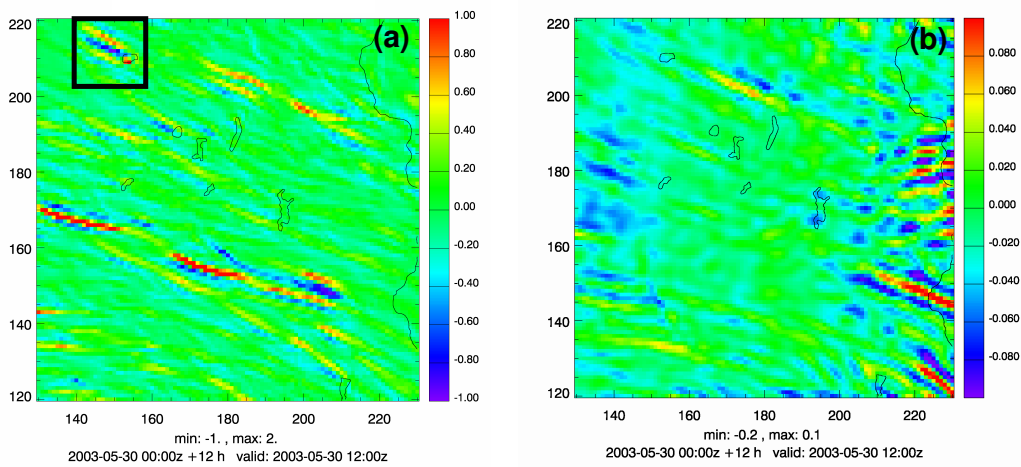


Figure 2.14: Horizontal plots of grid scale vertical wind speed (in m/s) at level 50 (approximately 800 m AGL) on 30 May 2003 at 1200 UTC (+12 h forecasts). COSMO-1 simulations with (a) heterogeneous (realistic) and (b) homogeneous surface conditions. Note the one order of magnitude difference in the colour scale between the two plots. Numbers on the axes indicate the distance in kilometres from the lower left corner of the domain. Thin black solid lines give the outlines of water bodies in the domain.

The heterogeneous run is characterized by organized up- and downdrafts in the PBL, which are aligned to the south-easterly mean horizontal wind. The amplitude of these PBL-waves is considerably large and can reach 1-2 m/s (grid scale values). The initiation of these strong perturbations is usually connected to abrupt changes in surface parameters, especially water bodies. The homogeneous sensitivity run simulates a less vigorous PBL with one order of magnitude smaller up- and downdraft velocities than in the case of the heterogeneous run. Consequently, these interesting PBL structures are caused by heterogeneous surface conditions. The main features of this “lake effect” are analysed in the following.

The effect of water bodies on the PBL structure is studied on a small lake close to Berlin (Grosser Muggelsee, approx. 4 km x 2 km), north-west from the LITFASS-domain (indicated with black rectangle on Figure 2.14a). Figure 2.15a again shows the grid scale vertical wind in the area of interest together with the horizontal wind at the lowest model level (10 m AGL).

This figure demonstrates that the flow patterns of the “lake effect” structures are coherent in the whole boundary layer. The downdraft on the lee side of the lake causes a divergent wind field on the surface, and thus the downdraft is compensated by updrafts on its both sides. The lee-side downdraft is triggered by the water body which is approximately 10 degrees colder than the surrounding soil (Figure 2.15b). Sensitivity experiments proved that the change in roughness length between water and land amplifies this PBL phenomenon, however, the main driving factor is the surface temperature difference (not shown).

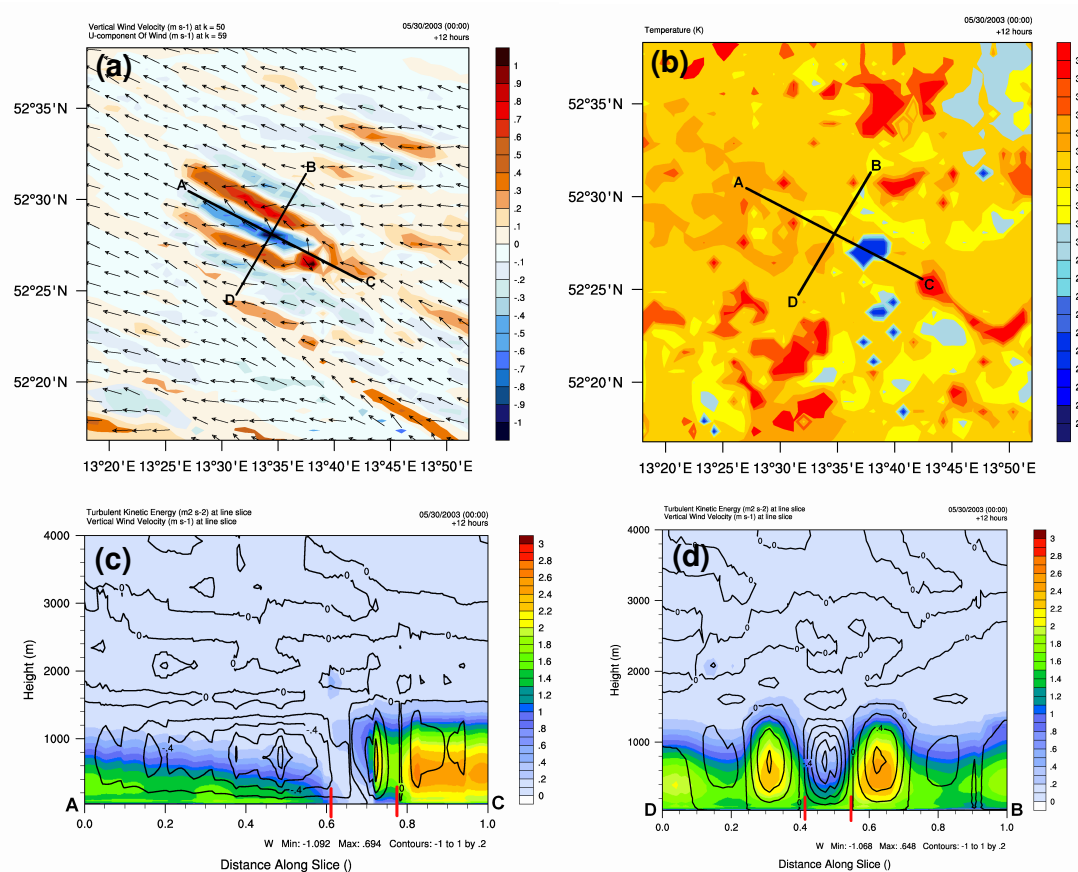


Figure 2.15: Investigation of the “lake effect” in the COSMO-1 simulation. All plots are for 30 May 2010 at 1200 UTC (+12 h forecasts). (a) Horizontal plot of the vertical wind at level 50 (shaded in m/s) and of the horizontal wind at the lowest model level (arrows), (b) Surface temperature (in K), (c) and (d) along wind and cross wind sections of the Turbulent Kinetic Energy field along the lines indicated on (a). Red lines on (c) and (d) indicate the position of the lake.

Figure 2.15c,d show along-wind and cross-wind sections of the Turbulent Kinetic Energy field. The stabilizing effect on the lee side of the lake is evident. TKE nearly vanishes over the lake surface and starts to grow slowly again over land. There is a considerable difference in the PBL height between the up- and downdraft regions as well. Over areas without PBL waves the average boundary layer depth is around 1200 m, which decreases to 600 m in the downdraft and grows up to 1500 m in the updraft regions (Figure 2.15d).

Investigation of the whole diurnal cycle of the simulation shows that the up- and downdrafts associated with water bodies are quite persistent features. The position of the structures changes only slightly during the course of the day following the direction of the horizontal wind. The PBL waves are starting to develop around 1100 UTC and their amplitude grows until around 1500 UTC when they are beginning to melt into each other.

It is interesting to investigate the sensitivity of the simulation of such structures towards the horizontal resolution of the model. Figure 2.16 shows the grid scale vertical wind simulated by the COSMO model at 2 km horizontal resolution. It is important to note that for this simulation the operational COSMO-2 configuration was used and consequently no horizontal diffusion (neither physical nor numerical) was applied.

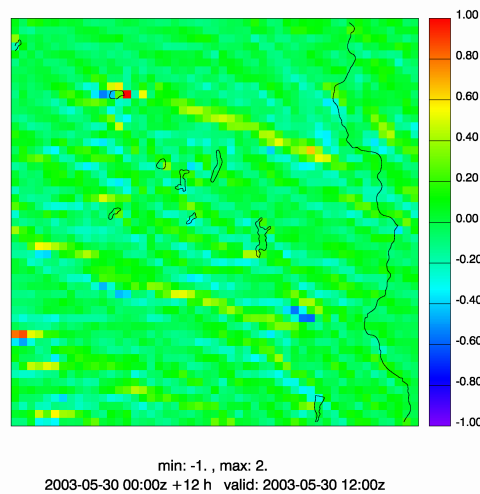


Figure 2.16: Same as Figure 2.14a, but simulated with 2 km horizontal resolution.

The wavelike structures are also present in the COSMO-2 run, but the amplitude of the waves is considerably reduced. Initiation of the up- and downdrafts is connected to water bodies in the 2 km simulation as well. The use of horizontal diffusion causes a slight smoothing in the prognostic fields of COSMO-2, but this effect is very weak (not shown).

2.3.5 Sensitivity to horizontal diffusion

In this Section the sensitivity of the COSMO-1 simulation towards the horizontal diffusion is studied. In particular, the impact on the above described PBL waves is investigated. As mentioned before, for the standard COSMO-1 simulations presented above, the isotropic three-dimensional turbulence scheme was applied (further referred to as the “3D_diff” run). In the following, two other methods, namely the numerical horizontal diffusion and the Smagorinsky closure are tested for the LITFASS-2003 case.

Numerical horizontal diffusion

As described in Section 1.2, in the COSMO model there is an option to apply a fourth order numerical filter in the horizontal direction for the prognostic variables. The purpose of this filter is to smooth the prognostic fields and remove small scale disturbances from the solution. Therefore, it is expected that the numerical horizontal diffusion has a similar effect on the PBL waves as the horizontal part of the three-dimensional turbulence scheme.

To test this hypothesis, first a control run was made without any horizontal diffusion in the inner part of the domain (Figure 2.17a). However, a relatively strong numerical horizontal diffusion had to be applied at the model boundaries (on a frame about twenty grid points wide) to damp unphysical waves which arise due to the lateral coupling with the driving model. It is important to note that this configuration is applied operationally at MeteoSwiss for COSMO-2. Without horizontal diffusion the simulated PBL in COSMO-1 shows quite unrealistic features with grid scale vertical winds on the order of 10 m/s. Next to the increase of the amplitude, the wavelength of the PBL waves is reduced, thus the simulation shows a rather noisy picture in the PBL. It is interesting to note that the vertical profiles of temperature, humidity and horizontal wind hardly change if compared to the standard COSMO-1 run presented above (not shown).

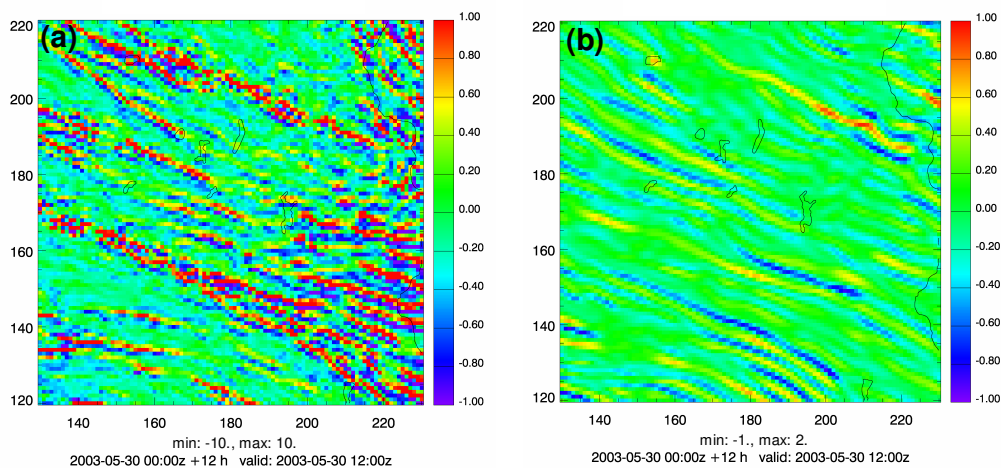


Figure 2.17: Same as Figure 2.14a, but for COSMO-1 run with the one-dimensional (vertical) turbulence scheme (a) without and (b) with numerical horizontal diffusion.

Figure 2.17b shows the simulated vertical wind field of COSMO-1 when applying numerical horizontal diffusion (further referred to as the “num_diff” run). The numerical filter was applied to all possible prognostic model variables (wind components, pressure, temperature and humidity), with a relatively high coefficient (0.75 in this case, which is the same value as applied on the model boundary). Due to the numerical filter, the amplitude of

the PBL waves is significantly reduced (with one order of magnitude) and the wavelength is increased, if compared to the control run without any horizontal diffusion (Figure 2.17a). It has to be noted that the “num_diff” run shows a qualitatively similar picture to the “3D_diff” run, as presented above (Figure 2.14a). However, in the case of the “num_diff” run the amplitude of the PBL waves is hardly changing over the domain of interest, while in the case of the “3D_diff” simulation “dominant” waves can be observed which are caused by the “lake effect”, as described above. In the case of the “num_diff” run the initiation of the PBL waves cannot clearly be correlated to the surface inhomogeneities.

Comparing these results with the COSMO-2 simulation (Figure 2.16), it can be concluded, that by increasing the horizontal resolution from 2 to 1 km, the importance of horizontal diffusion significantly increases. Consequently, it is worth to study this feature of the COSMO-1 simulation in more details. One possibility is, to test another scheme for horizontal diffusion, which is discussed in the following.

Smagorinsky closure for horizontal diffusion

The first order closure of Smagorinsky et al. (1963) was one of the first schemes applied for horizontal diffusion in a numerical weather prediction model. Several state-of-the-art NWP models still apply this scheme to calculate the turbulent diffusion coefficients in the horizontal direction. In the Weather Research and Forecasting Model (Skamarock et al., 2005) the Smagorinsky closure can be chosen optionally as an alternative to the fourth-order numerical diffusion scheme. After calculating the diffusion coefficient, the horizontal flux divergence is calculated explicitly. In most applications of the WRF model at 1 km resolution, this horizontal diffusion scheme is used together with a PBL parameterization in the vertical direction (Belusic and Güttler, 2010). In the Unified Model (Lean et al., 2008) a hybrid approach is used, where the coefficients for the fourth-order numerical diffusion are inferred from the Smagorinsky closure.

In the current version of the COSMO model there is an option to use an isotropic three-dimensional turbulence scheme where the diffusion coefficients are calculated with a Smagorinsky-like closure approach (Herzog et al., 2002). This scheme was developed in the framework of the LLM (LITFASS-Lokal-Model) Project, and consequently, its use is recommended with mesh sizes on the order of 100 m. To investigate the sensitivity of COSMO-1 towards the horizontal diffusion, the option to use the Smagorinsky closure in the horizontal direction independently of the vertical turbulence scheme was implemented and tested. In the following, some details of the implementation are described, followed by results for the LITFASS-2003 case.

The original Smagorinsky closure calculates the diffusion coefficient for momentum as a function of a length scale and the horizontal shear of the horizontal wind:

$$K_{Mh} = C_s^2 l^2 \left[\left(\frac{\partial u}{\partial y} + \frac{\partial v}{\partial x} \right)^2 + \left(\frac{\partial u}{\partial x} - \frac{\partial v}{\partial y} \right)^2 \right]^{\frac{1}{2}}, \quad (2.10)$$

where K_{Mh} is the horizontal diffusion coefficient for momentum, C_s is the Smagorinsky coefficient, with a typical value of 0.25, u and v are the zonal and meridional wind components and the length scale (l) is usually equal to the horizontal mesh size of the model.

In the terrain following coordinates of the COSMO model the metric terms also have to be taken into account when computing the components of the deformation tensor in Equation 2.3. This has been done by using the previous results of Baldauf (2006). After calculating K_{Mh} , the diffusion coefficient for heat (K_{Hh}) and scalars can be calculated using the Prandtl number (P_r):

$$K_{Hh} = \frac{K_{Mh}}{P_r}, \quad (2.11)$$

where the numerical value of P_r is set to 1/3 according to Deardorff (1972). After obtaining the horizontal diffusion coefficients the horizontal flux divergences are calculated explicitly, as in the case of the isotropic three-dimensional turbulence scheme used in the reference run of COSMO-1.

The newly implemented Smagorinsky closure was tested on the LITFASS-2003 convective case, with the operational TKE closure being used in the vertical direction. Figure 2.18 shows the structure of the simulated grid scale vertical wind in the boundary layer. Comparing this result to the previous experiments it can be concluded, that the Smagorinsky closure produces very little mixing in the horizontal direction. The wavelength of the PBL waves hardly changes as compared to the run without any horizontal diffusion. The amplitude of the waves is slightly reduced (from 10 m/s to 3 m/s), but is still unrealistically high.

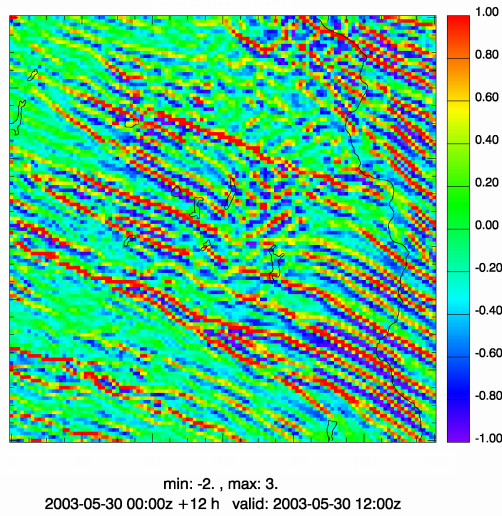


Figure 2.18: Same as Figure 2.14a, but the horizontal diffusion coefficients calculated using the Smagorinsky closure.

The reason for the minor effectiveness of the Smagorinsky closure is that the horizontal shear of the horizontal wind is nearly negligible in the present case, which is characterized by flat synoptic conditions. Figure 2.19 shows the diffusion coefficients for momentum for the vertical and horizontal directions as simulated by COSMO-1.

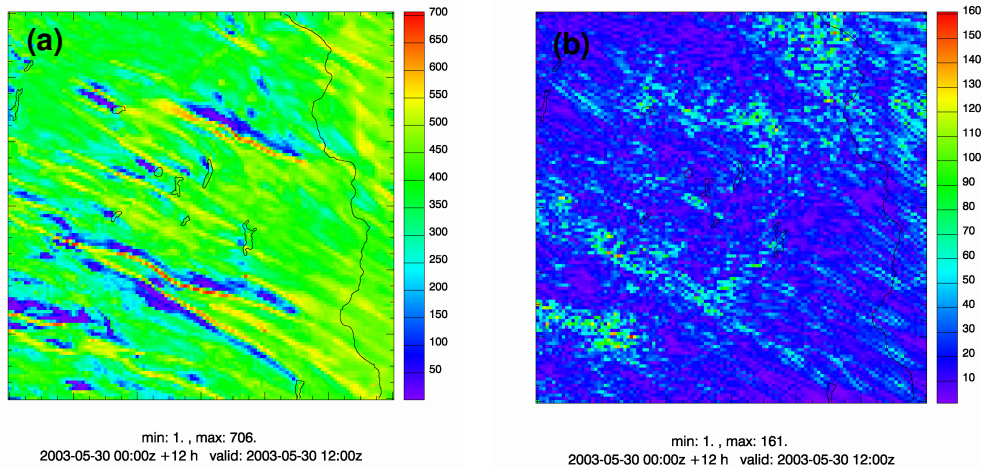


Figure 2.19: Horizontal plots of (a) vertical and (b) horizontal diffusion coefficients for momentum (in m^2/s) at level 50 (approximately 800 m AGL) in the COSMO-1 simulation which applies the operational TKE closure in the vertical and the Smagorinsky closure in the horizontal direction. Note the different colour scales.

It can be seen that the vertical turbulence scheme predicts an average diffusion coefficient of some $400 \text{ m}^2/\text{s}$ while the coefficients calculated by the Smagorinsky closure are one order of magnitude lower. The reference COSMO-1 run with the isotropic three-dimensional turbulence scheme uses the diffusion coefficients on Figure 2.19a in the horizontal direction,

while the run with the Smagorinsky closure uses the values on Figure 2.19b in the horizontal direction. This significant difference in the diffusion coefficients results in the notably diverse PBL simulation of the two COSMO runs. Based on these findings it might be worth to consider the inclusion of the horizontal shear of the vertical wind in the formulation of the Smagorinsky scheme by NWP models with 1 km horizontal resolution. However, this development is beyond the scope of the present study.

2.3.6 Analysis of the TKE budget

As shown above, the COSMO simulation of the selected convective day is characterized by a too cold (if we take into account the possible cold bias of the radio sounding), too moist and too shallow PBL (Figure 2.13). This is even more surprising if we consider that the surface sensible heat flux is overestimated and the surface latent heat flux is underestimated by the model (Figure 2.12). Thus it seems very likely that some kind of heat input to the PBL is missing in the COSMO simulation. In the following this problem is investigated by the component testing of the turbulence scheme, and a possible solution is proposed.

Figure 2.20a depicts the profile of Turbulent Kinetic Energy simulated by COSMO-1 (reference “3D_diff” run with 60 vertical levels), as compared to the LES profile. The drawbacks of the COSMO simulation are similar to those described for the ideal convective case (Section 2.2), namely, the shape of the simulated TKE profile has a pronounced maximum in the middle of the PBL, while LES results suggest a more well-mixed distribution. The reason for the wrong TKE profile is highlighted by Figure 2.20b, where the terms of the TKE budget are plotted separately. The turbulent transport term (which accounts for the vertical diffusion of TKE) is too weak as compared to the Large Eddy Simulation, what is attributed to the simple down gradient approach in the parameterization of this term. Apart from the wrong vertical distribution of TKE this fact has another considerable effect. TKE cannot be transported upwards to the PBL top, thus no mixing occurs in the capping inversion and the entrainment flux in the COSMO simulation is missing. The missing entrainment of relatively warm and dry air from the free atmosphere could be the reason of the too cold and too moist PBL in COSMO.

The problem arising in the TKE budget of COSMO can also be observed in the comparison with the tower turbulence measurements. For this, first the TKE budget terms had to be computed from the raw turbulence dataset, which consists of high frequency (13 Hz) measurements of the wind components, temperature and humidity at 50 and 90 m height above ground level.

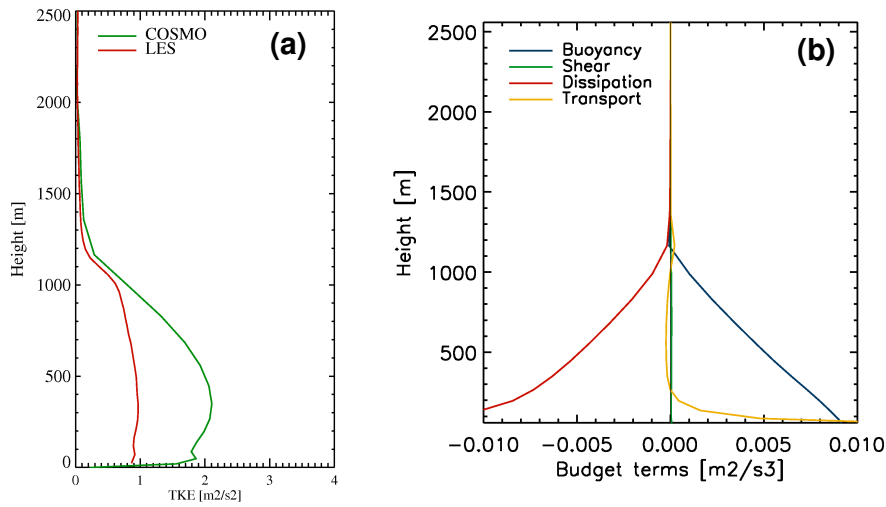


Figure 2.20: Simulated vertical profiles at on 30 May 2003 at 1200 UTC for the location of the Falkenberg tower. (a) Profiles of TKE simulated by the “3D_diff” COSMO-1 run with 60 vertical levels (green) and by the LES model (red). (b) Profiles of the TKE budget terms in COSMO-1.

The dissipation term was computed from the power spectrum of turbulence with a post-processing program developed at University Basel (Christen et al, 2009). All the other budget terms were computed with a modified version of the TK2 program from University of Bayreuth (Mauder and Foken, 2004).

Figure 2.21 presents time series of TKE and the budget terms in the TKE equation for the location of the Falkenberg tower. Time series of the LES values are also indicated for the time interval between 1200 and 1900 UTC.

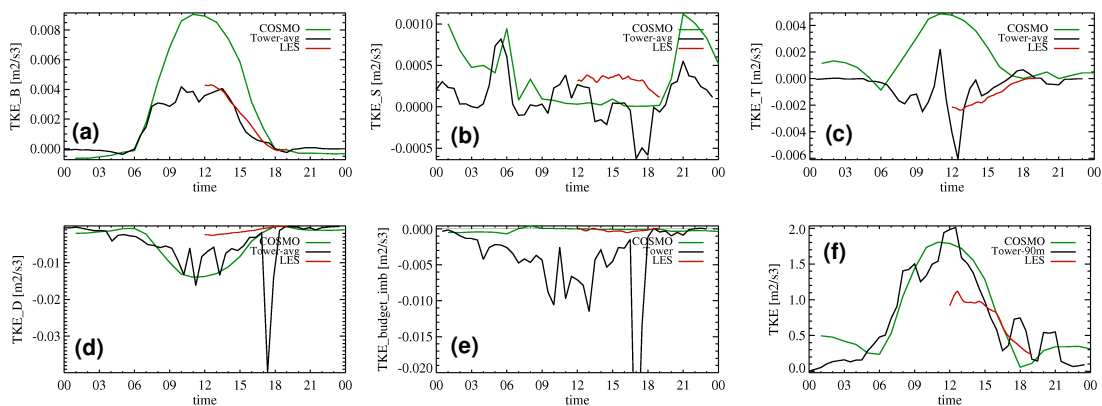


Figure 2.21: Time series of the TKE (f) and its budget terms: buoyancy production or destruction (a), shear production (b), turbulent transport (c), dissipation (d) and budget imbalance (e). “3D_diff” COSMO-1 (green), measurement (black) and LES (red) time series between 30 May 2003 0000 UTC and 31 May 2003 0000 UTC, at 70 m height (averaged values from 50 m and 90 m measurements).

The diurnal cycle of TKE is generally well predicted by COSMO-1. However, there is a considerable overestimation in the first hours of the simulation. As it can be noticed also on

Figure 2.20b, the shear production term during daytime is negligible in the TKE budget for the selected day. The buoyancy production is overestimated by COSMO, which is explained by the overestimated surface heat flux. The absolute values of the dissipation term calculated from measurements are much larger than the values predicted by LES, which might be attributed to a measurement problem rather than the error of the post-processing program (see further in Section 2.4.2). Because of the possibly wrong dissipation rates the measured TKE budget is not closed.

Most problematic is the simulation of the transport term, which has a different sign and nearly the same amplitude as in the measurements and LES data. This shows that the local down-gradient approach, which is used to parameterize this term, completely fails in such a strongly convective case. In COSMO the turbulent transport term is a source term near the surface (at 70 m height), because TKE, which has a maximum near the middle of the PBL, is diffused downwards from this maximum height according to the down-gradient approach. However, in a real convective boundary layer TKE is transported by large eddies – strongly non-local phenomena – from the surface upwards, which results in the negative sign of this term in the measurements. In the following, two attempts are presented to improve the TKE budget in the COSMO model.

Higher vertical resolution

As described in Section 1.2, the COSMO model utilises a vertically stretched coordinate system, which has the finest vertical resolution near the surface and the level thickness grows with height. With the operational 60 vertical levels, the level thickness is 20 m near the surface, but rapidly grows to more than 200 m at 2000 m above ground level, at the height of the capping inversion in this case. One possibility to enhance the entrainment flux at the PBL top would be to increase the vertical resolution of the model at higher levels, which might lead to a better description of boundary layer processes. Consequently, for the present case study a new vertical level distribution was tested with 74 vertical levels and a more uniform level thickness in the PBL. It has to be noted, that with the increased vertical resolution the explicit handling of the TKE diffusion is not plausible any more (see Section 2.2.1), and thus an implicit formulation was applied for this term.

Vertical profiles of potential temperature and TKE, as well as the TKE budget terms from this COSMO-1 simulation are depicted on Figure 2.22.

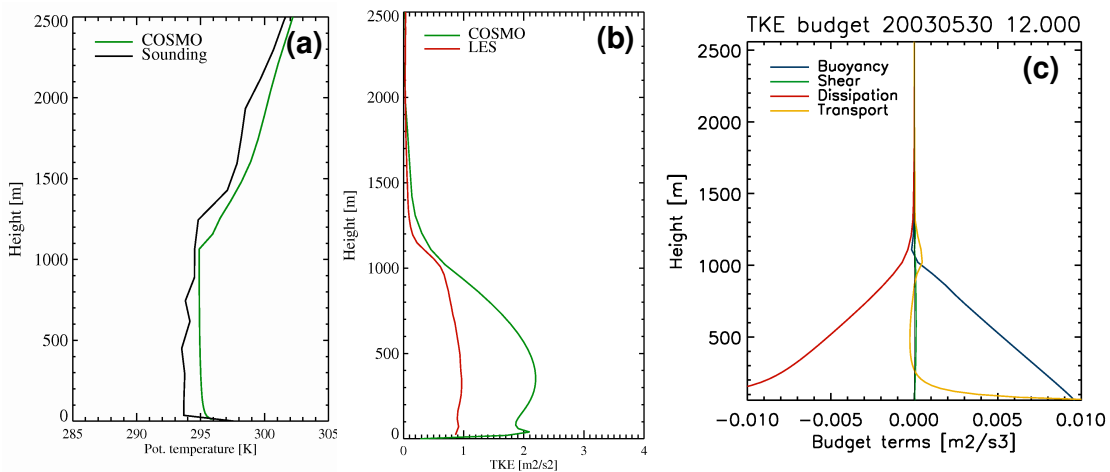


Figure 2.22: Simulated vertical profiles at on 30 May 2003 at 1200 UTC for the location of the Falkenberg tower. (a): Profiles of potential temperature from the radio sounding measurement (black) and simulated by the COSMO-1 run with 74 vertical levels (green). (b) Profiles of TKE simulated by COSMO-1 (green) and by the LES model (red). (c) Profiles of the TKE budget terms in COSMO-1.

Comparing the potential temperature profile with the reference run (Figure 2.13), it can be noted that the PBL height is still underestimated. However, the thickness of the capping inversion is significantly reduced and is much closer to the entrainment zone thickness detected by the radio sounding. Nevertheless, profiles of TKE and the TKE budget terms show the same problems as the reference run with 60 vertical levels. This implies that increasing the vertical resolution alone does not help to increase the turbulent transport of TKE and enhance the entrainment flux.

Increased TKE diffusion

The major deficiency of the 1.5-order closure framework in describing the inherently non-local nature of the convective boundary layer (CBL) has been pointed out from a very early stage of PBL research (e.g. Deardorff, 1966, 1972; Schumann, 1987). To overcome the problem of the so-called counter-gradient heat flux, which is an essential feature of the CBL, two main approaches are followed. Either a mass-flux approach is implemented to account for the non-local transport, or a counter-gradient term is applied by the computation of the heat flux, retaining the 1.5-order closure framework. A comprehensive overview of these approaches can be found in Mironov (2008) and in Tomas and Masson (2006).

In this work a more pragmatic approach is followed. A very simple possibility to increase the TKE diffusion is to keep the down-gradient formulation for the transport term but use a larger diffusion coefficient (α). The default numerical value of this coefficient is chosen as 0.2 in the COSMO model, but in the modelling community this coefficient is considered as a

tuning factor, the value of which might be adjusted in order to achieve better model performance.

As a first step, several sensitivity tests were conducted, in which the value of α was increased to 1.0, 2.0, 5.0 and 10.0 over the whole model domain. Significant differences from the run with the default value were observed only if values above 5.0 were used. Figure 2.23 shows profiles of TKE and the TKE budget terms for the run using $\alpha = 10.0$.

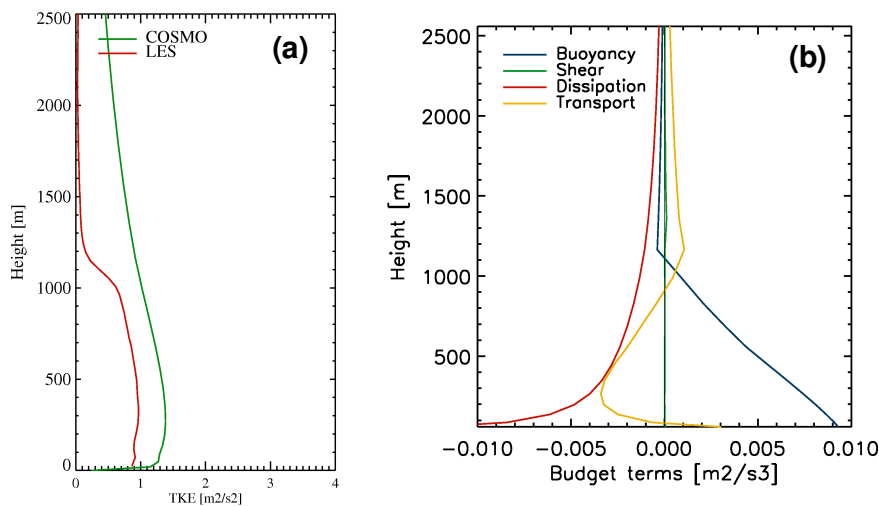


Figure 2.23: Same as Figure 2.20, but for the COSMO-1 simulation with increased TKE diffusion coefficient ($\alpha = 10.0$) on all levels.

The higher diffusion coefficient results in a significantly increased turbulent transport of TKE, especially in the lower part of the PBL, if compared to LES results. However, it has to be noted, that in both idealized and real-world LES runs the turbulent transport of TKE is restricted to the PBL, which is not the case for the COSMO simulation. In COSMO, the transport term has a long tail reaching far above the PBL top. Consequently, TKE is over-diffused and a PBL top is hardly recognisable in the TKE-profile of COSMO.

If we consider that the increase of the TKE diffusion coefficient was aiming at a better description of some non-local effects within the PBL, it is straightforward that this modification should be applied only in the PBL, where these non-local effects effectively take place. Thus in the second step, α was increased to 10.0 in the PBL only, and above the PBL top the default value of 0.2 was retained (Figure 2.24). For the determination of the PBL height the bulk Richardson number was used (Szintai and Kaufmann, 2008). The long tail of the TKE transport term disappears in this run and the budget terms show a much better similarity to the LES results than in the case of the reference simulation (Figure 2.20b). The PBL height estimated from the TKE profile increases by 500 m and is in good agreement with the PBL height estimated from the radio sounding. TKE in the boundary layer is well-mixed and its shape is closer to the LES profile.

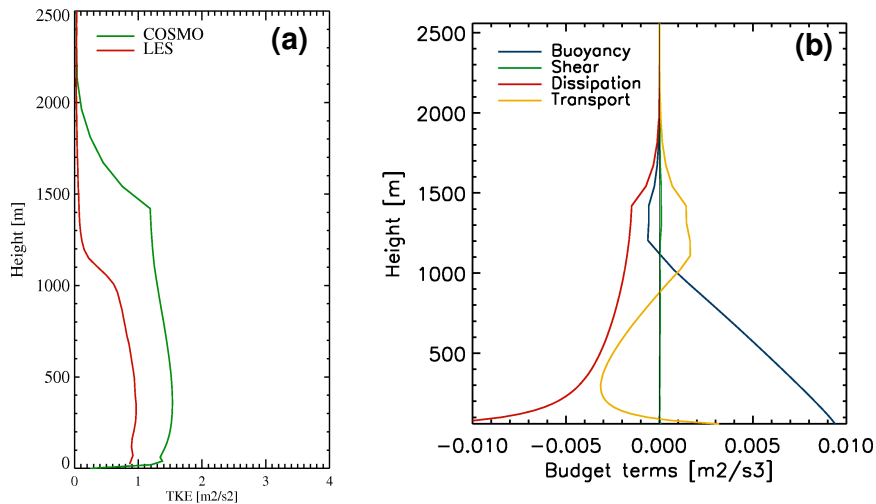


Figure 2.24: Same as Figure 2.20, but for the COSMO-1 simulation with increased TKE diffusion coefficient only in the PBL.

The entrainment flux also increases to some extent as compared to the reference run. However, it is still lower than the values suggested by LES. Due to the still low entrainment flux, profiles of temperature and specific humidity do not significantly change in the experiment with increased TKE diffusion. Nevertheless, the better profile of TKE alone might be a reason for further investigations in this topic. It is interesting to note that the application of other PBL height formulations for the determination of the highest level of the increased diffusion coefficient leads to significantly different – and worse – results (not shown). The experiments performed at the German Weather Service (Ekaterina Machulskaya, personal communication) showed that neither the TKE profile, nor the heat flux profile as PBL height indicator gives better results.

The above described modification also has an impact near the surface, which can be observed on the comparison with tower time series (Figure 2.25). The high positive values of the transport term seen on Figure 2.21 are somewhat corrected. Consequently, the dissipation rates predicted by COSMO are also closer to the LES values (as mentioned above, the measured dissipation rates are deemed to be problematic in this case). As the budget of TKE is closed in COSMO for the daytime hours, smaller positive values of the transport term cause the TKE to decrease.

It is interesting to compare the results related to the TKE budget terms to the previous work of Ament (2006), who already performed 1 km COSMO simulations for the LITFASS-2003 campaign.

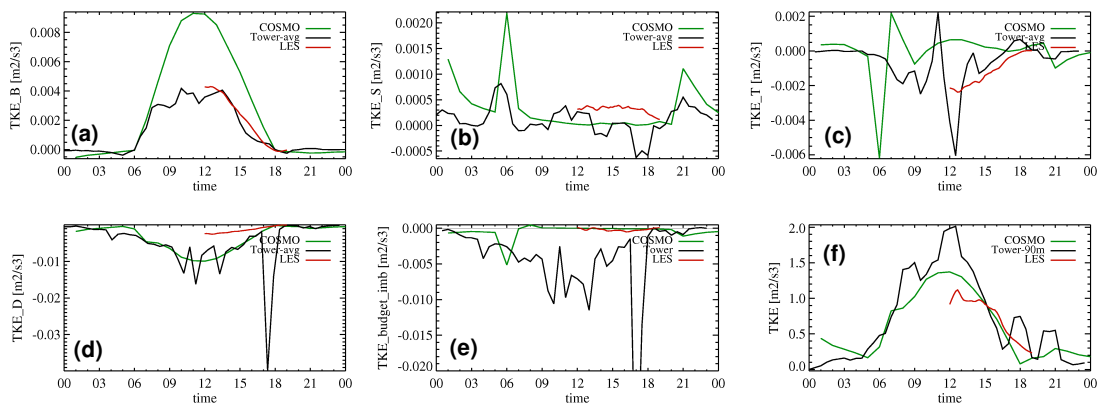


Figure 2.25: Same as Figure 2.21, but for the COSMO-1 simulation with increased TKE diffusion coefficient only in the PBL.

In this work it was concluded that the entrainment flux is seriously underestimated by COSMO. The proposed solution for this problem was to decrease the activity of the turbulence scheme (by reducing the master length scale) and see whether COSMO is able to resolve the missing entrainment flux on the grid scale. It was found that even with 1 km horizontal resolution it is not possible to produce entrainment fluxes at the PBL top, which implies the necessity for a relatively active subgrid-scale turbulence scheme. The modifications in the turbulence scheme of COSMO proposed in the present work account for at least a certain part of the missing entrainment flux.

2.3.7 Verification of a longer period

The above described modifications were also tested on a longer continuous time period using both COSMO-7 and COSMO-2. The selected period starts on 1 July 2009 and lasts for 27 days. The period is characterized by mostly flat convective conditions with a pronounced daily cycle of afternoon showers. The main goal of the experiment is to investigate whether the increased TKE diffusion has an impact on the amount and timing of convective precipitation. It has to be noted that the increased TKE diffusion leads to higher TKE fluxes in the model, thus to achieve a stable model performance the TKE diffusion term should be calculated implicitly (see Section 2.2.1). To be able to investigate the impact of these two modifications separately, two consecutive parallel experiments were performed:

- Experiment **504**: reference run
- Experiment **503**: same as 504 but the TKE diffusion term is calculated implicitly
- Experiment **502**: run with enhanced TKE diffusion ($\alpha = 10.0$ in the PBL), using the implicit formulation in the TKE diffusion term

All the three experiments were started from their own separate assimilation cycle. During the assimilation radar precipitation products were not assimilated. As the operational vertical level distribution with 60 levels is assumed to have layers which are thick enough not to cause numerical instabilities with the unmodified TKE diffusion, experiments 504 and 503 are expected not to differ significantly.

The forecasts of the three experiments were evaluated with different verification techniques:

- SYNOP messages from the whole European domain were used to compute standard point-to-point verification scores.
- Upper-air observations (TEMP messages) were applied to verify the forecasted model profiles.
- Forecasted precipitation fields were compared to Radar measurements using the neighbourhood verification technique.
- Radio sounding measurements were used to diagnose observed PBL heights which were compared to the forecasted PBL height field of the COSMO model.

The SYNOP verification results show a mostly neutral impact of the modifications on the model performance. The most notable impact is on the total cloud cover (Figure 2.26). As expected experiments 504 and 503 are very similar, but experiment 502 gives higher cloud cover in the afternoon hours, which improves the forecast. This effect is also present in COSMO-2, but is more significant in the COSMO-7 forecasts.

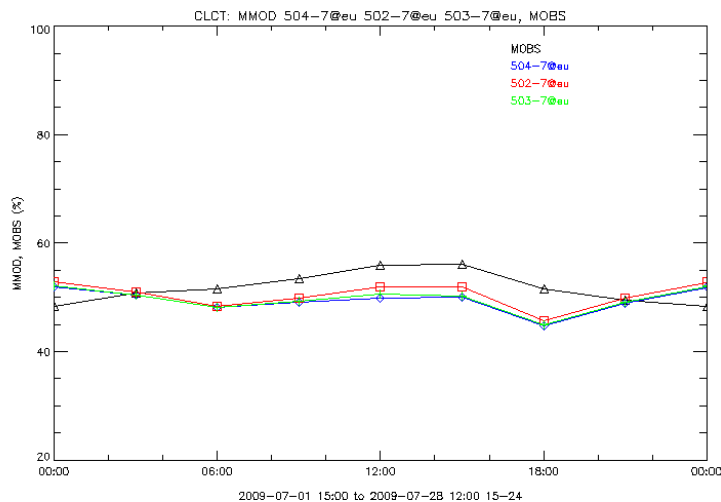


Figure 2.26: The mean daily cycle of observed (black line) and modelled (coloured lines) total cloud cover between 1 July 2009 and 27 July 2009. Always the first 24 hours of the COSMO-7 forecast was verified on the whole European domain. The different model experiments are described in the text.

The overall verification results of forecasted atmospheric profiles against radio sounding measurements do not show a significant impact of the increased TKE diffusion. For certain stations a small impact on the temperature and humidity profiles can be seen at the height of the entrainment zone for the 1200 UTC sounding, however, these impacts are smoothed out if all the measurement stations are verified together.

As it is rather difficult to verify convective precipitation using localized SYNOP messages, Radar measurements of precipitation were also applied to validate the COSMO forecasts. The evaluation was done for 3h accumulations for 0000 and 1200 UTC runs leaving out the first three hours. Details of the verification approach are given in Weusthoff et al (2010). Suffice here to say that different scores are analysed by successively increasing the spatial scale and the threshold (in mm/3 hrs for the present case). Lead times from +4 h to +15 h were evaluated for both models. For the ETS (Equitable Threat Score) and FSS (Fractions Skill Score) measures hardly any differences are detectable between the experiments (502, 503) and the reference version (504) (not shown). For the frequency BIAS between reference version and experiment 502 (Figure 2.27) some larger differences can be observed: for smaller thresholds the reference version tends to have better scores. However, for larger thresholds the experiment with enhanced TKE diffusion verifies better on certain spatial scales, especially for COSMO-2. For experiment 503 the scores are somewhat better than for experiment 502 in the case of COSMO-7. For COSMO-2, the two experiments perform similarly regarding the frequency BIAS score.

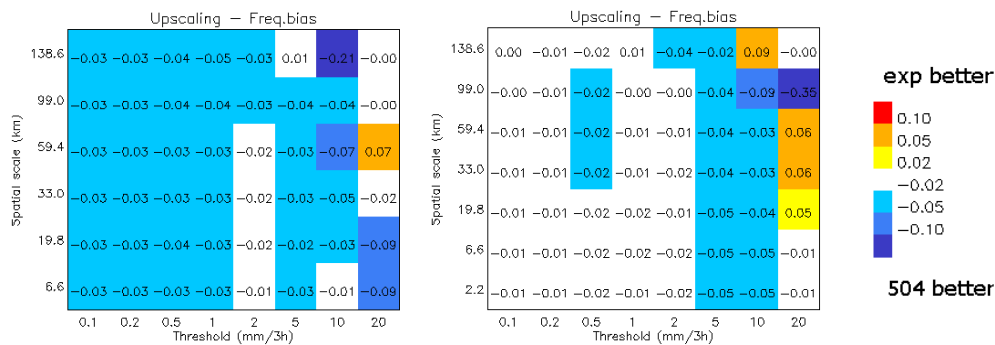


Figure 2.27: Neighbourhood verification (frequency bias score) of COSMO-7 (left) and COSMO-2 (right) precipitation forecasts using Radar measurements for the continuous period between 1 July 2010 and 27 July 2010. Lead times from +4 h to +15 h were evaluated for both models. The frequency bias difference is calculated between the reference version (504) and experiment 502.

The mean diurnal cycle of precipitation is better captured by COSMO-2, especially in the afternoon. The three experiments show again only slight differences, but the enhanced TKE diffusion (502) causes systematically less precipitation. For COSMO-7 this precipitation reduction deteriorates the forecast, but for COSMO-2 the modifications cause a slight improvement in the afternoon (Figure 2.28). It is also interesting that the modifications in the

turbulence scheme have a larger impact on the COSMO-7 forecasts where convection is parameterized as compared to COSMO-2 where convection is resolved explicitly. This is somewhat in contradiction with the expectation, which deems a stronger coupling between turbulence and convection is convection resolving models.

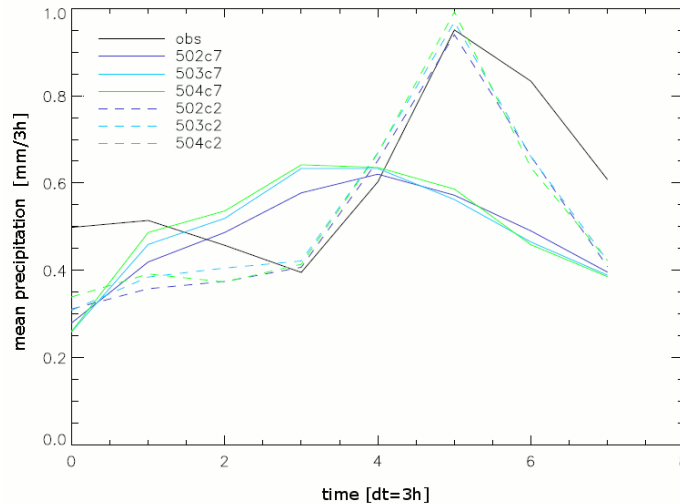


Figure 2.28: Mean diurnal cycle of Radar-observed (black line) and forecasted (coloured lines) precipitation for the continuous period. In the legend the first three digits indicate the experiment number, the last two digits the model version (c7: COSMO-7; c2: COSMO-2).

Based on the results of the case studies described in the previous sections, it is expected that the enhanced TKE diffusion also has an impact on the forecasted PBL height. Consequently, PBL height was also evaluated for the continuous period. COSMO forecasts were compared to PBL heights diagnosed from radio-sounding measurements. For the diagnosis of PBL heights, the bulk Richardson number method was used both for observations and model forecasts. Figure 2.29 shows time series of observed and simulated PBL heights for July 2009. All the three experiments generally overestimate the PBL height, but the impact of the modifications is negligible. For certain days, experiment 503 gives the lowest PBL height and thus the best forecast, but for most of the days the experiments are very close to each other. This result, together with the evaluation of atmospheric profiles, indicates that the modified TKE profile does not significantly modify the temperature and humidity profiles in the PBL. The reason for the missing coupling between TKE and other prognostic variables is unclear at the moment and would need further investigation that goes beyond the scope of the present work.

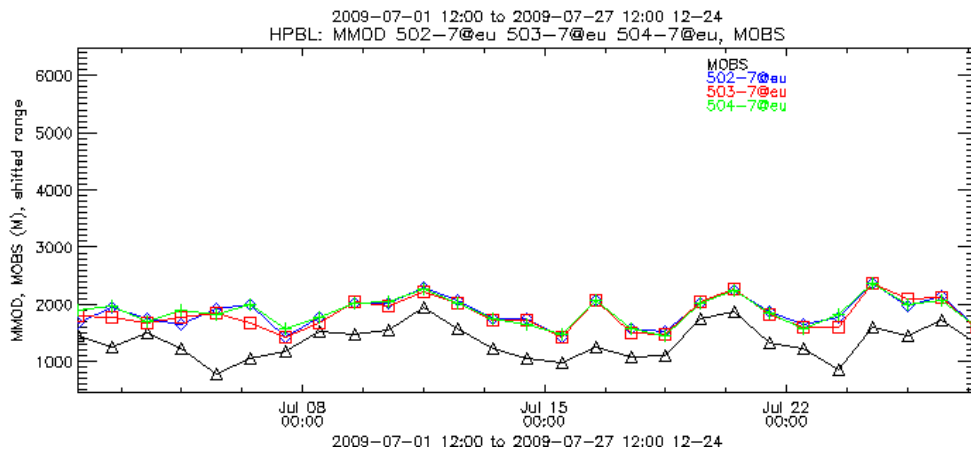


Figure 2.29: Observed and modelled PBL heights for the continuous period in July 2009. PBL heights diagnosed from 1200 UTC soundings are compared to +12 h forecasts of COSMO-7 for twelve radio sounding stations in Europe.

After analyzing the verification results it can be concluded that the enhanced TKE diffusion has only a neutral to minor impact on the verified fields of the COSMO model. A slight improvement can only be seen in the total cloud cover and in the afternoon convective precipitation. Similarly to the case studies, the prognostic TKE shows a more realistic profile during the continuous period: TKE near the PBL top is increasing (Figure 2.30).

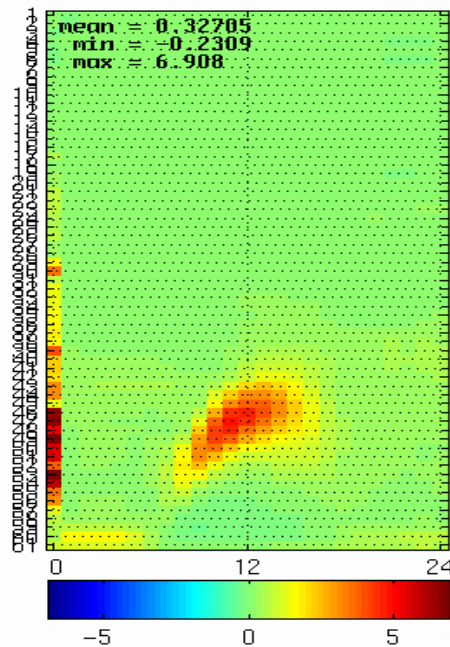


Figure 2.30: Domain averaged relative difference of the prognostic TKE between experiment 502 and the reference run (504) for 16 July 2009. On the x-axis the time (in UTC) is shown, on the y-axis the level numbers are depicted. The relative difference is indicated by the colour scale (e.g. a value of 5.0 indicates that the TKE value in experiment 502 was five times higher than in the reference).

As the COSMO model is used operationally to provide wind and turbulence input fields for dispersion models both by MeteoSwiss and the German Weather Service (DWD), and these profiles are based on TKE (at least in the operational version), this last result implies that it might be beneficial to apply these modifications also in the operational COSMO forecasts. However, it would be important to first understand why the modified TKE profile does not have a direct impact on other prognostic fields like temperature and humidity.

2.4 Simulation of a real, stable boundary layer with COSMO-SC

In the previous Sections the performance of the COSMO model during convective conditions was investigated. It was found that if the surface forcing is adequately represented, COSMO is able to correctly capture the main features of the evolution of the convective PBL. However, some major deficiencies were identified in the simulated budget of Turbulent Kinetic Energy, and a solution for this problem was proposed.

In the present Section the ability of the COSMO model in simulating the development of the Stable Boundary Layer (SBL) is investigated. Next to the testing of the turbulence scheme, the aim of the present experiment is to produce a controlled simulation and measurement dataset which can later be used to validate the input parameters of dispersion models (see Section 3.3).

2.4.1 Description of the GABLS3 experiment

For the testing of the model performance, the GABLS3 model intercomparison case was selected (Bosveld, 2008). GABLS stands for GEWEX Atmospheric Boundary-Layer Study, and focuses on a better representation of stable boundary layers in atmospheric models (Holtslag, 2006). In GABLS, both Large Eddy Simulation and Single Column models are participating. The first GABLS experiment was a highly idealized SBL case (Cuxart et al., 2006) with prescribed surface forcing. In this study, several single column models were compared to a set of Large Eddy Simulation results (Buzzi et al., 2010 present the results for COSMO-SC, which were obtained after the 'official' GABLS phase). The second GABLS case was selected from the CASES 99 field experiment and aimed at the simulation of a whole diurnal cycle (Svensson and Holtslag, 2007) (again, the COSMO-SC reproduced the case after the official intercomparison had terminated, Buzzi, 2008). This experiment showed the difficulty of comparing single column models to field measurements. One of the main

conclusions was that great care has to be taken in selecting the case study and it is inevitable to prescribe correct boundary conditions for the single column models.

The third GABLS case was selected from the long measurement time series of the Cabauw measurement site in the Netherlands. Special care was taken to choose a case with possibly constant or slowly changing geostrophic wind. The selected case starts on 1 July 2006 at 1200 UTC and lasts 24 hours. During night time a stable boundary layer develops with a pronounced low-level jet (LLJ) around 200 m above ground level, which is caused by the decoupling from the surface and an inertial oscillation (Basu et al. 2010). After 0300 UTC the LLJ loses its strength and at 0600 UTC a convective boundary layer starts to grow.

To validate the single column and Large Eddy Simulation models, various observations were available. A 200 m tower is in operation at the site with wind, temperature and humidity measurements at several heights. Sonic anemometers were also mounted at 5, 60, 100 and 180 m heights, measuring turbulence characteristics. Radio sounding measurements were conducted four times a day, complemented by windprofiler measurements. Surface variables, like surface radiation budget and turbulent fluxes between the surface and atmosphere were also measured.

The main drawback of using measurements for the validation of the turbulence scheme of COSMO is the limited vertical resolution of the measured turbulence characteristics. Because of this, information from Large Eddy Simulation models was also used. In the LES intercomparison for the GABLS3 case eleven groups participated. The LES setup was slightly idealized, with prescribed surface cooling rates, and only night time and morning hours between 0000 and 0900 UTC were simulated. LES models used an isotropic resolution of 6.25 m and the simulation domain was 800 m × 800 m × 800 m. Until now, the exact dataset from one group was available for the present study, results from other groups can be found in Basu et al. (2010).

The COSMO-SC simulation for the GABLS3 case was conducted by Matthias Raschendorfer and Jürgen Helmert at the German Weather Service (DWD). The task of the author was to compare the simulation results with turbulence measurements and LES data, and to compute and analyse the TKE budget terms. As for all the participating single column models, a soil model coupled to the atmospheric model was used, and initial soil moisture was adjusted to obtain a Bowen ratio of 0.33 at the beginning of the simulation. Initial profiles, changing geostrophic wind, horizontal and vertical advective tendencies were prescribed for the case. Table 2.1 summarizes the differences in the COSMO model setup between the GABLS3 case and the operational settings at MeteoSwiss.

Table 2.1: Details of the model configuration for the GABLS3 experiment and for the operational COSMO model at MeteoSwiss (both COSMO-7 and COSMO-2).

	GABLS3 (COSMO-SC)	MeteoSwiss oper. (COSMO-7, COSMO-2)
Vertical levels	40	60
First full model level [m]	10	10
K_min [m²/s]	0.01	1.0
Explicit humidity corr.	not used	used
Pattern length [m]	1.7	500.0

Main differences between the GABLS3 setup and the operational MeteoSwiss settings are in the number of levels in the boundary layer, the minimum diffusion coefficient, and the parameter controlling the circulation terms (“Pattern length”).

2.4.2 Simulation of the SBL evolution

In the following, the performance of the COSMO model in simulating the whole diurnal cycle is investigated, with special attention to the night-time Stable Boundary Layer. After the validation of the surface forcing, the profiles of mean variables and TKE are presented, followed by the analysis of the TKE budget.

Figure 2.31 depicts the time series of measured and modelled surface sensible and latent heat fluxes. It has to be noted that the modelled Bowen ratio in the first four hours of the simulation is smaller than the measured value, which is attributed to a dry air advection in the area of the measurement site in reality. However, it is assumed that this initial inconsistency does not have a major effect on the simulation of the SBL after 1800 UTC.

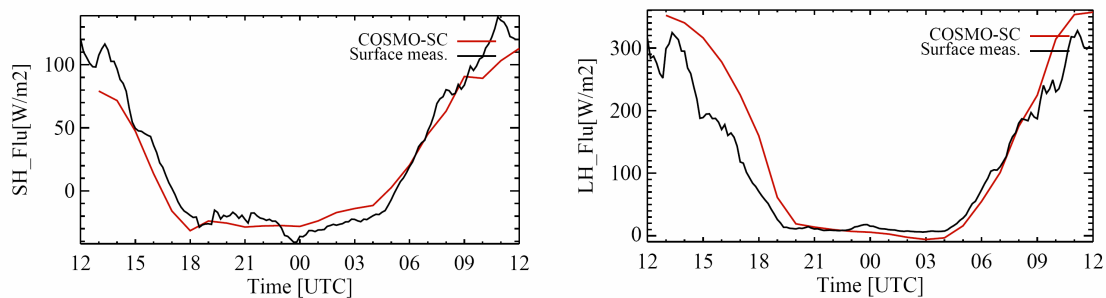


Figure 2.31: Time series of surface sensible (left) and latent (right) heat fluxes of the COSMO model (red) compared to measurements (black) for the GABLS3 experiment between 1 July 2006 1200 UTC and 2 July 2006 1200 UTC.

In the night time hours the surface fluxes of sensible and latent heat are simulated adequately, and the sign change of the sensible heat flux during the morning transition is well captured.

One of the main challenges of single column models is to correctly simulate the height and intensity of nocturnal low-level jets (Buzzi, 2008). As mentioned before, the GABLS3 case was characterized by a strong LLJ, with a peak intensity around 0000 UTC and a dissolution around 0500 UTC. Figure 2.32 presents the measured and modelled profiles of horizontal wind speed and potential temperature. Between 0000 and 0300 UTC the LLJ peak in the measurements is sinking from 200 m to 100 m and its intensity is decreasing from 13 m/s to 9 m/s. COSMO is able to reproduce the decreasing intensity of the LLJ, however, the height of the LLJ is nearly constant in COSMO between 0000 and 0300 UTC. The profiles of potential temperature show an overestimated cooling rate in COSMO, which results in the underestimation of temperature of about 2 K in the lowest 100 m. The evolution of the temperature profile and the intensity of the LLJ is well simulated by the LES model. Still, the decreasing height of the LLJ peak is badly reproduced, similarly to COSMO.

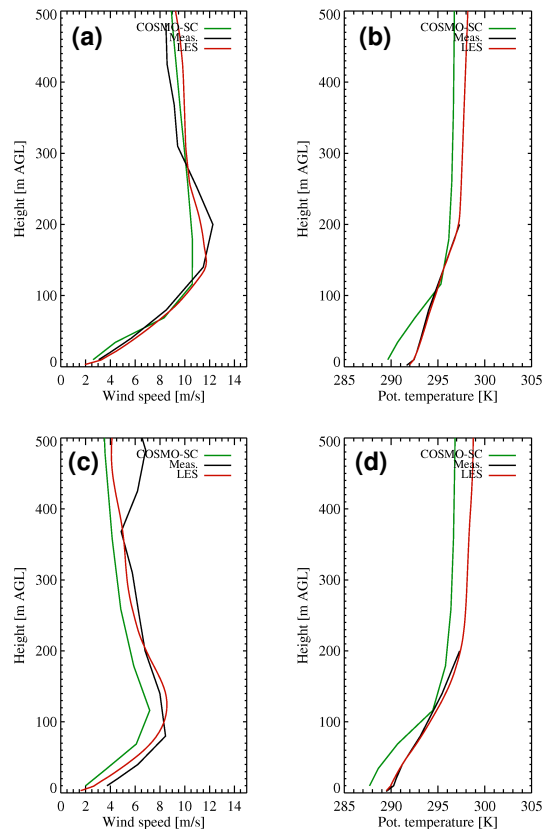


Figure 2.32: Profiles of horizontal wind speed (a and c) and potential temperature (b and d) on 2 July 2006 at 0000 UTC (a and b) and at 0300 UTC (c and d). COSMO profiles (green) are instantaneous values, measured (black) and LES (red) profiles are centred one hour averages. Below 200 m height the tower measurements, above 200 m the windprofiler data are used.

Figure 2.33 shows profiles of Turbulent Kinetic Energy from COSMO compared to tower observations and LES data. From LES, only the resolved part of TKE is available, thus LES values are lower than the measured TKE. Generally it can be concluded that the shape of

the TKE profile is accurately simulated by COSMO below the low-level jet. However, TKE is slightly overestimated at 0000 UTC near the surface. Above the LLJ peak at 0300 UTC, the simulated TKE profile significantly deviates from the measured values. Apparently, COSMO is unable to simulate the pile-up of turbulence above the LLJ, which is an indication of an upside-down boundary layer and is assumed to be generated by wind shear (Mahrt and Vickers, 2002). As shown by Basu et al. (2010), LES models also seem to have difficulty in modelling this SBL phenomenon.

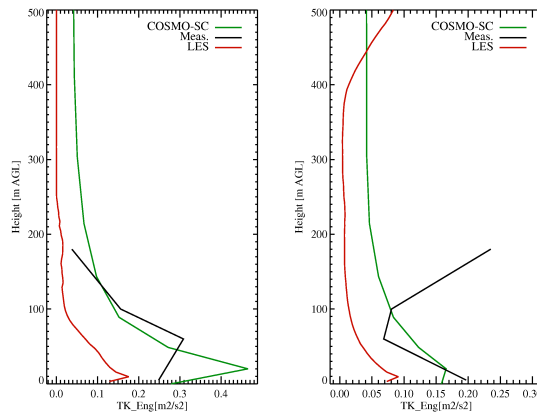


Figure 2.33: Profiles of TKE on 2 July 2006 at 0000 UTC (left) and at 0300 UTC (right). COSMO profiles (green) are instantaneous values, measured (black) and LES (red) profiles are centred one hour averages. Note that LES TKE only contains the resolved-scale partition of TKE.

In Section 2.3.6, the budget of Turbulent Kinetic Energy in the COSMO model was compared to observations and LES data for a convective case. In that experiment some major deficiencies in the TKE budget of COSMO were identified, and a measurement problem related to the dissipation rate was also detected. In the following, the same exercise is repeated for the GABLS3 stable case. However, COSMO time series are only compared to measurements, as it was not possible to derive all the TKE budget terms from the LES dataset.

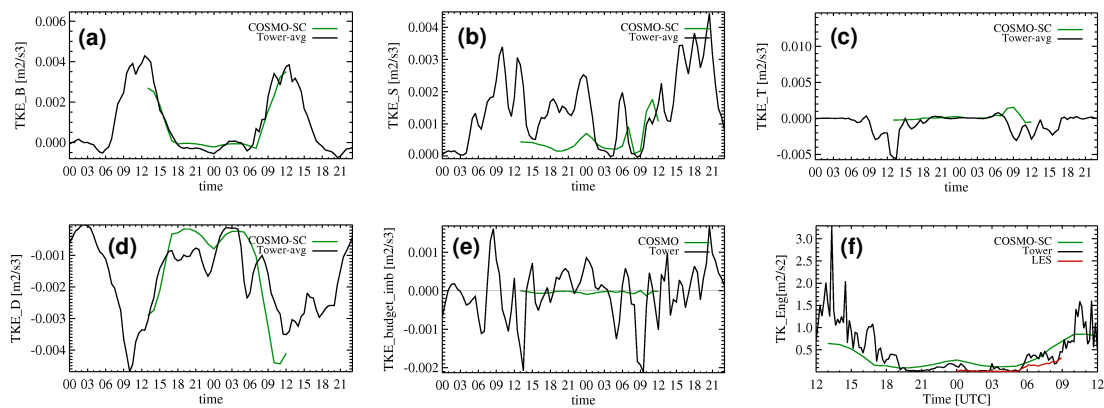


Figure 2.34: Time series of the TKE (f) and the TKE budget terms: buoyancy production or destruction (a), shear production (b), turbulent transport (c), dissipation (d) and budget imbalance (e). COSMO (green), measurement (black) and LES (red) time series between 1 July 2006 0000 UTC and 3 July 2006 0000 UTC (for TKE the first and last 12 hours are not shown). A level at 80 m above ground is shown.

Figure 2.34 depicts TKE budget time series at 80 m above ground level (time series at different heights show similar behaviour). It can be seen that during night time shear production and dissipation are the dominating terms, buoyancy destruction and turbulent transport are negligible. Generally it can be concluded, that the magnitude of the separate budget terms as well as that of TKE is adequately simulated during night time conditions by COSMO, but shear production and dissipation are underestimated between 1800 and 0000 UTC. The measured budget imbalance shows large scatter, but is close to zero on average. This indicates that the measurement problem seen by the LITFASS-2003 case (Section 2.3.6) is not present for the GABLS3 dataset.

It is important to discuss the results of the GABLS3 simulation with respect to previous experiments in simulating the SBL with the COSMO model. Analyzing the first GABLS case, Buzzi (2008) found that the COSMO model is extremely sensitive to the choice of the minimum diffusion coefficient and recommended an optimal value on the order of $0.01 \text{ m}^2/\text{s}$ for this parameter. This value is applied for the GABLS3 experiment and indeed results in a fairly accurate simulation of the SBL. The numerical instabilities described by Buzzi (2008) when using the reduced minimum diffusion coefficient are however not observed for the GABLS3 case. This is due to two factors: First, in the experiment of Buzzi (2008), a very fine vertical resolution was used (6.25 m equidistant level distribution), while in the case of the GABLS3 experiment the vertical resolution was much coarser (with the lowest level at 10 m height). Secondly, the circulation terms were switched off for the first GABLS case and switched on for GABLS3. As the circulation terms are positive definite source terms in the TKE budget, this settings for GALS3 also stabilizes the numerics of the model.

2.5 Summary and conclusions

In this chapter the performance of the COSMO model has been evaluated in the Planetary Boundary Layer. Next to the mean prognostic variables, the turbulence characteristics of the model have also been verified. An attempt has been made to understand the behaviour of the turbulence scheme in different situations by analyzing the TKE budget terms separately.

First, an idealized dry convective case was investigated, and simulations of the COSMO-SC model were compared to LES data. After several experiments, a COSMO-SC model solution of the ideal convective boundary layer was achieved that is independent of the vertical resolution and the time step, consequently representing the physical capabilities of the current turbulence scheme in such a situation. Compared to the LES results, the turbulent transport of TKE is too weak in the COSMO model, and as a consequence TKE values near the PBL top are too low. This results in an insufficient negative buoyancy flux in the entrainment zone. The experiments have also shown the drawbacks of the explicit handling of the transport term, which can be improved by applying a semi-implicit solver for the vertical diffusion of TKE.

Following the idealized study, the performance of the COSMO model was tested on a real-world dry convective case over heterogeneous flat terrain. It has been shown that the COSMO model is able to reproduce the main evolution of the boundary layer if the external parameters are realistic and if the initial conditions are adequate. The sensitivity of the COSMO model with respect to several factors was investigated. First, the sensitivity to the horizontal resolution was studied. It was shown that the vertical profiles are not sensitive to the horizontal resolution, but the three-dimensional structure of the PBL is significantly different in COSMO-1 than in COSMO-2. Secondly, the sensitivity of the COSMO-1 simulation to the horizontal diffusion was investigated. The standard isotropic three-dimensional turbulence scheme was compared to the fourth-order numerical diffusion and to the newly implemented first-order Smagorinsky closure. It can be concluded that without horizontal diffusion the COSMO-1 simulation exhibits unrealistically strong waves in the PBL. Both physical and numerical horizontal diffusion seem to have the same – beneficial – impact on the PBL waves. Based on these findings, it is recommended to use the three-dimensional turbulent diffusion scheme with horizontal mesh size on the order of 1 km, because it is more physically based than the fourth-order numerical filter. For flat convective conditions with very low horizontal wind field deformation, the Smagorinsky closure in its classical formulation generates too little mixing, whereas the extension of the scheme to include the horizontal shear of vertical wind might be beneficial for these cases.

Finally, the budget terms in the TKE equation were investigated separately. The turbulent transport term was identified as the most problematic term in the prediction of TKE.

The underestimation of the turbulent TKE transport was even noticed by Mellor and Yamada (1982), but in operational NWP models applying this scheme no solution has been found for this problem so far. In the present work a solution to increase the TKE transport in the PBL was proposed, resulting in a more realistic TKE profile and higher entrainment fluxes. Unfortunately, the better TKE profile does not lead to an improvement of the temperature profile in the PBL. According to Buzzi (2008), changes in TKE might be compensated by the stability functions in the computation of the diffusion coefficients, which then leads to an unmodified temperature profile.

In order to assess the performance of the COSMO model during stable conditions, the single column simulations performed by DWD for the GABLS3 case were compared to tower turbulence measurements and LES data. Special attention was paid to the simulation of the nocturnal low-level jet and TKE profiles. It was found that COSMO is able to simulate the gross properties of the LLJ, what is attributed to the usage of reduced minimum diffusion coefficients (Buzzi, 2008). Fine details however, like the sinking of the LLJ with time, are not captured by the model. The investigation of the measured TKE profiles revealed an upside-down structure of the boundary layer, where TKE is produced at higher levels and then transported towards the surface. This phenomenon of the SBL is not captured by COSMO for the present case.

Acknowledgements

The author would like to thank Dmitrii Mironov and Ekaterina Machulskaya (DWD) for providing the LES dataset for the idealized convective case and useful discussions. Thank goes to Felix Ament (University of Hamburg) for providing the 1 km external parameters for the LITFASS-2003 simulations. I would like to thank Frank Beyrich and Gerd Vogel (DWD) for providing the LITFASS-2003 measurement dataset and Jens Bange (TU Braunschweig) for making the Helipod measurements available. The help of Matthias Mauder (IMK-IFU), Thomas Foken (University of Bayreuth) and Dominik Michel (MeteoSwiss) in the post-processing of turbulence data is highly acknowledged. The indispensable contribution of Daniel Nadeau and Chad Higgins (EFLUM-EPFL) in connection with the LES simulations for the LITFASS-2003 case is greatly appreciated. Many thanks for Matthias Raschendorfer and Jürgen Helmert (DWD) for providing the GABLS3 COSMO-SC simulations. I would also like to thank Sukanta Basu (NCSU), Fred Bosveld (KNMI) and Bert Holtslag (Wageningen University) for providing measurement and LES data for the GABLS3 case. Thanks goes to Vanessa Stauch, Tanja Weusthoff and Christophe Hug (MeteoSwiss) for helping me by the verification of the parallel experiments.

3 Deriving turbulence characteristics from the COSMO model for dispersion applications

3.1 Introduction

In the emergency response system of MeteoSwiss the LPDM of DWD, which is a Lagrangian particle dispersion model, is used to simulate the transport and diffusion of pollutants. For this type of dispersion model, information from the mean atmospheric variables as well as from the turbulence state of the atmosphere is required. In most operational systems, the mean meteorological variables can directly be extracted from a numerical weather prediction model but turbulence characteristics have to be parameterized. This is done by using a meteorological pre-processor or interface.

In this chapter two different interfacing approaches are validated against Large Eddy Simulation data and turbulence measurements. First, the basic equations of the two parameterizations are presented. Secondly, the possible methods for diagnosing the PBL height – which is an important input parameter for one of the interfacing approaches – are presented and verification results are discussed. Finally, the diagnosed turbulence characteristics are verified on several case studies.

3.1.1 Direct usage of TKE

The task of the coupling interface between COSMO and LPDM is to determine two variables needed by LPDM as three-dimensional fields: the standard deviation of velocity fluctuations (σ) and the Lagrangian integral timescales (T_L) in both the horizontal and vertical directions. The coupling approach which is used operationally at MeteoSwiss uses the prognostic TKE and the turbulent diffusion coefficients of the COSMO model directly. The standard deviations of velocity fluctuations are determined from:

$$\sigma_k = \sqrt{2m_k e}, \quad (3.1)$$

where m_k is the portion of TKE (e) for the given coordinate direction (horizontal or vertical). The Lagrangian integral timescale is determined following Batchelor (1949) for both the horizontal and vertical directions as:

$$T_L = \frac{K_m}{\sigma^2}, \quad (3.2)$$

where K_m is the turbulent diffusion coefficient for momentum.

The main difficulty of the “Direct” coupling approach is to determine the vertical portion of TKE, in order to diagnose the vertical and horizontal velocity fluctuations separately. In the case of the currently operational approach the equation for the TKE partitioning (Eq. 4.8) is derived from the governing equations of the Mellor and Yamada (1974) level 2 closure. This approach (further referred to as the “Direct-lev2” approach) is described in detail in Section 4.3.3. The main concern with this approach is that its derivation is not consistent with the turbulence parameterization of the COSMO model, which is based on the Mellor and Yamada (1982) level 2.5 approach.

To diagnose the turbulence variables for the dispersion model consistently with the turbulence scheme of COSMO, the governing equations of the level 2.5 closure have to be used to derive the vertical portion of TKE (Mellor and Yamada, 1982):

$$m_3 = \frac{\sigma_w^2}{2e} = \frac{1}{3} - 2A_1 S_M G_M + 4A_1 S_H G_H, \quad (3.3)$$

where G_M and G_H are dimensionless gradients, which are functions of TKE and the wind and temperature gradients, respectively. S_M and S_H are stability functions, which can be calculated from Eq. 2.5 and Eq. 2.6 (the diffusion coefficients can be written in the COSMO output files), and A_1 is a model constant. In the following sections this new, consistent coupling approach (further referred to as the “Direct-lev2.5” approach) is compared to the operational “Direct-lev2” method.

3.1.2 Similarity theory approach

The COSMO model is using a relatively sophisticated turbulence scheme, which carries a prognostic equation for turbulent kinetic energy. As it has been shown in the previous section, TKE can directly be used to derive the necessary turbulence characteristics for a Lagrangian particle dispersion model. However, in the case of other NWP–dispersion model

pairs, usually this kind of direct coupling is not possible. Consequently, other approaches have to be applied.

A different approach to diagnose the turbulence variables for a dispersion model is to apply similarity theory considerations. In this case usually the surface fluxes and a diagnosed planetary boundary layer (PBL) height is needed from the NWP model. This approach is used, e.g., in the Lagrangian dispersion model FLEXPART (Stohl et al., 2005).

In the FLEXPART model the turbulence characteristics needed by the dispersion model are parameterized according to Hanna (1982). The main concept of this parameterization is substantially different from those applied in the interface of LPDM (described in the previous section), which is also reflected by the fact that in this case not the model coordinate directions, but a natural coordinate system is used for wind fluctuations, with u and v referring to the along-wind and the cross-wind component. For the parameterization of the necessary turbulence variables the boundary layer parameters h , L , w_* , z_0 and u_* are used, i.e., the PBL height, the Obukhov length, the convective velocity scale, the roughness length and the friction velocity, respectively. For the present purpose, the PBL height was derived according to the bulk Richardson number method (Szintai and Kaufmann, 2008).

The Obukhov length is calculated as:

$$L = \frac{-\Theta_v u_*^3}{kg \overline{w' \theta'_{vs}}}, \quad (3.4)$$

where Θ_v is the mean virtual potential temperature, u_* is the friction velocity, $k=0.4$ is the von Karman constant, $g=9.81 \text{ m/s}^2$ is the acceleration due to gravity and $\overline{w' \theta'_{vs}}$ is the kinematic surface heat flux. u_* is the square root of the kinematic surface momentum flux:

$$u_* = \sqrt[4]{\overline{u' w_s'^2} + \overline{v' w_s'^2}}, \quad (3.5)$$

where $\overline{u' w_s'} = \frac{M_u}{\rho}$ and $\overline{v' w_s'} = \frac{M_v}{\rho}$ are the zonal and meridional components of the kinematic surface momentum flux. The kinematic surface heat flux can be derived as:

$$\overline{w' \theta'_{vs}} = \frac{H}{\rho \cdot c_p}, \quad (3.6)$$

where c_p is the specific heat of air. It has to be noted, that both the momentum and heat fluxes are averaged over the forecast period in the standard model output. Consequently, the

actual values should be extracted first from the values of two consecutive timesteps. The convective velocity scale is defined as:

$$w_* = \left[\frac{ghw'_{vs}\theta'_v}{\Theta_v} \right]^{1/3}. \quad (3.7)$$

Here h is the boundary layer height. Turbulence post-diagnosis methods based on similarity theory approaches usually distinguish three stability classes (unstable, neutral and stable conditions), and apply different parameterizations for these. The stability of the atmosphere can be defined with different indicators, e.g., the Richardson number, potential temperature profile or the surface sensible heat flux. In this study the stability was determined with the surface sensible heat flux (H). During unstable conditions ($H > 10 \text{ W/m}^2$) horizontally isotropic turbulence is assumed in Hanna (1982), which leads to:

$$\frac{\sigma_u}{u_*} = \frac{\sigma_v}{u_*} = \left(12 + \frac{h}{2|L|} \right)^{1/3} \quad (3.8)$$

$$T_{L_u} = T_{L_v} = 0.15 \frac{h}{\sigma_u} \quad (3.9)$$

$$\frac{\sigma_w}{w_*} = \left[1.2 \left(1 - 0.9 \frac{z}{h} \right) \left(\frac{z}{h} \right)^{2/3} + \left(1.8 - 1.4 \frac{z}{h} \right) u_*^2 \right]^{1/2}. \quad (3.10)^2$$

In the surface layer, i.e., for $z/h < 0.1$, and for heights $z - z_0 > -L$ the vertical Lagrangian timescale is computed as:

$$T_{L_w} = 0.15 \frac{z}{\sigma_w [0.55 - 0.38(z - z_0)/L]}. \quad (3.11)$$

² Equation 3.10 is taken from the documentation of Flexpart 6.2. In the documentation of Flexpart 8 this equation was modified to the following, dimensionally correct one:

$$\sigma_w = \left[1.2 w_*^2 \left(1 - 0.9 \frac{z}{h} \right) \left(\frac{z}{h} \right)^{2/3} + \left(1.8 - 1.4 \frac{z}{h} \right) u_*^2 \right]^{1/2}$$

As the new equation was noted only during the final revisions of the thesis, for all the results presented in this work Equation 3.10 was used. First tests indicate only minor differences between the results of the two equations, however, the impact should be tested more extensively in future.

For $z/h < 0.1$ and for heights $z - z_0 < -L$:

$$T_{L_w} = 0.59 \frac{z}{\sigma_w}. \quad (3.12)$$

For the mixed layer, i.e. for $z/h > 0.1$:

$$T_{L_w} = 0.15 \frac{z}{\sigma_w} \left[1 - \exp\left(-\frac{5z}{h}\right) \right] \quad (3.13)$$

For neutral conditions ($-10 \text{ W/m}^2 < H < 10 \text{ W/m}^2$) the scaled standard deviations of the velocity fluctuations are parameterized as an exponential function of height:

$$\frac{\sigma_u}{u_*} = 2.0 \exp(-3fz/u_*) \quad (3.14)$$

$$\frac{\sigma_v}{u_*} = \frac{\sigma_w}{u_*} = 1.3 \exp(-2fz/u_*) \quad (3.15)$$

$$T_{L_u} = T_{L_v} = T_{L_w} = \frac{0.5z/\sigma_w}{1 + 15fz/u_*}, \quad (3.16)$$

where $f = 1 \cdot 10^{-4} \frac{1}{s}$ is the Coriolis parameter.

For stable conditions ($H < -10 \text{ W/m}^2$) turbulence is assumed to decrease linearly with height:

$$\frac{\sigma_u}{u_*} = 2.0 \left(1 - \frac{z}{h} \right) \quad (3.17)$$

$$\frac{\sigma_v}{u_*} = \frac{\sigma_w}{u_*} = 1.3 \left(1 - \frac{z}{h} \right) \quad (3.18)$$

$$T_{L_u} = 0.15 \frac{h}{\sigma_u} \left(\frac{z}{h} \right)^{0.5} \quad (3.19)$$

$$T_{L_v} = 0.07 \frac{h}{\sigma_v} \left(\frac{z}{h} \right)^{0.5} \quad (3.20)$$

$$T_{L_w} = 0.1 \frac{h}{\sigma_w} \left(\frac{z}{h} \right)^{0.5}. \quad (3.21)$$

Standard deviations of the wind fluctuations derived according to this method will be further referred to as the “SIM” method.

3.1.3 Parameterizations of ADPIC

ENSI (Swiss Federal Nuclear Safety Inspectorate) uses the dispersion model ADPIC to calculate the transport of radioactive pollutants in the close vicinity of NPPs. The input variables of ADPIC concerning atmospheric turbulence are the standard deviation of lateral wind speed (σ_v) and the standard deviation of wind direction (σ_θ).

In the case of the ADPIC model the required turbulence variables are parameterized from COSMO model outputs in the following way:

$$\sigma_v = u_* \sqrt{2 - \frac{z}{h} + 0.35 \left(\frac{h}{k \cdot L} \right)^{2/3}}, \quad (3.30)$$

for unstable conditions and

$$\sigma_v = u_* \sqrt{2 \left(1 - \frac{z}{h} \right)} \quad (3.31)$$

for stable conditions (Gryning et al., 1987). The PBL height (h) is determined according to the bulk Richardson method, similarly to the previous section. Standard deviations of the cross-wind fluctuations derived according to this method will be further referred to as the “ENSI” method.

The standard deviation of the wind direction (in radian) is then computed as:

$$\sigma_\theta = \frac{\sigma_v}{\overline{U(z)}}, \quad (3.32)$$

where $\overline{U(z)} = \sqrt{u(z)^2 + v(z)^2}$ is the mean wind speed at height z .

This method will only be evaluated for the CN-Met measurement campaign (see section 3.3.4).

3.2 PBL height determination from the COSMO model

3.2.1 Methodology

In the previous sub-section the similarity theory approach for turbulence post-diagnosis was presented. The governing equations of this parameterization show that the height of the Planetary Boundary Layer is an important input parameter for this approach. As the PBL height was not a standard output variable of the COSMO model, first, it had to be implemented. For the diagnosis of the PBL height either from measurements or from NWP outputs, several methods exist. Seibert et al. (2000) give a comprehensive overview about the currently used approaches.

In the present study methods using the following characteristics were applied to COSMO model fields to diagnose the height of the PBL:

- Gradient Richardson number
- Bulk Richardson number
- TKE
- Momentum and heat fluxes
- Theoretical approaches based on surface fluxes

The Richardson number is a non-dimensional quantity widely used in turbulence theory to characterize the strength of turbulence and to distinguish between turbulent and non-turbulent flows. It is derived from the TKE equation, by taking the ratio of the buoyancy production/destruction term and the shear generation term. Assuming horizontal homogeneity the so-called flux Richardson number (R_f) can be defined, using the notation of Section 2.1:

$$R_f = \frac{\frac{g}{\theta_v} \overline{w'\theta'}}{\overline{u'w'} \frac{\partial U}{\partial z} + \overline{v'w'} \frac{\partial V}{\partial z}}. \quad (3.22)$$

From measurements or NWP model data it is usually more convenient to obtain gradients of temperature and wind than fluxes of heat and momentum, thus we can simplify the above definition by assuming a down-gradient relation between fluxes and gradients with an equal diffusivity for heat and momentum transfer. In this way we can define the gradient Richardson number (R_i):

$$Ri = \frac{\frac{g}{\theta_v} \frac{\partial \Theta}{\partial z}}{\left(\frac{\partial U}{\partial z}\right)^2 + \left(\frac{\partial V}{\partial z}\right)^2}. \quad (3.23)$$

The above definition contains local gradients which could be difficult to assess at higher levels in the atmosphere. Consequently, in several applications the local gradients are approximated by finite differences. For the determination of the PBL height the special definition of the bulk Richardson number (Ri_b) is used, which assumes the lower reference level to be fixed near the surface:

$$Ri_b = \frac{gz(\Theta_{v,z} - \Theta_{v,surf})}{\theta_v(U_z^2 + V_z^2)}, \quad (3.24)$$

where $\Theta_{v,z}$, U_z and V_z are the virtual potential temperature and the two horizontal wind components at height z and $\Theta_{v,surf}$ is the virtual potential temperature at the reference level close to the surface.

When using the gradient Richardson number to determine the PBL height, a constant critical value of 0.38 is used (Barbara Fay, DWD, personal communication). The PBL top was defined as the first model level where the local Ri reaches the critical value. To calculate the bulk Richardson number, the diagnosed 2-m temperature was used as a reference. According to the literature, a critical Ri_b of 0.22 (Vogelenzang and Holtslag, 1996) was used for unstable conditions and a critical value of 0.33 (Wetzel, 1982) in stable situations.

When applying TKE for PBL height determination, first the maximum value of TKE was searched in a predefined lower part of the atmosphere (2000 m for unstable and 500 m for stable conditions), and the critical TKE value (TKE_c) was defined with a certain threshold (th): $TKE_c = TKE_{max} * th$. During the evaluation different threshold values were tested for stable and unstable stratification. For the momentum fluxes the same methodology was used, however, always the surface momentum flux was used as a reference to calculate the critical value. The PBL top was then determined at the height where TKE or the momentum flux first dropped below the critical value. When using the heat flux of the model the PBL height was determined as the level of the heat flux minimum. As the momentum and heat fluxes are not operational outputs of the COSMO model, these first have to be calculated from the turbulent diffusion coefficients and the temperature and wind gradients, following Equations 2.3 and 2.4.

Theoretical approaches to determine the PBL height have also been implemented. These methods are based on the surface heat and momentum fluxes and the background stratification above the PBL. For the convective boundary layer, the slab model equation of Batchvarova and Gryning (1991) was used to calculate the growth rate of the boundary layer:

$$\frac{dh}{dt} = (1 + 2A) \frac{\overline{w'\theta'_{vs}}}{\gamma_{\theta}h} + 2B \frac{u_*^3}{\gamma_{\theta}\beta h^2}, \quad (3.25)$$

where h is the PBL height, $\overline{w'\theta'_{vs}}$ is the surface potential temperature flux, u_* is the friction velocity, β is the buoyancy parameter, γ_{θ} is the background stratification above the PBL and A and B are model constants. The integration of the above equation was started at sunrise, when the surface sensible heat flux becomes positive, and it was initiated with a PBL height of 50 m.

For the height of the stable boundary layer the diagnostic equation of Zilitinkevich et al. (2007) was applied:

$$\frac{1}{h^2} = \frac{f^2}{(C_R u_*)^2} + \frac{N|f|}{(C_{CN} u_*)^2} + \frac{|f\beta\overline{w'\theta'_{vs}}|}{(C_{NS} u_*^2)^2}, \quad (3.26)$$

where f is the Coriolis parameter, N is the Brunt-Väisälä frequency and C_R , C_{CN} and C_{NS} are empirical constants. Equation 3.26 is a so-called multi-limit formulation, where the terms on the right hand side account for different basic types of the stable boundary layer. The first term corresponds to the “truly neutral” PBL, with a constant potential temperature profile. The second term refers to the “conventionally neutral” PBL, with a well-mixed layer near the surface and an elevated inversion above. The last term represents the “nocturnal” stable boundary layer with a surface inversion resulting from strong surface cooling.

3.2.2 PBL height validation against radio soundings

Validating the PBL heights diagnosed by the COSMO model proved to be a rather difficult task, as no routine measurements are available for this variable. Furthermore, there is no agreement in literature about the exact definition of the PBL height and the methods to diagnose it from, e.g., radio soundings. In the following a method is presented to obtain the PBL height automatically from routine radio sounding measurements. These values are then compared to the different PBL height determination methods applied to COSMO model

forecasts. First, ideal convective and stable cases are studied, which is followed by the investigation of a one-month continuous period.

Measurements

The first task in the evaluation of diagnosed PBL heights was to obtain a reliable and objectively determined dataset on observed PBL heights. As a reference, PBL height was subjectively determined for several cases from measured radio sounding profiles following the method described in Joffre et al. (2001). The aim was to construct an automatic objective method which results in values that correlate well with the subjective dataset. For this task ten stable and ten unstable days were chosen and ten European radio sounding stations were used each day (see details of the dataset in the next sub-section).

To determine the boundary layer height objectively from the radio soundings, the bulk Richardson number was applied for the measured virtual potential temperature and wind profiles. For convective days a critical Ri_b of 0.22 was used, which turned out to be a reliable measure and showed good agreement with the subjectively defined PBL top. For stable days a critical Ri_b of 0.33 was applied, which value worked adequately for well mixed stable boundary layers with an elevated inversion.

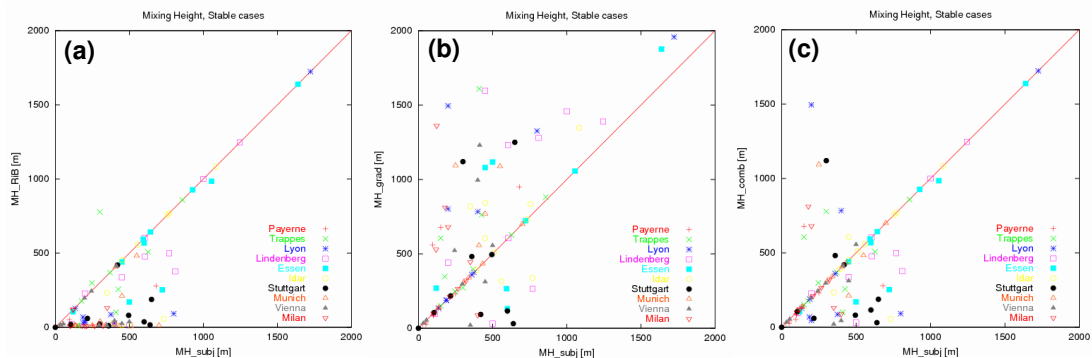


Figure 3.1: Scatter plot diagrams showing the correlation of the different objectively evaluated PBL heights (y-axis) with the subjectively determined values (x-axis): (a) method based on the bulk Richardson number method, (b) close-to-adiabatic temperature gradient and (c) combined method. Different symbols are indicating the different radio sounding stations used for validation. Different colours refer to different radio sounding sites (see legend).

However, especially in the case of radiation dominated stable boundary layers this method often failed to determine a realistic PBL height (Figure 3.1a). In these cases Ri_b exceeded the critical value already at the first measurement level. Consequently, a second method was implemented when the first height starting from the surface was searched, where the potential temperature profile was "close" to adiabatic, i.e., the potential temperature gradient

was smaller than 0.72 K/100 m. This method gives reasonable results for the radiation dominated SBL, however, considerably overestimates the cases with elevated inversion (Figure 3.1b). The combination of these two methods showed reasonable agreement with the subjectively defined PBL top (Figure 3.1c), however, to achieve a more robust method to determine PBL height objectively in stable situations is still an unresolved problem.

Ideal cases

PBL heights determined subjectively from the measurements of five radio sounding stations on the COSMO-2 domain were compared to 12 hour forecasts of the COSMO model during ten stable and ten convective days, with anticyclonic conditions. In the experiments the model version 4.0 (MeteoSwiss local version 4.0.4) was used. Both horizontal resolutions of the COSMO model were tested, namely, COSMO-7 with 7 km horizontal resolution and 45 vertical levels (operational configuration in 2007) and COSMO-2 with 2.2 km horizontal resolution and 60 vertical levels. COSMO-7 was initialized from its own assimilation cycle, while the initial conditions for COMSO-2 were interpolated from the COMSO-7 analysis due to the fact that in 2006 no assimilation cycle was running at MeteoSwiss for COSMO-2. The PBL height determination methods were applied for the COSMO model to the grid point which was closest to the radio sounding location. For the PBL height methods based on the TKE and the momentum flux two different threshold were also tested to investigate the sensitivity of these two – not so widely applied – approaches.

For the verification, different scores (relative bias, relative standard deviation and relative root mean square error) were calculated and scatter plot diagrams were analyzed. The relative bias or relative mean error of a dataset is computed as:

$$BIAS_{rel} = \frac{1}{N} \sum_{i=1}^N \left(\frac{X_{p,i} - X_{o,i}}{X_{o,i}} \right), \quad (3.27)$$

where $X_{p,i}$ is the i -th predicted value of the variable X , $X_{o,i}$ is the i -th observed value of the variable X and N is the number of observations. The standard deviation of errors is defined as:

$$STDEV_{rel} = \sqrt{\frac{1}{N} \sum_{i=1}^N (\varepsilon_i - \bar{\varepsilon})^2}, \quad (3.28)$$

where ε_i is the relative error of the i -th predicted value and $\bar{\varepsilon}$ is the mean of relative errors. The quality of a population of predicted values can be characterized with giving the $BIAS_{rel}$ and $STDEV_{rel}$ scores at the same time. The relative root mean square error ($RMSE_{rel}$) is a single score characterizing the quality a forecast dataset:

$$RMSE_{rel} = \sqrt{\frac{1}{N} \sum_{i=1}^N \left(\frac{X_{p,i} - X_{o,i}}{X_{o,i}} \right)^2} \quad (3.29)$$

For the model evaluations presented in the following, usually the bias score is shown to indicate whether a given method under- or overestimates the PBL height, and the forecasts of the different methods are compared to each other based on the $RMSE_{rel}$ score.

Figure 3.2 shows verification scores for the ten unstable days for both COSMO-7 and COSMO-2. A strong underestimation can be observed for the Ri and the heat flux method, and a considerable overestimation for the Ri_b method and the slab model. In the case of the $RMSE_{rel}$, the different methods are much closer to each other. For COSMO-7 the slab model and the momentum flux method perform best, while for COSMO-2 the Ri method and the TKE method give the most accurate predictions. It has to be noted that from the two different thresholds (5% and 10% of the surface value) the higher seems to be giving the more accurate diagnosis.

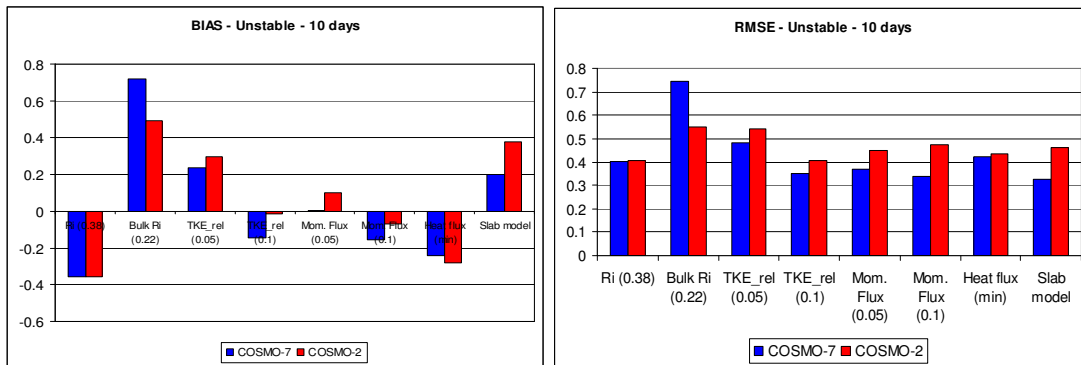


Figure 3.2: Relative bias (left) and relative root mean square error (right) of the predicted PBL height for the ten ideal unstable days in the case of COSMO-7 (blue) and COSMO-2 (red). A score of 0.1 means 10% relative error. In parentheses the applied critical values or model thresholds are indicated. Case numbers are slightly different for the two model resolutions and for the different methods.

Figure 3.3 highlights the dependence of model errors on the observed PBL height for different methods. With every method – except for the bulk Richardson number method – the same features can be observed, namely, the shallower (approx. 700 m) boundary layers are overestimated, while the higher (approx. 2500 m), well-developed boundary layers are

underestimated by the COSMO model (Figure 3.3a and b). This might indicate that the turbulence scheme of COSMO is unable to catch the extreme values of the turbulence characteristics and predicts rather uniform PBL statistics in every situation. For the Ri_b method PBL height is generally overestimated regardless of the observed PBL height value (Figure 3.3c), which is a better indication for possible applications, as a uniform bias is easier to correct with e. g. statistical post-processing.

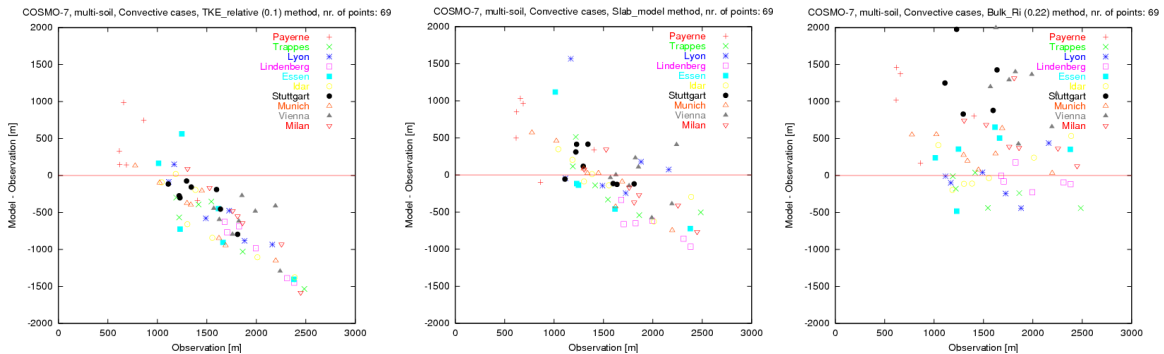


Figure 3.3: Scatter plot diagrams showing the dependence of the model error (model-observation, y-axis) on the observed PBL height (x-axis) for the ten ideal unstable days in the case of COSMO-7: (a) method based on TKE, (b) slab model and (c) bulk Richardson number. Number of observation-model pairs is 69.

For stable days the same methods were investigated as for convective cases, however, with somewhat higher thresholds. Both with the TKE and momentum flux method a threshold of 20% proved to be the most appropriate, in contrast to the 10% threshold used during unstable days. The use of higher thresholds was necessary due to a known problem of the COSMO model in stable situations. As a minimum turbulent diffusion coefficient of $1 \text{ m}^2/\text{s}$ is applied in the COSMO model, it causes the very stable boundary layer to be more active than in reality, and consequently higher thresholds are needed to find a suitable PBL top from the model.

While during convective days usually all the methods were successful in finding a PBL top, this was not the case for stable situations (Figure 3.4). A method was considered unsuccessful in this respect, if either the diagnosed PBL top was at the first model level (i.e., 30 m for COSMO-7 and 10 m for COSMO-2), or no PBL top was found below 5000 m. The first case was mainly associated with the Richardson number methods, while the second case with methods based on TKE or the turbulent fluxes. The number of successful diagnoses for stable days was the highest with the momentum flux method and lowest with the gradient Richardson number method, the latter method being successful in diagnosing a realistic PBL height only in 10% of the cases.

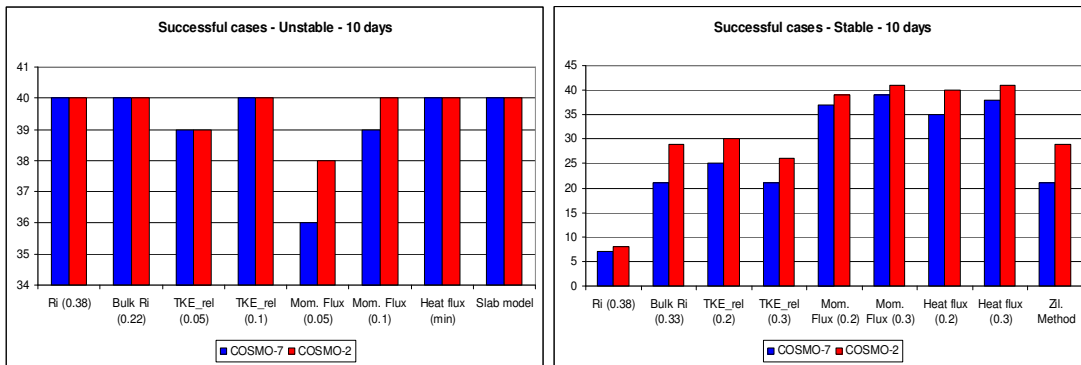


Figure 3.4: Number of cases during unstable (left) and stable (right) days, when the different methods were able to diagnose a PBL height (see details in text). Number of validated cases are 40 (unstable) and 48 (stable).

To be able to perform a fair intercomparison between the different methods, verification scores were calculated only for those cases when all the methods were successful in finding a PBL top. When using only five radio sounding stations from the COSMO-2 domain, this condition results in only four cases both for COSMO-7 and COSMO-2, which is very few for a statistical evaluation. Because of this, the verification scores were not calculated for COSMO-2, and for COSMO-7 five more stations were used from the outer parts of the model domain to evaluate the different methods (Figure 3.5).

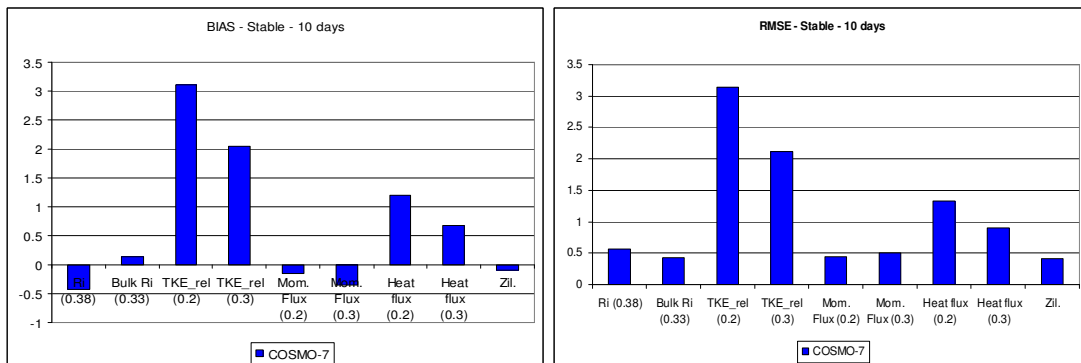


Figure 3.5: Same as Figure 3.2, but for stable cases and only for COSMO-7. Number of cases is 14 for all the methods.

For the ideal stable cases the gradient Ri method and the momentum flux method are underestimating, the TKE method and the heat flux method are overestimating the PBL height. The bulk Ri method and the Zilitinkevich equation predict the PBL height practically bias-free. Based on the $RMSE_{rel}$ score the best methods for predicting the height of the stable boundary-layer are the Zilitinkevich equation and the bulk Ri and momentum flux methods.

Continuous period

Next to ideal cases the PBL height determination methods were also evaluated on a one-month continuous period, between 20 February and 20 March 2008. The first half of the period was characterized by a strong anticyclone causing warm and sunny weather, while the second half was determined by several cyclone passages. Both versions of the COSMO model from the operational forecast cycle were used. COSMO-7 with 6.6 km horizontal resolution and 60 vertical levels was integrated for 72 hours while COSMO-2 with 2.2 km resolution and the same vertical level distribution was integrated for 24 hours. For the evaluation only the 0000 UTC runs were used. COSMO forecasts of the PBL height were validated using the 0000 UTC and 1200 UTC measurements of four radio sounding stations.

Figure 3.6 shows $RMSE_{rel}$ scores for the predicted PBL heights validated with 1200 UTC soundings (12 hour forecasts) and 0000 UTC soundings (24 hour forecasts). The methods based on the Richardson number perform best, similarly to the ideal cases. Theoretical approaches (slab model and Zilitinkevich equation) also have relatively good scores. The method based on the TKE profile performs worst, especially for 0000 UTC soundings and for COSMO-2, when PBL heights are seriously overestimated. Except for the gradient Richardson number method all the approaches overestimate the PBL height (not shown).

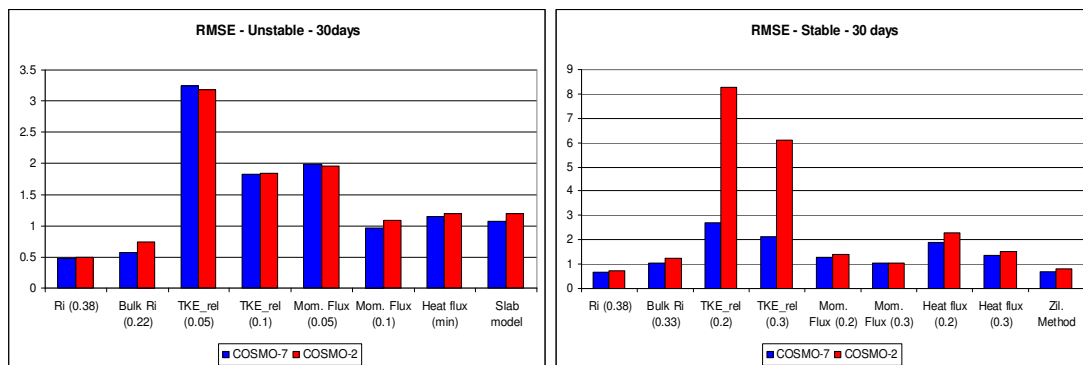


Figure 3.6: Relative root mean square error ($RMSE_{rel}$) of the predicted PBL height by different methods for the one-month continuous period. Scores for 12 hour (left) and 24 hour (right) forecasts are shown, model start time is always 0000 UTC. The verification was done for 30 days and four radio sounding stations, only those cases were considered when all the methods were successful in diagnosing a PBL height. For unstable cases this results in 41 (37) data points for COSMO-7 (COSMO-2). For stable cases 61 (59) data points were validated for COSMO-7 (COSMO-2).

Considering the reliability of the methods, all the approaches perform very well being successful in about 90% of the cases except for the gradient Ri method with about 50% rate.

For the one-month period the lead time dependence of PBL height determination was also investigated for COSMO-7 (Figure 3.7).

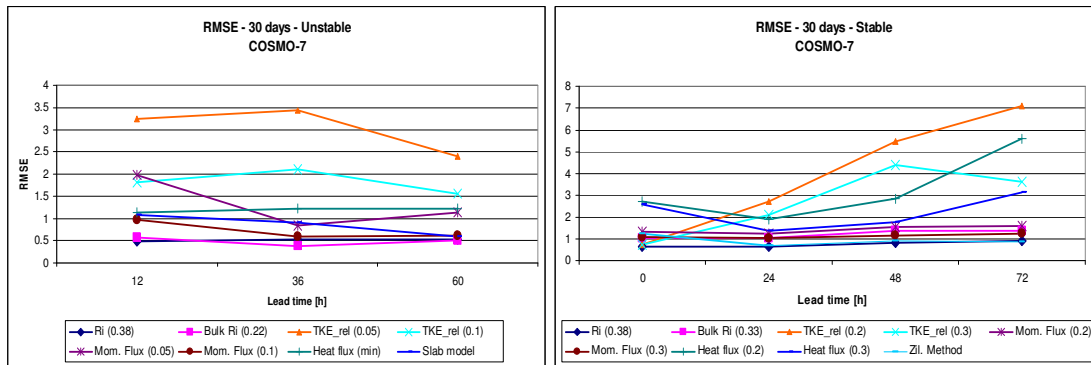


Figure 3.7: Lead time dependence of the error of the PBL height prediction (relative $RMSE_{rel}$) for COSMO-7 in the case of the one-month period for 1200 UTC (left) and 0000 UTC (right) soundings. On the x-axis the lead time (in hours) of the COSMO-7 forecast is shown.

In the case of 1200 UTC soundings (unstable situations) no significant dependence can be found for the $RMSE_{rel}$ score in the first three days of the forecast, except for the momentum flux (5%) method, which improves significantly in the second day. For the 0000 UTC soundings (stable situations) the forecast skill is deteriorating with the lead time for the TKE and heat flux methods, while for the other approaches the skill is constant. This indicates that the turbulence parameterization of the COSMO model is more robust during daytime and more sensitive to initial- and boundary conditions during nocturnal stable situations.

The serious overestimation of the TKE method was also studied. The investigation of single case studies from the one-month period showed that the overestimation of the PBL height by the TKE method is very often associated with the presence of low- and middle level clouds in the COSMO simulation. In the following this relationship is described for a case study. Figure 3.8 shows vertical profiles of cloud cover and TKE in COSMO-2 at 0000 UTC on 28 February 2008 for the Stuttgart radio sounding station. For this case a PBL height of 142 m above ground level is diagnosed from the radio sounding profile. From the COSMO-2 model outputs, all the other PBL height determination methods give a PBL height between 50 and 500 m, while the TKE method diagnoses a PBL height of 2600 m which is a serious overestimation. The TKE profile of COSMO also shows a 400 m thick turbulent layer above the surface, however, the low-level clouds at 1500 m height generate strong turbulence which is diffused up- and downwards in the model.

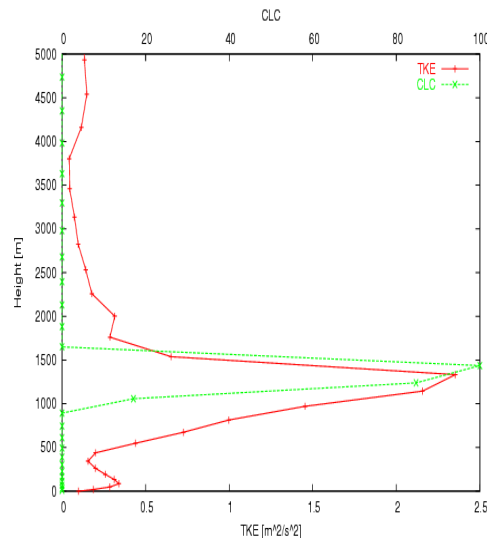


Figure 3.8: Simulated vertical profiles of cloud cover (green dashed line) and TKE (red solid line) in COSMO-2 at 0000 UTC on 28 February 2008 for the Stuttgart radio sounding station. On the y-axis the height above ground level (in metres) is shown, on the lower x-axis TKE in (m^2/s^2) on the upper x-axis the cloud cover (in %) is shown.

Consequently, TKE drops below the predefined threshold value only at a very high altitude, causing the above mentioned overestimation. The generation of TKE by buoyancy effects at the edge of clouds was also discussed by Mellor and Yamada (1982), however, the validation of the TKE values in the vicinity of clouds is extremely difficult due to the lack of reliable measurements.

Based on the evaluation of the ideal cases and the continuous period the bulk Richardson number method, the momentum flux method and the theoretical approaches (slab model and Zilitinkevich equation) were found to be the most reliable and accurate methods to diagnose the PBL height from the COSMO model. As a compromise between the presented results and operational convenience the bulk Richardson number method was chosen for operational application. This method was implemented both in the official COSMO code and in 'Fieldextra', the official post-processing program of the COSMO consortium (see <http://www.cosmo-model.org>).

3.3 Evaluation of diagnosed turbulence characteristics

The different approaches for turbulence diagnosis described in Section 3.1 are validated on several measurement datasets, which are discussed in the following. First, an ideal convective case is investigated, followed by two real-world measurement campaigns. Finally, validation results against longer continuous turbulence measurements are presented.

3.3.1 Ideal convective case

The ideal convective case used for the evaluation of the COSMO-SC model is described in detail in Section 2.2. Here, the validation of turbulence characteristics against Large Eddy Simulation data is presented. For the diagnosis of turbulence variables the reference COSMO-SC run with the operational 60 vertical levels is used.

Figure 3.9 shows profiles of the standard deviations of wind fluctuations after the steady state was reached in the simulation. In the horizontal direction the standard deviation is considerably overestimated by the “SIM” approach throughout the whole PBL, while the “Direct-lev2” approach gives good results, especially in the middle of the PBL.

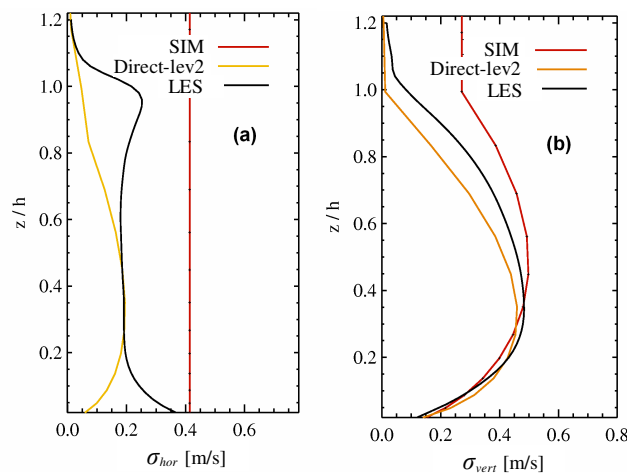


Figure 3.9: Profiles of the (a) horizontal and (b) vertical standard deviations of wind fluctuations for the ideal convective case. Turbulence variables are diagnosed with two different approaches (“Direct-lev2” and “SIM”) from single column simulations of the COSMO model. The reference is output from LES simulations according to Mironov et al (2000). On the y-axis the dimensionless height (ratio of the height above ground and the PBL height) is indicated.

The vertical standard deviation is simulated well by both methods, however, in the upper PBL the “SIM” method overestimates while the “Direct-lev2” method underestimates the LES values. It has to be noted that in the case of the “SIM” approach, the bulk Richardson number was used to determine the PBL height, which shows good agreement with the PBL height evaluated subjectively from the heat flux profile of the LES.

3.3.2 LITFASS-2003 convective case

COSMO simulations and turbulence measurements from the LITFASS-2003 campaign were also used to validate the input turbulence characteristics of dispersion models. Details of the

measurement dataset and the COSMO simulations are described in Section 2.3. For the present validation the reference COSMO-1 simulation with 60 vertical levels and three-dimensional turbulence scheme (“3D_diff” run) was used.

Figure 3.10 shows the diurnal cycle of diagnosed velocity fluctuations compared to tower turbulence measurements at 90 m height. For the selected LITFASS case three different post-diagnosis methods are compared: the similarity theory approach (“SIM”), and two approaches using the prognostic TKE of the COSMO model directly, applying either a level 2 closure (“Direct-lev2”) or a level 2.5 closure (“Direct-lev2.5”) for the partitioning of TKE.

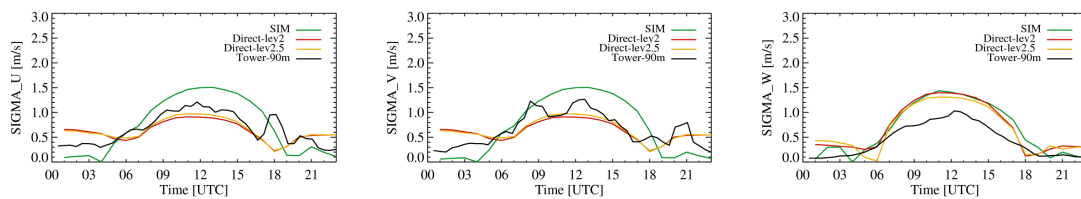


Figure 3.10: Time series of the standard deviations of along-wind (left), cross-wind (middle) and vertical (right) wind fluctuations at 90 m height for 30 May 2003 for the Falkenberg tower location during the LITFASS-2003 campaign. Colour lines: turbulence characteristics post-diagnosed from the COSMO-1 simulation with different approaches (see text); black line: tower turbulence measurements.

During daytime the “Direct” approaches predict the horizontal fluctuations with good accuracy, with a slight underestimation, while the vertical fluctuations are overestimated. During night time turbulence intensity is generally overestimated by the “Direct” approaches, which can be attributed to the overestimation of TKE by the COSMO model (see Figure 2.21f). Only very small differences can be detected between the level 2 and level 2.5 approaches, with the latter performing slightly better. The “SIM” approach overestimates both the horizontal and vertical fluctuations during daytime, which is caused by the overestimated surface heat flux in the COSMO simulation (see Figure 2.12). During night time turbulence variables are diagnosed slightly better by the “SIM” method than by the “Direct” approaches. It has to be added that for the other sonic anemometer at 70 m height the validation results are similar to that of the 90 m sensor (not shown). The other group of input turbulence variables for dispersion models, i.e., the Lagrangian time scales were not validated for the LITFASS-2003 campaign, as the calculation of Lagrangian statistics from Eulerian (fixed in space) measurements could be subject to large uncertainties.

3.3.3 GABLS3 stable case

Next to the above described convective case, the GABLS3 stable case was also investigated with respect to the diagnosed turbulence characteristics. The available measurements and the COSMO-SC simulation for this case are described in details in Section 2.4.

First, the different approaches for PBL height determination were tested on the diurnal cycle of GABSL3 (Figure 3.11). For the validation of the methods, different sources of measurements are available. During daytime conditions, PBL height was determined from windprofiler measurements, which method is in turn not reliable during night time due to the low turbulence intensity and the thin turbulent layer. Consequently, for stable conditions a very simple, but robust method was applied, namely, starting from the surface searching for the maximum of the temperature profile measured at the 200 m high tower (Fred Bosveld, personal communication). The drawback of this method is that it is not able to detect a stable boundary layer height above 200 m. At 0000 UTC the PBL height was also determined subjectively from radio sounding profiles.

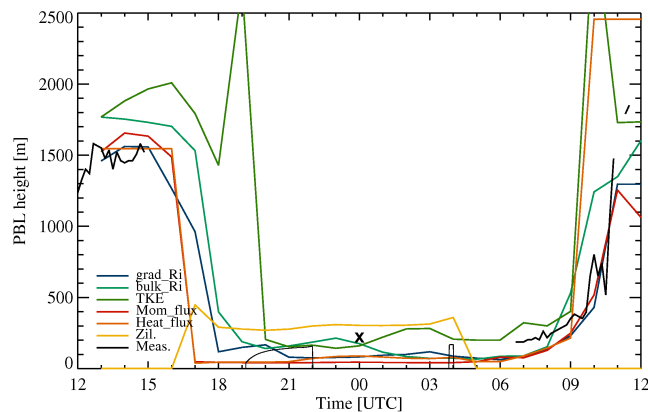


Figure 3.11: Time series of measured (black lines) and simulated (colour lines) PBL heights between 1 July 2006 1200 UTC and 2 July 2006 1200 UTC for the GABLS3 case. Thick black line: PBL height from windprofiler; thin black line: temperature profile method; black “x”: PBL height diagnosed from radio sounding profiles.

During the very stable night time hours the methods based on the gradient Ri , heat and momentum fluxes are considerably underestimating the PBL height, while the Zilitinkevich equation overestimates it. The bulk Ri and the TKE method diagnose a fairly accurate PBL height as compared to available measurements. The morning transition is best captured by the Ri methods and the momentum flux method, while the TKE method has notable difficulties during transition times. Based on these findings, similarly to the previous case studies, the bulk Ri method is used during the post-diagnosis of turbulence variables.

Figure 3.12 compares the diagnosed turbulent fluctuations to the tower turbulence measurements for the GABLS3 case.

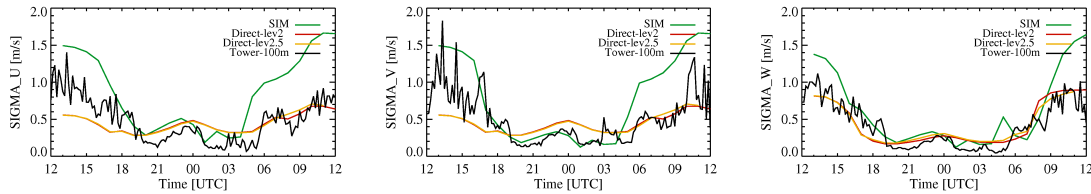


Figure 3.12: Time series of the standard deviations of along-wind (left), cross-wind (middle) and vertical (right) wind fluctuations at 100 m height between 1 July 2006 1200 UTC and 2 July 2006 1200 UTC for the GABLS3 case. Colour lines: turbulence characteristics post-diagnosed from the COSMO-SC simulation with different approaches (see text); black line: tower turbulence measurements.

For the unstable daytime hours the results are similar to those discussed for the LITFASS-2003 case, namely, the overestimation of turbulence intensity by the “SIM” approach and the adequate diagnosis of the “Direct” approaches. During the night time hours the “SIM” and “Direct” approaches are closer to each other, each of them performing well. The difference between the “Direct-lev2” and “Direct-lev2.5” methods is negligible in this case.

3.3.4 The CN-Met measurement campaign

In case of a nuclear emergency at a Swiss nuclear power plant (NPP), two different dispersion models are used for the calculation of the transport of radioactive pollutants. One is the ADPIC model, which is used by ENSI, the other is the LPDM of DWD, which is used by MeteoSwiss. Both these dispersion models need two types of information from the atmospheric flow: information on the mean wind (speed and direction) and information on the state of the atmospheric turbulence. Both types of information (mean wind and turbulence) can be derived from the COSMO numerical weather prediction model. A recent MeteoSwiss project called CN-Met (Centrale Nucléaire et Météorologie) aimed at updating the system delivering weather information used for emergency response purposes. As a part of this project the validation of turbulence characteristics derived from the COSMO-2 model against measurements was conducted.

Turbulence measurements during CN-Met

Turbulence measurements are carried out by the CN-Met measurement equipment at four sites in the close vicinity of the Swiss NPPs (Mühleberg, Beznau, Goesgen and Leibstadt). Table 3.1 describes the exact location and height of these sites.

Table 3.1: Location and height of the CN-Met turbulence measurement sites: Mühleberg (MUB), Beznau (BEZ), Goesgen (GOE) and Leibstadt (LEI).

	MUB	BEZ	GOE	LEI
Swiss coordinates - X	587.788	659.808	640.417	656.350
Swiss coordinates - Y	202.478	267.694	245.937	272.100
Altitude [m ASL]	480	326	381	341

In all the cases measurements are made at 10 m height above ground level, with Metek USA-1 sonic anemometers, with a measurement frequency of 20 Hz. The averaging period for the measured data is 10 minutes. The velocity variances are computed both in the geographical (north-south, east-west) and in the natural (along-wind – cross-wind) coordinate system. The time period used for the verification is 1 August 2008 – 31 October 2008.

Verification strategy

To evaluate the capability of COSMO-2 for predicting atmospheric turbulence, the diagnosed turbulence characteristics are compared to the measurements of the sonic anemometers. The verification was focusing on the variables listed in Table 3.2.

For the CN-Met project COSMO-2 runs are made with a 10-minute output frequency, similarly to the measurement averaging time. However, the parameterizations in the COSMO model were devised with respect to longer averaging periods, and hence it cannot be expected from such a model to correctly reproduce the atmospheric variability on the order of 10 minutes. Consequently, measurements and model results have been averaged over one hour before the comparison. When averaging 10-minute measurements both the high and low frequency part of turbulence should be calculated. This means, e.g., for variances that first the one-hour average of 10 minute variances should be computed (high-frequency part) and added to the variance of the 10 minute mean wind speed (low frequency part). On the contrary, the turbulence variables of the model can be used directly, as the turbulence parameterizations applied are already based on hourly or half-hourly averages, thus cover the entire spectrum.

Table 3.2: Verified turbulence variables during the CN-Met campaign.

Name	Short name	Dimension	Measurement height	Height in model
Standard deviation of zonal wind fluctuations ("Direct-lev2" method)	sigma_x	m/s	10 m	20 m
Standard deviation of meridional wind fluctuations ("Direct-lev2" method)	sigma_y	m/s	10 m	20 m
Standard deviation of vertical wind fluctuations ("Direct-lev2" method)	sigma_z	m/s	10 m	20 m
Standard deviation of along wind fluctuations ("SIM" method)	sigma_u	m/s	10 m	10 m
Standard deviation of cross wind fluctuations ("SIM" method)	sigma_v	m/s	10 m	10 m
Standard deviation of vertical wind fluctuations ("SIM" method)	sigma_w	m/s	10 m	10 m
Standard deviation of cross wind fluctuations ("ENSI" method)	sig_v_hsk	m/s	10 m	10 m
Standard deviation of wind direction ("ENSI" method)	sig_th_hsk	rad	10 m	10 m
Turbulent Kinetic Energy	TKE	m ² /s ²	10 m	20 m
Mean wind speed	Wind speed	m/s	10 m	10 m

In the following, verification results based on the averaging method described above will be presented. First, time series of measured and modelled turbulence variables will be compared, in order to have a closer look at the diurnal evolution of turbulence. Secondly, scatter plot diagrams will be examined to study the dependency of errors on the amplitude of the variable. Finally, verification scores (bias and standard deviation) will be shown for the whole time period, and the different interfacing approaches will be compared to each other. As COSMO-2 is integrated every three hours operationally, only the first three hours of a COSMO-2 integration were used during the verification. The dependency of the results on the lead time has not been investigated in this study.

Time series of turbulence variables

Turbulence in the PBL can either be generated by wind shear or by buoyancy effects. If a significant synoptic forcing is absent, then wind speed is stronger during daytime than during night time. This results in an increased shear production of turbulence during daytime. The buoyancy effects result in a turbulence production during unstable conditions (daytime) and turbulence destruction during stable conditions (night time). These two factors cause a typical diurnal cycle of turbulence evolution in the PBL, with high values during daytime and low or intermittent turbulence during night time. This diurnal cycle can be studied with the help of time series of turbulence variables.

Figure 3.13 depicts the time series of measured and modelled values of the standard deviation of vertical velocity fluctuations (after the “Direct-lev2” modelling approach), for a five-day period.

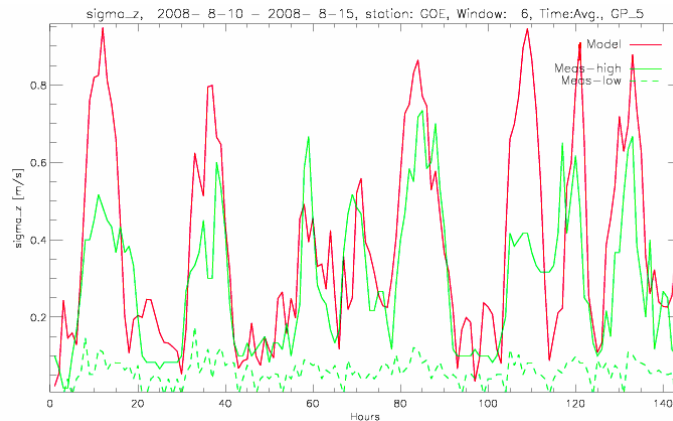


Figure 3.13: Time series of measured and modelled values of the standard deviation of vertical velocity fluctuations between 10 August 2008 at 0000 UTC and 16 August 2008 at 0000 UTC for the measurement site Goesgen. Green solid line: high-frequency part of measured turbulence. Green dashed line: low-frequency part of measured turbulence. Red solid line: modelled turbulence (after the “Direct-lev2” modelling approach).

The first two days show a clear diurnal cycle of turbulence, as described above, with high values during daytime and low values in the night. These two days were characterized by low winds and clear skies. On the figure the high- and low-frequency parts of the measured turbulence are plotted separately. The high-frequency part is clearly dominant, however, during night time the low-frequency part can also have a substantial contribution to the total turbulence.

To evaluate the performance of COSMO-2, first the primary model variables should be studied and only after this the post-diagnosed characteristics. Figure 3.14 shows measured and modelled time series for Turbulent Kinetic Energy (TKE), which is a primary model variable.

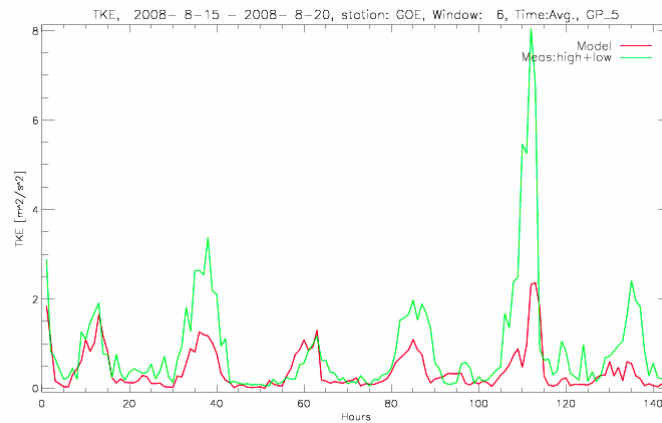


Figure 3.14: Time series of measured and modelled values of Turbulent Kinetic Energy (TKE) between 15 August 2008 at 0000 UTC and 21 August 2008 at 0000 UTC for the measurement site Goesgen. Green line: high- and low-frequency part of measured TKE. Red line: modelled TKE.

It can be seen that the high TKE values during daytime are underestimated. These high TKE values (e.g., the fifth day in the time series, 19 August 2008) are mostly associated with high wind speeds (17 m/s gusts on 19 August 2008), thus high TKE is generated mainly by shear production. This process is not adequately simulated by the model, which could be caused by the difference of roughness length in the model and reality (this problem will be further analyzed later).

Scatter plot diagrams

Figure 3.15 shows scatter plot diagrams for wind speed, TKE and two different post-diagnosed approaches for the standard deviation of the vertical wind fluctuations for the measurement site Goesgen. On the diagram for wind speed it can be seen, that the measured wind speed was very frequently lower than 1 m/s during the three-month period, and these very low wind speeds were usually overestimated by the model. The model tends to underestimate TKE for the whole measurement range, however, the underestimation is more pronounced for higher values of TKE, as it was shown for the measurement time series as well. The model performance for TKE and other turbulence variables is closely related to the roughness length in the model. Consequently, for a measurement site with higher roughness length in the model (e.g., Beznau, see Table 3.3), an overestimation of the lower TKE values would be the result. However, the underestimation of higher TKE values is still present even at this site. This might imply that the very high TKE values are caused by different physical processes than surface layer phenomena (e.g., the interaction of convection and turbulence) which mechanisms are not adequately described in the COSMO model. The last two scatter plot diagrams show results of the two different approaches

(“Direct-lev2” and “SIM”) for the diagnosis of the vertical part of turbulence. Overall, the two approaches are very close to each other, in good agreement with the measurements. However, the “Direct-lev2” approach tends to overestimate the higher turbulence values, while the “SIM” approach mainly underestimates the moderate turbulence values.

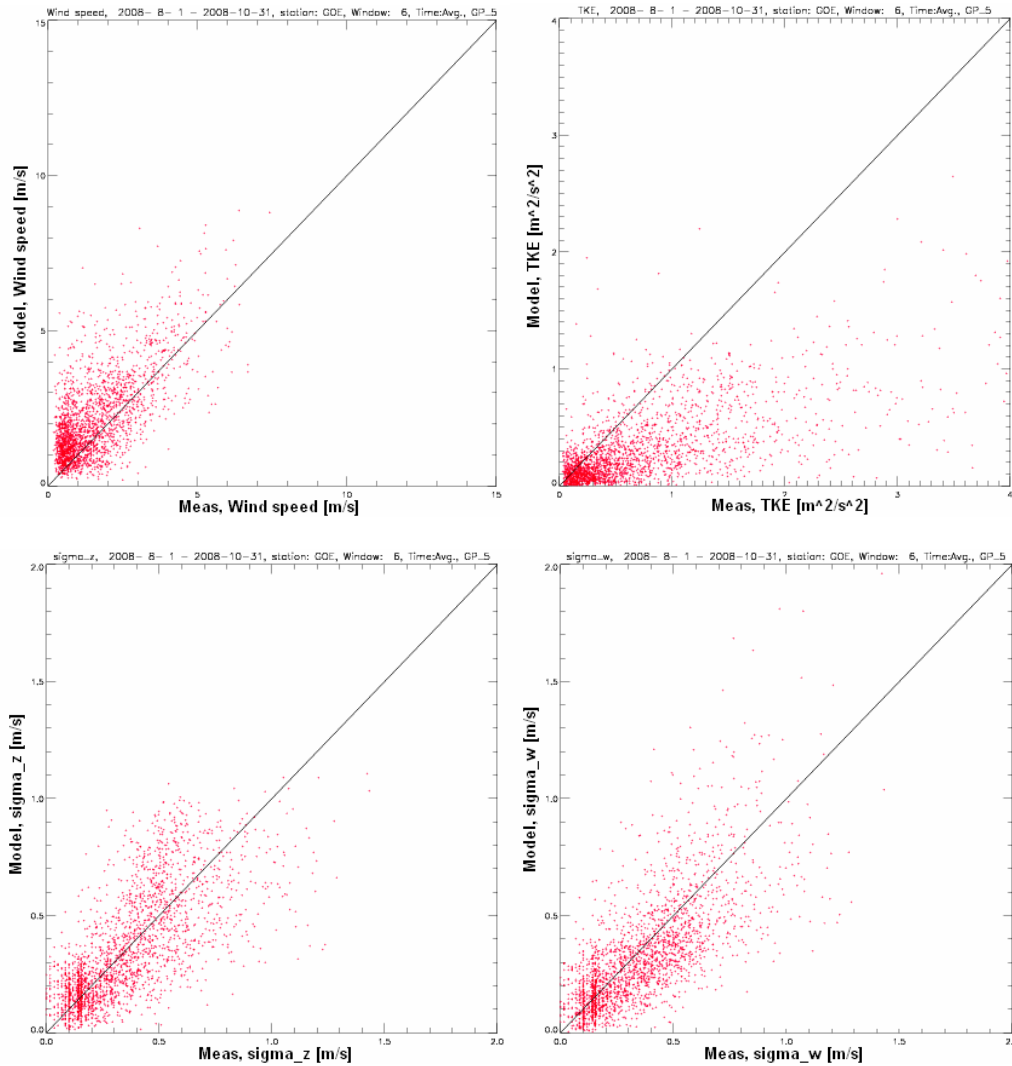


Figure 3.15: Scatter plot diagrams for wind speed (upper left), TKE (upper right) and two different post-diagnosed approaches for the standard deviation of the vertical wind fluctuations (“Direct-lev2”: lower left, “SIM”: lower right) for the measurement site Goesgen for the whole three-month verification period.

Note that the scatter plot diagrams of the other measurement sites show similar characteristics (not shown), however, results for the Beznau site are a bit different from the three other sites, which may again be attributed to a different roughness length in the model. This problem will be further analyzed in the next sub-section.

Verification scores

For the hourly averaged three-month dataset verification scores (bias and standard deviation of errors) were calculated for the turbulence variables listed in Table 3.2. As the amplitude of measured turbulence values can range over orders of magnitudes, relative scores were computed to allow for a fair comparison. If using relative errors, a verification threshold value should be set, for avoiding extremely high relative errors in the case of very small values. This threshold was $0.1 \text{ m}^2/\text{s}^2$ for TKE, 0.1 m/s for the other turbulence variables, and 1 m/s for wind speed. By interpreting the verification scores it has to be considered, that the estimated measurement error of the Metek USA-1 sensor regarding standard deviations of wind fluctuations is on the order of 10% (Christen et al., 2001). Consequently, relative model errors on the order of 10% for these turbulence variables should not be considered as significant results.

For the verification either the nearest grid point of COSMO-2 was chosen or an average of nine grid points was computed. The roughness lengths of these grid points in COSMO-2 are given in Table 3.3.

Table 3.3: Roughness lengths [m] of verified COSMO-2 grid points for the four measurement sites. No. 5 is the closest grid point, while no. 1 is the lower left and no. 9 is the upper right grid point.

	MUB	BEZ	GOE	LEI
1	0.73	1.04	0.89	0.62
2	0.04	0.59	0.44	1.02
3	0.10	0.87	1.02	0.85
4	0.18	1.03	0.39	0.79
5	0.21	1.04	0.14	0.40
6	0.76	0.56	0.25	0.22
7	0.08	1.02	0.25	0.12
8	0.14	1.01	0.56	0.39
9	0.39	0.39	0.79	0.70
Average	0.29	0.84	0.53	0.57

Figure 3.16 shows relative bias and standard deviation scores for the nearest grid point for the whole three-month period (hourly averages). As it was seen before on the scatter plot diagrams, TKE is underestimated by about 20-30% by the model, except for the Beznau site. This can be regarded as a good result for a mesoscale model with 2.2 km horizontal resolution over such a heterogeneous terrain as the Swiss Midlands (see e.g., Trini Castelli et al. (2006) for similar evaluations). Vertical turbulence is predicted with a relatively small bias (less than 10%) and larger standard deviation (around 50%). The two different approaches (“Direct-lev2” and “SIM”) are close to each other with smaller overestimation in the case of the similarity theory approach. The comparison of the two approaches for horizontal turbulence is not straightforward, as the “SIM” approach calculates the turbulence

characteristics in the natural coordinate system, thus distinguishes between along- wind and cross-wind turbulence. In the case of the “Direct-lev2” approach horizontal isotropy is assumed, thus the zonal and meridional turbulence intensity is always equal in the model. As opposed to vertical turbulence, horizontal turbulence is underestimated by the methods with around 50% relative bias in the case of the “Direct-lev2” approach and maximum 30-40% in the case of the “SIM” approach. The standard deviation of errors is smaller for horizontal turbulence (around 30%) than for the vertical turbulence.

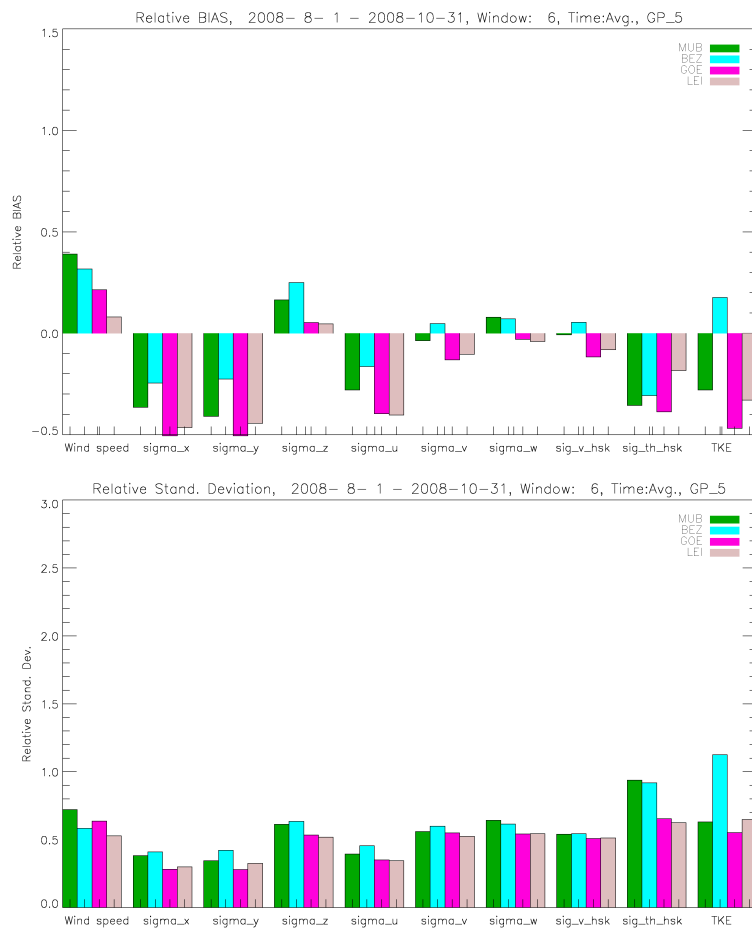


Figure 3.16: Relative bias (upper panel) and relative standard deviation (lower panel) scores, for the nearest grid point for the whole three-month period (hourly averages), for the four measurement sites (in different colours, see legend).

The turbulence measurements and the evaluated model variables are at 10 or 20 m height - both levels that are always located in the surface layer of the PBL. In the surface layer, the surface characteristics (e.g., roughness length) have a substantial impact on the turbulent state of the atmosphere. Consequently, the verified model variables are extremely sensitive to the surface characteristics. In some cases the measurement site may not be representative for the whole grid box, i.e., the local surface properties are different from the

grid box average. In such cases investigating neighbouring grid points or a grid point average with different surface properties can bring a benefit, as the surface property of a neighbouring cell or an average might better match the one at the measurement site. Figure 3.17 shows verification scores for the nine point averaged model values.

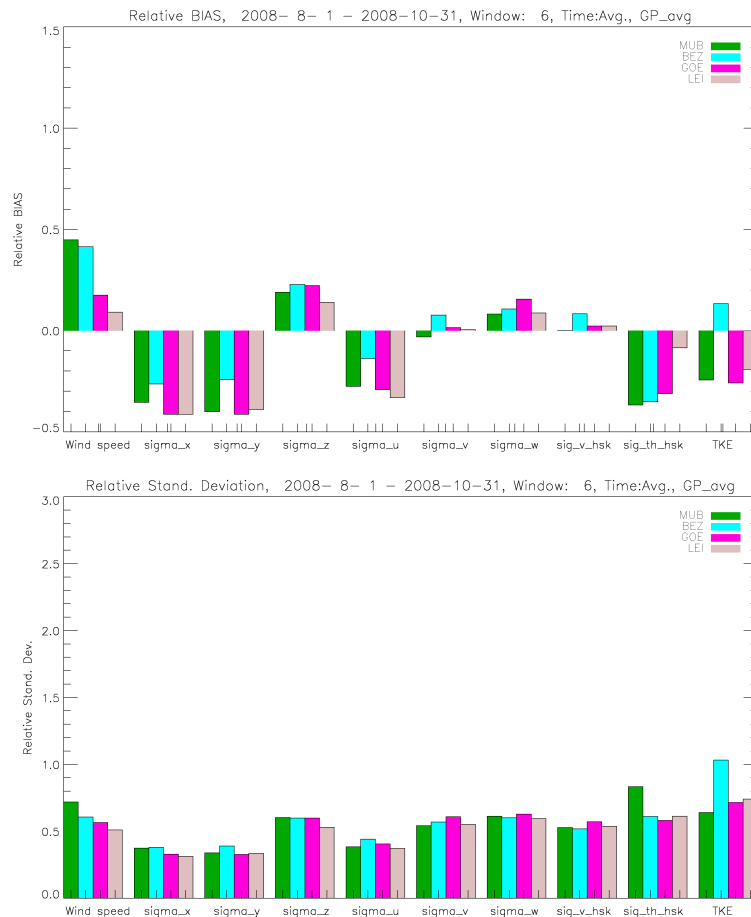


Figure 3.17: Same as Figure 3.16, but for the nine-point average.

By comparing Figure 3.16 and Figure 3.17 it can be concluded, that due to a higher roughness length of the averaged grid points (except for Beznau), higher turbulence values are present in the case of nine point averages than in the case of the nearest grid point. These higher values lead to improvement of the biases in the case of formerly underestimated variables (mainly TKE and horizontal turbulence). However, they result in a more pronounced overestimation for other variables (mainly vertical turbulence). Nevertheless, the nine point average roughness length is only by chance higher than the roughness length of the nearest grid point, thus the above statement cannot be generalized. In the case of the standard deviations, a slight increase can be seen for all averaged values.

The one-by-one analysis of all the neighbouring grid points reveals that the smallest biases of turbulence variables are obtained with a roughness length of approximately 0.5 m.

This value may seem still too high, as all the measurement sites are located on farmland or grassland, with a characteristic roughness length of 0.1 – 0.2 m. However, surface texture in the vicinity of the sites is quite heterogeneous, with patches of forests or buildings. During stratified conditions, this can result in small scale circulations which increase turbulence intensity (especially in the low frequency part). In near-neutral conditions the abrupt changes in the roughness length can cause the advective enhancement of turbulence. This effect can be modelled by introducing a so-called “secondary” roughness length, in addition to the “local” value (Schmid and Bünzli, 1995). These two processes (small scale circulations and advective enhancement) can explain, why the relatively high value of 0.5 m that proved to be optimal for the CN-Met measurement sites, is reasonable for this application.

When interpreting the results, it has to be kept in mind that in the case of the turbulence variables (“Direct-lev2” approach and TKE), model values at 20 m (first half level) were compared to measurements at 10 m (Table 3.2). This is due to the fact that the COSMO model uses staggered coordinates in the vertical, and although the first model level (for wind speed) is at 10 m, the first half level, where TKE is computed, is at 20 m. A possible solution for this problem could be to use the TKE values at the surface from the model, and average the surface and 20 m values. This approach results in slightly smaller turbulence values, but differences are negligible (not shown). This small sensitivity to the height of turbulence computation is also present in the values of the “SIM” parameterization if recomputed using 20 m height instead of the original 10 m (not shown). In any case, if the given application of COSMO-2 turbulence forecasts permits, it is desirable to use the turbulence values at their model height of 20 m.

3.4 Conclusions and outlook

In this chapter the second component of the emergency response system of MeteoSwiss, namely, the meteorological pre-processor was evaluated. The verification of the turbulence related input parameters of a dispersion model is not straightforward, as these atmospheric variables are not measured routinely. Consequently, data from several case studies and measurement campaigns was collected for this purpose.

The height of the Planetary Boundary Layer is one of the most important input parameters for many dispersion models. As the PBL height was not a standard output parameter of the COSMO model, seven methods were tested to diagnose this variable from standard COSMO output fields. These methods were validated against radio sounding measurements for ten ideal convective and stable cases and a one-month continuous period. Results suggest that the bulk Richardson number and the momentum flux profile are the

most reliable indicators of the PBL height. With these methods the PBL height can be diagnosed with a relative bias of 40% and relative standard deviation of 80% for unstable conditions. For stable conditions the corresponding scores are 80% (bias) and 200% (standard deviation). As the bulk Richardson number is more robust and easier to implement, this method was included in the official code of the COSMO model. Furthermore, a major advantage of the bulk Richardson number with respect to operational applications is the fact that it is based on the routinely verified atmospheric profiles of wind and temperature.

The validation exercise showed the drawback of radio soundings for PBL height determination (especially for stable cases) and pointed out the need for more accurate PBL height measurements with better time resolution. Measured aerosol backscatter ratios from Lidar (Light Detection and Ranging) instruments represent a unique source of information for the determination of the PBL height. A next step in the validation of the PBL heights predicted by the COSMO model should be a detailed comparison with Lidar measurements. In the COSMO consortium two projects have recently started with the active participation of the author. First, MeteoSwiss installed its own Lidar system in Payerne in 2008, which is now able to measure the aerosol backscatter ratio as well. Implementation of automated algorithms for the diagnosis of the PBL height from these measurements is currently underway. Secondly, in the framework of the BASE:ALFA project (Caporaso et al., 2010) an extensive measurement campaign was carried out involving Lidar measurements of the PBL height. Figure 3.18 presents a first intercomparison of different PBL height determination methods from COSMO outputs and Lidar measurements.

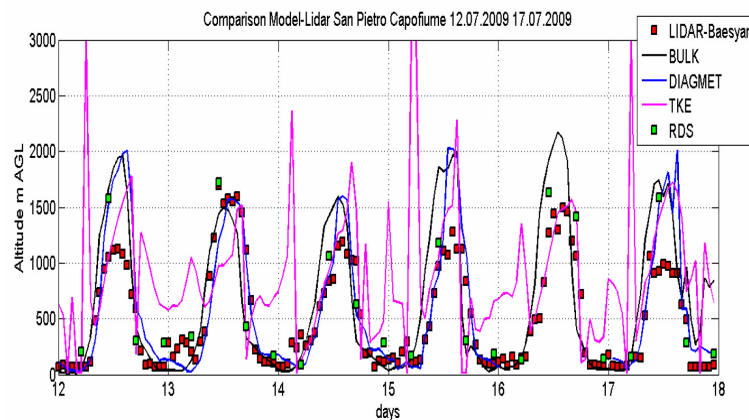


Figure 3.18: Time series of measured and modelled PBL heights from the BASE:ALFA measurement campaign between 12 July 2009 at 0000 UTC and 18 July 2009 at 0000 UTC at the San Pietro Capofume (Italy) station. Red squares: Lidar measurement; green squares: PBL height diagnosed from radio soundings with the bulk Richardson method; blue line: DIAGMET pre-processor; PBL heights diagnosed from COSMO outputs with the bulk Richardson number (black line) and TKE methods (pink line). This figure was produced by Luca Caporaso (SIMC ARPA Emilia Romagna).

These results highlight the excellent time resolution of Lidar measurements as compared to radio soundings. Similarly to the radio sounding verification, the bulk Richardson number method gives the most reliable diagnostics among the different approaches described in this chapter. It has to be noted though that the validation of PBL heights should be repeated or even performed routinely as soon as reliable Lidar observations are available for this variable on a regular basis.

After the evaluation of the diagnosed PBL heights the input turbulence variables of Lagrangian dispersion models were evaluated. As reliable measurements of the Lagrangian timescales were not available from observations, the evaluation was restricted to the standard deviations of the velocity fluctuations. Three selected case studies were investigated during this task: an idealized LES case of the dry convective boundary layer, a real-world dry convective case from the LITFASS-2003 campaign and the GABLS3 diurnal cycle. During convective situations the similarity approach tends to overestimate the turbulence intensity, while the approaches based on the direct usage of TKE give more accurate results. For stable conditions the different approaches are closer to each other and give reasonable predictions. The difference between the “Direct” approaches based on the level 2 and level 2.5 closures is nearly negligible, consequently, it is recommended to use the level 2.5 approach for turbulence post-diagnosis, as it is consistent with the turbulence parameterization of the COSMO model. The verification exercise also showed the need for reliable LES data for the evaluation of dispersion related turbulence parameters, as especially during convective conditions the upper parts of the PBL are extremely difficult to be measured by direct sensors.

Three-month continuous turbulence measurements of the CN-Met campaign were also used for model evaluation. The verification results show an overall good performance of the COSMO-2 model, with all the selected turbulence parameters being in an acceptable range (20-30% relative bias and 50% relative standard deviation). Turbulent kinetic energy, which is the only turbulence related model variable in COSMO, is generally underestimated by the model, except for the one site, where the model grid points are characterized by a significantly higher roughness length, compared to other sites. This indicates that due to local characteristics (e.g., shading by nearby objects or the above discussed secondary roughness length) the measurement sites might not be representative for a whole grid box of the COSMO-2 model and thus the results should be handled with certain care. Reasonable performance was observed in the case of vertical turbulence, which is the most important turbulence variable with respect to mesoscale dispersion modelling. The standard deviations of horizontal wind speed are not as well predicted as that for the vertical component. The method based on similarity theory shows slightly better performance than that based on the direct use of TKE from the COSMO model, which is caused by the assumption of horizontal isotropy in the case of the latter approach.

After the analysis of all the results from the evaluation of turbulence variables for dispersion models it is very difficult to decide which method (the “SIM” or the “Direct” approach) could be recommended for operational applications. The different validation exercises favour different choices. For the case studies, which are idealized settings or “very simple” atmospheric situations, the “Direct” approach turned out to fit the observations and LES data better, however, for the longer evaluation campaign (CN-Met Project) the similarity approach gave better scores. To decide between the coupling approaches these sources of validation information should be weighted. In the author’s opinion, at this first step of meteorological pre-processor evaluation (at least in the COSMO consortium) more weight should be given to the idealized or very simple case studies, because these are the situations when the pure performance of the turbulence scheme can be understood. Of course, a longer measurement campaign is very useful to assess the general model performance for “everyday” cases, however, the compensating errors from different parts of the modelling system (e.g., numerics, different physical parameterizations like soil processes or cloud microphysics) might make it difficult to understand the results in depth.

Following this reasoning the turbulence coupling method based on the direct usage of TKE is recommended for operational use, because it performed better for the investigated case studies. One further advantage of the “Direct” method is that it does not use the PBL height which means an additional uncertainty when using the similarity approach. The major deficiency of the currently applied “Direct” approach is the isotropic parameterization for horizontal turbulence, which should be improved. One possible solution would be to use similarity considerations to diagnose the ratio of along-wind and cross-wind turbulence for the horizontal part of the prognostic TKE. It also has to be noted that the direct usage of TKE for dispersion modelling applications means a very strong coupling between the NWP and the dispersion model, which requires a tight collaboration between these two modelling communities. Any changes in the turbulence scheme of the NWP model (or other components related to it) should be carefully tested with respect to dispersion results as well.

Finally, it has to be emphasized that these findings are based on only a limited number of cases thus it would be desirable to conduct other validation studies in connection with the turbulence coupling of NWP and dispersion models. For such kind of an evaluation campaign the following points are recommended based on this study:

- Measurement campaigns should be performed (or previous campaigns revisited) both for stable and unstable conditions on carefully selected locations, where the shading of the measurement sensors is avoided.
- During the campaign turbulence measurements should be conducted not only near the surface but also at higher levels.

- Next to the turbulence intensity, the height of the Planetary Boundary Layer should also be measured with remote sensing instruments (e.g., Lidar) at high vertical and temporal resolutions.
- Tracer experiments should be conducted to be able to assess the impact of turbulence on the dispersion process.
- Selected cases from the measurement campaign should be investigated with Large Eddy Simulation models which give a full three-dimensional picture of the turbulent flow and might be very useful for the evaluation of NWP and dispersion models.

One of the most important questions arising after the evaluation results presented in this chapter are to what extent these turbulence variables are affecting the concentration forecasts and what are the roles of other uncertainties in the modelling system. In the next chapter these topics are investigated based on a modelling exercise of a real tracer experiment in highly complex terrain.

Acknowledgements

The author would like to thank Hubert Glaab and Barbara Fay (DWD) for useful discussions about the 'Lagrangian Particle Dispersion Model' of DWD. Thank goes to Luca Caporaso and Francesca Di Guiseppe (ARPA-SIMC) for sharing their research results in connection with the BASE:ALFA campaign.

4 Simulation of pollutant transport in complex terrain with a NWP – particle dispersion model combination³

4.1 Introduction

The continuous development of atmospheric weather prediction models has led to the application of increasingly finer grids on which these models are integrated. The finer resolution inevitably results in a more complex model orography over mountainous areas, which can cause numerical difficulties in the models. The correct simulation of all the relevant processes related to complex topography is one of the most challenging tasks within the numerical modelling community. Due to developments in transportation and tourism, human presence in the mountains is increasing. Consequently, it is of major importance to accurately simulate meteorological conditions as well as air quality in mountainous terrain.

Mesoscale air quality modelling systems consist of two main parts. For the simulation of the atmospheric flow usually a numerical weather prediction (NWP) model is used, which provides three-dimensional fields of meteorological variables like wind, temperature and pressure. For the modelling of the transport, diffusion and interaction of pollutants an air quality model is applied. These two models have to be coupled by a so-called meteorological pre-processor, which provides all the parameters that are not readily available in the output of the NWP model.

Detailed numerical investigation of small-scale atmospheric flow in mountainous terrain has started only in the 1990s. The reason for this late start is twofold. On the one hand, to accurately simulate the flow over complex topography, a very fine numerical grid has to be used, which imposes high computational costs. On the other hand, non-hydrostatic motions play a dominant role on these relatively fine scales what prohibits the application of hydrostatic models, which were generally used before the 1990s. One of the first studies at very high resolution was that of Enger et al. (1993), who used 700 m horizontal resolution to simulate the flow in the Colorado River Valley. Zängl et al. (2004) used the MM5 model with 1 km mesh size to simulate a foehn event in the Alpine Rhine Valley. Several studies concentrated on the Riviera Valley in southern Switzerland. De Wekker et al. (2005) used the

³ This chapter is based on a paper with the same title by B. Szintai, P. Kaufmann and M. W. Rotach, accepted to *Boundary-Layer Meteorology*.

Regional Atmospheric Modeling System (RAMS) on a 333 m grid, while Chow et al. (2006) applied the Advanced Regional Prediction System (ARPS) with horizontal resolutions down to 150 m. In the framework of the ALPNAP Alpine Space project (Heimann et al. 2008) detailed investigations were conducted in connection with the meteorology and air quality of Alpine valleys. Schicker and Seibert (2009) simulated flow conditions in the Inn Valley with the MM5 model and found that an 800 m resolution is needed to correctly reproduce the characteristic features of the valley atmosphere.

In the past decades many air quality models have been evaluated over mountainous terrain. Due to the complex flow pattern, simplified Gaussian models are inadequate to simulate the transport and diffusion of pollutants, thus more sophisticated Eulerian or Lagrangian models have to be applied, coupled to mesoscale meteorological models. Enger and Koracin (1995) simulated SO₂-concentrations in the Colorado River Valley with an Eulerian dispersion model. Carvalho et al. (2002) evaluated a modelling system composed of the meteorological model RAMS and the particle model SPRAY for the TRACT field experiment (TRANsport of Air Pollutants over Complex Terrain) in the Rhine Valley. Trini Castelli et al. (2007) applied the same modelling system to simulate traffic pollution in the Susa (Italy) and Maurienne (France) valleys. Michioka and Chow (2008) used the ARPS model with as fine as 25 m horizontal resolution to simulate scalar transport in complex terrain.

In the standard output of most NWP models not all the variables that are necessary for dispersion models are present. Consequently, a meteorological pre-processor has to be used which derives all these – in most cases turbulence related – variables. Meteorological pre-processors are either integrated in the dispersion model, like in the case of the FLEXPART model (Stohl et al. 2005), or are separate programs, like in the case of the METRODOS pre-processor (Astrup et al. 2001) or the MIRS code (Model for Interfacing RAMS and SPRAY, Trini Castelli and Anfossi 1997). In most cases, to obtain profiles of turbulence characteristics some kind of similarity approach is used (Hanna 1982), where the standard turbulence profiles are scaled with surface variables and the height of the planetary boundary layer (PBL). These scaling relationships are usually based on turbulence datasets over flat and homogeneous surface. However, turbulence structure in complex terrain, such as in steep and narrow Alpine valleys, can be substantially different from flat conditions.

In this paper a new scaling approach from Weigel et al. (2007) suited for steep and narrow Alpine valleys is investigated with respect to pollutant dispersion. The new interfacing approach is compared to the classical flat-terrain approach and to tracer concentration measurements from the TRANSALP-89 campaign. For the simulation of the atmospheric flow and the tracer dispersion, the operational emergency response system of MeteoSwiss is used, which consists of the NWP model COSMO coupled to a Lagrangian Particle Dispersion Model (referred to as LPDM in the following).

The measurement campaign is briefly described in Section 4.2. In Section 4.3 the applied models and methods are introduced. Results from the simulations are described in Section 4.4, while Section 4.5 presents several sensitivity experiments. Findings are summarized in Section 4.6.

4.2 The TRANSALP-89 campaign

TRANSALP stands for “Mesoscale transport of atmospheric pollutants across the Alps” and is one of the two experimental activities of the TRACT project (Fiedler 1989). In the framework of TRANSALP three consecutive measurement campaigns with increasing size and complexity were carried out in southern Switzerland (Ambrosetti et al. 1998).

TRANSALP-89 was a small-scale tracer experiment conducted in October 1989 in the Riviera, Leventina and Blenio Valleys. The experiment domain is highly complex, with north-south directed steep and narrow valleys. The valleys are around 6 km wide (crest-to-crest) and 1500 m deep, with ridges over 2500 m a.s.l. The wider Riviera Valley runs from south to north and at Biasca it bifurcates to the smaller Leventina and Blenio Valleys (Figure 4.1d).

During TRANSALP-89 two tracer experiments were conducted on 5 and 19 October 1989. The meteorological situation on both days was characterized by an anticyclone, with weak large-scale forcing and cloud free conditions, which favoured the development of a valley wind system. Previous numerical studies of the TRANSALP-89 campaign concentrated on the second tracer release. Desiato et al. (1998) successfully simulated the valley wind with diagnostic wind field models. Using these wind fields Anfossi et al. (1998) simulated the tracer concentrations with two Lagrangian particle models. As opposed to these simulations the current work is based on prognostic models and thus enables the evaluation of a real emergency system which can be applied in hazardous situations.

In the present study both days of the campaign are investigated. For the experiments perfluoro-methyl-cyclohexane (C_7F_{14}) was released 8 m above ground at Iragna (287 m a.s.l.) between 1000 and 1100 UTC at a constant emission rate of 0.004 kg s^{-1} . The tracer was measured with 25 surface samplers at half-hourly intervals in both the Leventina and Blenio Valleys (Figure 4.1d). Samplers were located at different elevations on the valley floor and on the slopes. During TRANSALP-89 several meteorological measurement instruments (sodar, sonic anemometer, surface stations) were deployed as well. In this paper, the surface meteorological stations operated by MeteoSwiss are used for the evaluation of wind and temperature time series.

4.3 The modelling system

4.3.1 The COSMO model

The COSMO model is a non-hydrostatic, limited-area numerical weather prediction model (Doms and Schaettler 2002) which is being developed in the framework of the COSMO consortium (COnsortium for Small-scale MOdelling). At MeteoSwiss the COSMO model is run operationally at two horizontal resolutions. COSMO-7 has a horizontal resolution of 6.6 km and is integrated on a European domain (Figure 4.1a), while COSMO-2 has a 2.2 km horizontal resolution, and its nested domain covers the Alps (Figure 4.1b). For the present study the COSMO model was also run on a 1.1 km grid (COSMO-1), nested in COSMO-2, covering southern Switzerland (Figure 4.1c).

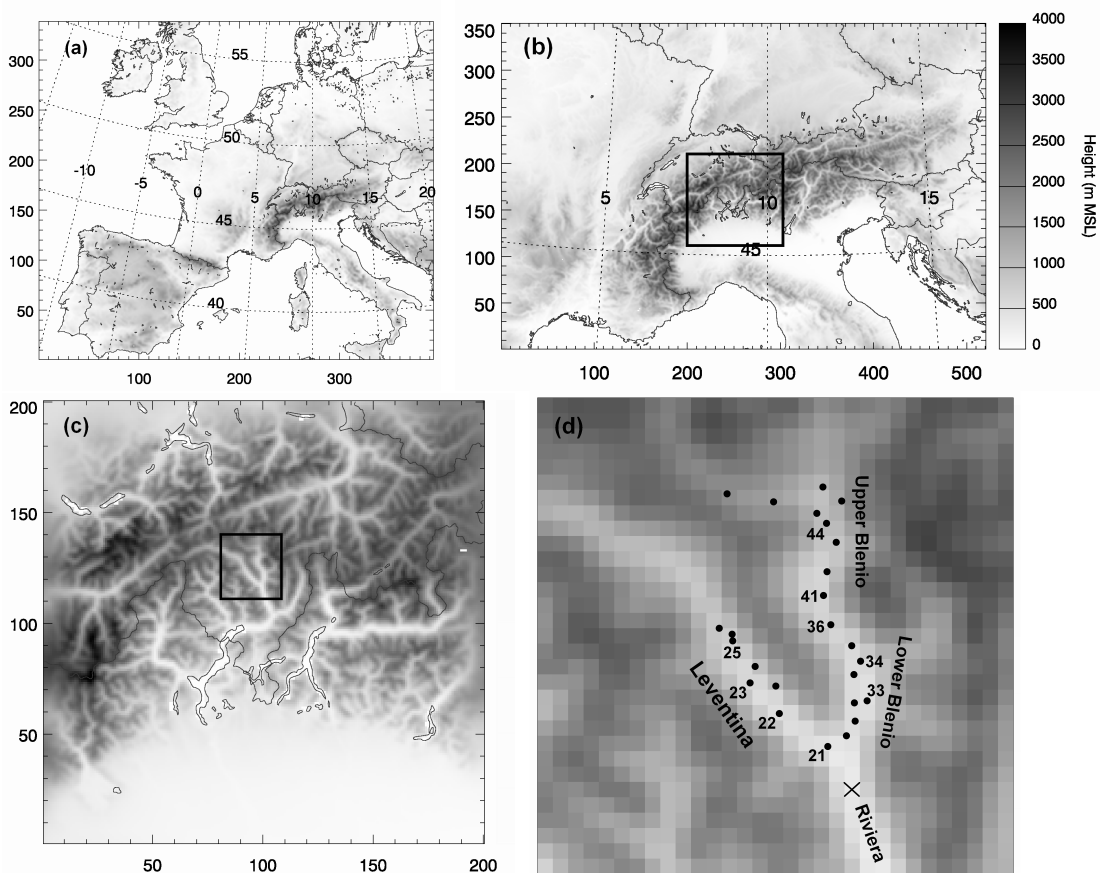


Figure 4.1: Model domains of the (a) COSMO-7, (b) COSMO-2 and (c) COSMO-1 simulations. Rectangle on (b) indicates the COSMO-1 domain. Rectangle on (c) marks the zoomed area of (d), where the valleys of interest and the locations of tracer measurement stations (black dots) are indicated. Tracer emission location is marked with X. On the axes the grid point numbers are indicated.

The initial and boundary conditions for COSMO-7 were obtained from the ERA-Interim Reanalysis; during the consecutive nesting no additional data assimilation was used. For all the three COSMO versions the same terrain-following stretched vertical coordinates were applied with 60 levels. The resolution was 20 m near the surface and reached 1000 m at the model top at some 23 km altitude. The timesteps for the integration were 60, 20 and 1 s for the 6.6, 2.2 and 1.1 km grid, respectively. The very small timestep which was necessary for a stable model performance at 1.1 km horizontal resolution could imply some deficiencies in the numerical core of COSMO in the presence of very steep model orography. However, further investigation of this problem is beyond the scope of the present study.

For the parameterization of atmospheric turbulence the COSMO model uses a 1.5-order closure (Buzzi et al. 2009), which corresponds to level 2.5 in the Mellor and Yamada notation (Mellor and Yamada 1982). This closure type carries a prognostic equation for turbulent kinetic energy (TKE). Numerical horizontal diffusion is only applied close to the lateral boundaries due to the relatively high numerical diffusivity of the Runge-Kutta time integration scheme. For deep convection, a mass-flux scheme after Tiedke (1989) is applied in COSMO-7. In COSMO-2 and COSMO-1 deep convection is supposed to be resolved explicitly and thus a simpler shallow convection scheme is used. A topographical radiation correction scheme is applied (Müller and Scherrer 2005; Buzzi 2008) to account for the correct description of surface radiation processes of sloped model surfaces. COSMO is coupled with an eight layer soil model (Schrodin and Heise 2001) with the deepest (climatological) layer at 14.5 m depth. Initial temperature and moisture in the soil are interpolated from the ERA-Interim Reanalysis.

The COSMO model predicts all the meteorological parameters (e.g., wind and temperature profiles) which are relevant for dispersion modelling with high accuracy. At MeteoSwiss the COSMO model is continuously verified against radio soundings (Arpagaus 2005) and surface observations (Kaufmann 2005).

4.3.2 The Lagrangian Particle Dispersion Model

The present Lagrangian Particle Dispersion Model was developed by Glaab et al. (1998) at the German Weather Service (DWD), and is used at MeteoSwiss for the calculation of pollutant dispersion in emergency situations. Since a rather generic name ('LPDM') has been used in previous papers (e.g., Glaab et al. 1998, Folini et al. 2008) this acronym will be used in the following. In LPDM the trajectory of each particle is calculated using the actual wind velocity at the position of the particle, which is decomposed into a mean and a turbulent component. In the horizontal direction isotropic turbulence is assumed, and consequently the actual velocity components can be written as:

$$u = \bar{u} + u' \quad (4.1)$$

$$v = \bar{v} + v' \approx \bar{v} + u' \quad (4.2)$$

$$w = \bar{w} + w', \quad (4.3)$$

where \bar{u} , \bar{v} and \bar{w} are the grid scale mean velocity components in zonal, meridional and vertical directions respectively and are taken directly from the COSMO model. u' and w' are the horizontal and vertical velocity fluctuations and are computed using the Langevin equation. In the horizontal direction LPDM assumes homogeneous Gaussian turbulence, thus the Langevin equation reads:

$$u'(t + \Delta t_h) = R_h u'(t) + \sqrt{1 - R_h^2} \sigma_h \xi, \quad (4.4)$$

where R_h is the autocorrelation function, σ_h is the standard deviation of velocity fluctuations and Δt_h is the timestep in the horizontal direction. ξ is a random number chosen from a Gaussian distribution. In the vertical direction inhomogeneous Gaussian turbulence is assumed, and the Langevin equation can be written as (Legg and Raupach 1982):

$$w'(t + \Delta t_w) = R_w w'(t) + \sqrt{1 - R_w^2} \sigma_w \xi + T_{L_w} (1 - R_w) \frac{\partial \sigma_w^2}{\partial z}. \quad (4.5)$$

with the same notation as for Equation (4.4). The first term on the right hand side of Equation (4.5) describes the correlated part of the wind fluctuation, while the second term denotes the random part. The third term is the so-called drift correction term which is applied so that the model fulfils the well-mixed criterion (Thomson 1987) also in the case of moderately inhomogeneous turbulence.

By comparing Equations (4.4) and (4.5) it can be noticed that in the horizontal direction no drift correction is applied in LPDM, due to the assumption of horizontally homogeneous turbulence. The complex topography of the TRANSALP simulation indeed gives rise to inhomogeneous turbulence fields also in the horizontal direction, which would require the application of a drift correction term in Equation (4.4). However, detailed investigation of simulated tracer concentration cross-sections has not revealed any unrealistic “pile-up” of the

tracer in the valley thus suggesting that at least the horizontal inhomogeneity is not the dominant factor determining the tracer concentrations. For the present case this might be attributed to the fact that due to the strongly convective conditions horizontal velocity variances (and their gradients) are usually an order of magnitude lower than the vertical variances and thus the tracer dispersion is dominated by vertical turbulent motions.

For the autocorrelation function an exponentially decaying function is assumed, both for the horizontal and vertical directions:

$$R = e^{-\frac{\Delta t}{T_L}}, \quad (4.6)$$

where T_L is the Lagrangian integral timescale, the derivation of which is described in the following section.

During the dispersion runs a 60 s timestep was used in the horizontal and 5 s in the vertical direction. The concentration grid was identical to the grid of the COSMO model. To simulate the tracer cloud, more than 100.000 particles were emitted from the source. As the tracer used in the TRANSALP-89 campaign was completely inert, dry and wet deposition was switched off in LPDM.

4.3.3 Turbulence coupling between COSMO and LPDM

The turbulence coupling of COSMO and LPDM is performed with a separate program, which allows performing sensitivity experiments in a more convenient manner. The task of this coupling interface is to determine two variables needed by LPDM as three-dimensional fields: the standard deviation of velocity fluctuations and the Lagrangian integral timescales in both the horizontal and vertical directions. Currently, there are three options implemented in the coupling interface to derive these variables, which are presented in the following.

Direct usage of TKE

In the case of the operational coupling option, TKE and turbulent diffusion coefficients are used directly from the COSMO model (in the following denoted as “Direct” approach). The standard deviations of velocity fluctuations are determined from:

$$\sigma_k = \sqrt{2m_k e}, \quad (4.7)$$

where m_k is the portion of TKE (e) for the given coordinate direction (horizontal or vertical). The formula computing the vertical portion of TKE can be derived from the Level 2 closure of Mellor and Yamada (1974):

$$m_w = \frac{\sigma_w^2}{2e} = \frac{1}{3} - 2L_c \frac{1 + 2R_f}{1 - R_f}. \quad (4.8)$$

R_f is the flux Richardson number derived from the gradient Richardson number following Mellor and Yamada (1974), which is in turn calculated from wind and temperature differences of adjacent model layers; $L_c=0.052$ is the ratio of the return-to-isotropy length scale (Rotta 1951a, 1951b) and the dissipation length scale (Kolmogorov 1941). Assuming a horizontally homogeneous turbulence, the horizontal portion of TKE reads as:

$$m_u = \frac{1}{2}(1 - m_w). \quad (4.9)$$

The Lagrangian integral timescale is determined following Batchelor (1949) for both the horizontal and vertical directions as:

$$T_L = \frac{K_m}{\sigma^2}, \quad (4.10)$$

where K_m is the turbulent diffusion coefficient for momentum. K_m in the vertical direction is taken directly from the COSMO model. However, as the COSMO model uses a one-dimensional turbulence scheme, there is no diffusion coefficient computed in the horizontal direction. Consequently, the parameterization proposed by Smagorinsky (1963) is applied for K_m in the horizontal direction. The Smagorinsky approach is a first order closure for turbulent diffusion, which relates the diffusion coefficient to the deformation of the horizontal wind field.

Similarity theory approach

In the second coupling approach, similarity theory considerations are used to derive the turbulence variables needed by LPDM (further referred to as the “SIM” approach). In the case of similarity approaches, usually the surface fluxes and a diagnosed PBL height are needed from the NWP model. The approach proposed by Hanna (1982) and applied in the coupling interface of LPDM is often used in Lagrangian dispersion models (e.g., Stohl et al. 2005). For the diagnosis of turbulence characteristics, the boundary layer parameters h , L , w_* , z_0 and u_* are used, i.e. the PBL height, the Obukhov length, the convective velocity scale, the roughness length and the friction velocity, respectively.

The surface variables can easily be extracted from the COSMO model, but the determination of the PBL height is not so straightforward, as several methods exist to derive this variable from NWP outputs (Seibert et al. 2000; Szintai and Kaufmann 2008). Based on a comparison with radio sounding profiles (Szintai et al. 2009), the bulk Richardson number method (Sørensen et al. 1996) was chosen for the coupling interface to determine the PBL height. Above the PBL the turbulence characteristics are kept constant in the “SIM” approach. In the horizontal direction the values at the PBL top are used in the free troposphere. However, in several sensitivity studies it became clear that in some situations the “SIM” approach results in too large values of the vertical turbulence parameters at the PBL top. Consequently, in the free troposphere a constant value of 0.3 m s^{-1} was used for σ_w and 200 s for T_{L_w} , as suggested by the average values of the “Direct” approach (note, that the TKE scheme of the COSMO model is applied on all model levels, also above the PBL).

It has to be considered that most of the similarity relations used in today’s dispersion models are based on field experiments which were performed over horizontally homogeneous and flat terrain. For instance, the approach proposed by Hanna (1982) is based on the Minnesota field experiment (Readings et al. 1974), which was conducted over a flat cropland. Consequently, the validity of approaches based on these flat-terrain datasets is questionable in highly complex topography such as the Alps. In the following, a new method is proposed which accounts for the special turbulence conditions observed in steep and narrow Alpine valleys.

Turbulence coupling in Alpine valleys

During the Riviera Project (Rotach et al. 2004) of the Mesoscale Alpine Program (MAP) meteorological conditions in a steep and narrow Alpine valley were extensively studied. Among others the scaling properties of TKE were investigated. Over flat, homogeneous terrain mixed-layer similarity predicts TKE to scale with the convective velocity scale (w_*) as a function of z/z_i . Naturally, the local w_* (i.e., the w_* determined from the surface heat flux directly under the profile of interest) would be chosen for the scaling of TKE. Analysis of airborne turbulence measurements in the Riviera Valley showed that daytime profiles of TKE did essentially not scale at all using the local w_* . Rather, it was found that TKE profiles scale very well if w_* is obtained from the sunlit eastern slope (i.e., the slope facing to the east) and not from the surface directly underneath the measured profiles (Weigel and Rotach 2004). This scaling behaviour was also reproduced by high-resolution Large Eddy Simulation runs (Weigel et al. 2007).

The findings of Weigel and Rotach (2004) are based on available observations, i.e. strictly speaking only valid for TKE profiles in the centre of a valley. Over the slopes the situation has not been investigated in detail. Also, the results of Weigel and Rotach (2004) and Weigel et al. (2007) reveal that the scaled TKE profiles in the valley centre are a function of z/z_i alone, viz.

$$TKE / w_{*,slope}^2 = f_{TKE}(z / z_i), \quad (4.11)$$

but this function has, due to the limited data available, not explicitly been determined. In order to test the hypothesis that this scaling behaviour has a substantial impact on pollutant dispersion characteristics, we make the following assumptions for an improved coupling interface in complex terrain (denoted “SIM-ct”, for similarity in complex terrain):

- The revised scaling is applied to all valley floor grid points (not only to valley centre), but not to grid points over the slopes.
- Due to the lack of better knowledge, for all grid points the well-known flat-terrain similarity relations are employed, but using a different w_* as a scaling variable for valley floor grid points (see details below).
- Application is restricted to those locations and conditions for which the scaling characteristics were actually observed. Whenever no information is available (on the slopes, non-convective conditions) the traditional similarity approach is used.

In the following the procedure to select “valley grid points” and the determination of the relevant surface fluxes is described in some detail.

First, a valley mask is defined on the model domain, where the new approach is applied. A model grid point is considered as “valley” point when the following two conditions apply:

- (i) The model surface height is below a predefined height. This threshold is changing in the meridional direction due to the geometry of the southern Alps.
- (ii) Both to the West and to the East of the considered grid point a “mountain” grid point can be found within a predefined horizontal distance (e.g., 10 km). A grid point is defined as “mountain” point if it is 200 m higher than the valley threshold.

With the above two conditions only north-south directed valleys are selected (Figure 4.2). The reason for this is the fact that the new scaling approach is based on studies from a north-south directed valley and does not necessarily apply to valleys with other orientation. Note, however, that this restriction is only marginally relevant in the present study because the tracer experiment also took place in a more or less north-south directed valley system.

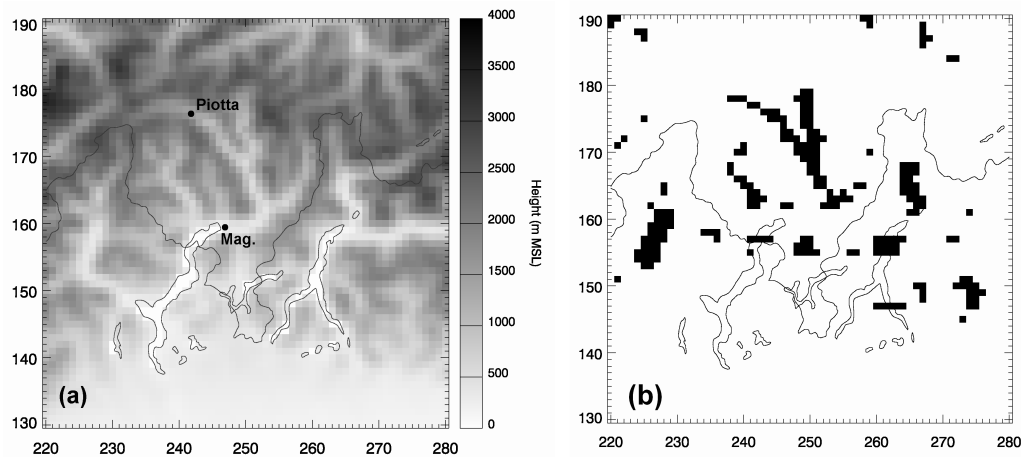


Figure 4.2: COSMO-2 model orography (a) and the valley mask (b, marked with black), as described in Section 4.3.3. Two surface meteorological stations (Magadino and Piotta) used for COSMO verification are also shown. On the axes the grid point numbers are indicated.

After the valley mask is defined the “SIM-ct” approach is applied to a given “valley” point (**A**) in the following way:

- 1) The first “non-valley” grid point (**B**) is searched to the east of **A** (this is the eastern slope of the valley). If **B** has a negative surface sensible heat flux (H_s), then the normal “SIM” approach is used for **A**, as the findings of Weigel et al. (2007) only apply to convective conditions. Moreover, the new scaling approach is applied only in the afternoon hours (between 1200 UTC and 1900 UTC, for both simulated days).

- 2) If H_s for **B** is positive, the scaling parameters w_* and L for **A** are computed using the H_s from **B**. All the other PBL parameters (h , z_0 and u_*) for **A** are computed from values of the **A** point. This “mixed” choice of the scaling parameters can be justified by the findings of Weigel et al. (2007), who pointed out that buoyancy effects on the sunlit slope play an important role in the generation of TKE in the valley.
- 3) The similarity relations described in Hanna (1982) are applied for **A** with the PBL parameters computed according to 2).

Turbulence variables on “non-valley” grid points are always computed according to the “SIM” approach. In the following section the “SIM-ct” approach is evaluated on the TRANSALP-89 tracer experiment, results are compared to the “SIM” and “Direct” approaches.

4.4 Evaluation of model results

In this section the performance of the model system is evaluated, regarding both the simulation of the meteorological conditions and the dispersion of the tracer cloud. With the COSMO–LPDM system both tracer experiments of the TRANSALP-89 campaign were simulated. In the following, results of COSMO-2 and LPDM simulations for the second tracer experiment (19 October 1989) are presented, while possible differences between the two days are also highlighted.

4.4.1 COSMO simulation

As described in Section 4.3.1 the COSMO-2 model is nested in the COSMO-7 model, which obtains its initial and lateral boundary conditions from the ERA-Interim Reanalysis. For the initialization of the COSMO-7 and COSMO-2 models no additional observations were used. The simulation started on 5 and 19 October 1989 at 0000 UTC and the COSMO models were integrated for 24 hours. The effect of both the so-called spin-up time and the impact of assimilated observations were assessed in a separate study by running a 24 hour assimilation cycle before the experiment day. This new run has some beneficial characteristics in the first 4-5 hours of the simulation, but afterwards the impact vanishes. In the following, results from the original COSMO runs without assimilation are presented.

During the TRANSALP-89 experiment the tracer was transported by the developing valley wind system. Consequently, it is of major importance that the NWP model should be able to simulate the onset and amplitude of the valley wind with good accuracy. The

forecasted wind fields of COSMO-2 were evaluated with eight surface meteorological stations operated by MeteoSwiss in the region of the experiment. According to the measurements, the onset of the valley wind occurs around 0900 UTC in the region of the tracer experiment, independently of the location within the valley. As the valleys are north-south directed, the daytime valley wind has a southerly direction. The maximum wind speed is between 3 and 4 m s⁻¹ in the region and is measured between 1100 and 1300 UTC.

Figure 4.3 shows measured and modelled wind direction and wind speed for two selected stations. For the Magadino station (location on Figure 4.2), which is close to the entrance of the Riviera Valley (and runs approximately east-west), the wind direction is simulated quite accurately. However, the onset of the valley wind and the maximum of the wind speed occur approximately 2 hours later in the model than in the measurement.

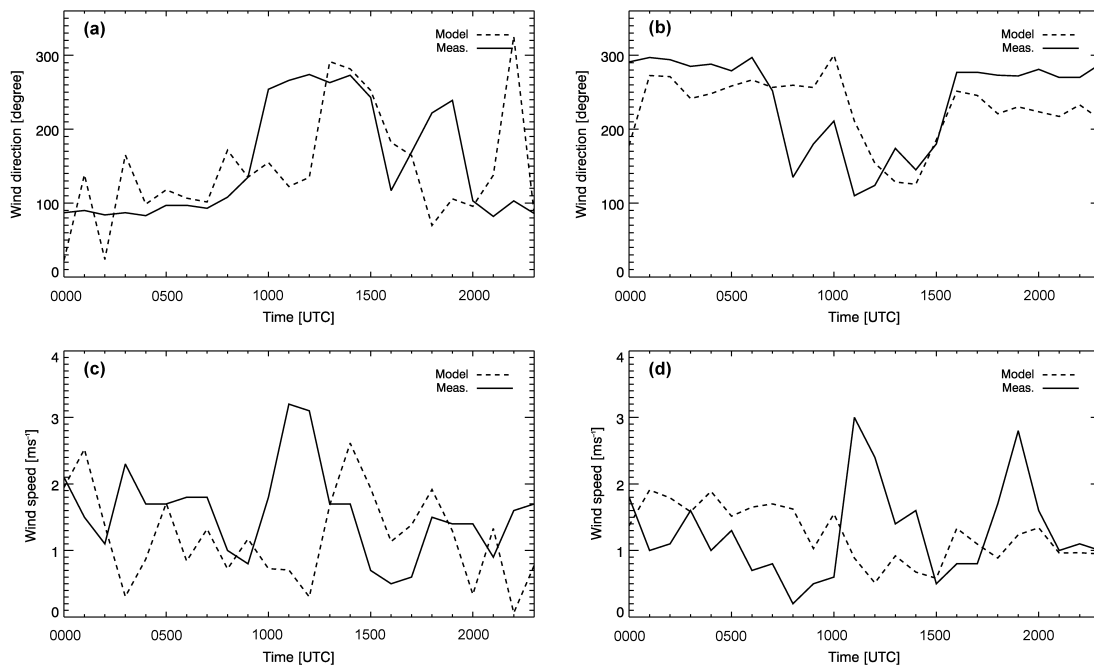


Figure 4.3: Measured (solid line) and modelled (dashed line) wind direction (a, b) and speed (c, d) for the Magadino (a, c) and Piotta (b, d) stations for 19 October 1989. COSMO-2 model run with unmodified soil moisture from the ERA-Interim analysis (“control” run).

For the station at Piotta, which is located in the Leventina Valley, the late onset of the valley wind is more pronounced. The change in the wind direction occurs three hours later in the model than observed, while the wind speed maximum measured around 1100 UTC is completely missing in the COSMO simulation.

Previous numerical experiments (e.g., Chow et al. 2006) have shown that the amplitude and timing of the valley wind can be highly sensitive to the soil moisture. This is due to the fact, that soil moisture directly influences the partitioning of available energy on the surface into sensible and latent heat flux. If soil moisture is higher, latent heat flux increases, which

leads to a decreasing sensible heat flux, provided the available energy is kept constant. Consequently, a too wet soil hinders the heating of the valley atmosphere and thus the development of the valley wind system.

It is assumed that the delayed simulation of the valley wind system by the COSMO model is caused by a too moist soil analysis. As no additional measurements were used to initialize COSMO, this problem could be traced back to the ERA-Interim Reanalysis. It has been shown that the precipitation-evaporation balance is slightly positive in ERA-Interim until 1991 (Uppala et al. 2008), which could lead to a too moist soil. A further problematic aspect could be the interpolation of the IFS soil moisture into the COSMO model, due to the different soil hydrology schemes in the two models (Gantner and Kalthoff 2009).

Figure 4.4 shows measured and modelled time series of 2-m temperature and relative humidity for the station at Piotta (other stations give similar results, not shown).

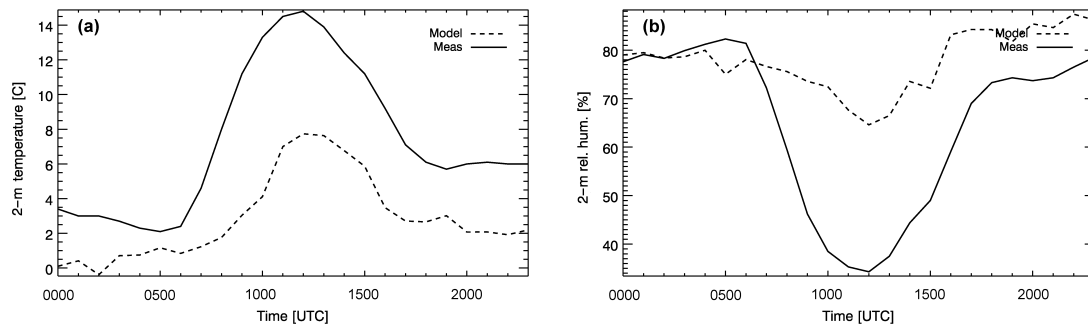


Figure 4.4: Measured (solid line) and modelled (dashed line) 2-m temperature (a) and relative humidity (b) for the Piotta station on 19 October 1989. COSMO-2 model run with unmodified soil moisture from the ERA-Interim analysis (“control” run).

Daytime temperature is underestimated, while relative humidity is overestimated by COSMO which strengthens our assumption of the too moist soil. The sensitivity of the COSMO simulation towards soil moisture is further investigated in Section 4.5.1. In the following the simulation of the tracer cloud is presented.

4.4.2 Verification of the tracer dispersion

Several LPDM runs were conducted using outputs of the COSMO-2 model for the tracer experiments of 5 and 19 October 1989. LPDM runs were started at the beginning of the tracer emission at 1000 UTC, and half-hourly concentration outputs were generated over the grid of COSMO-2. To investigate the impact of the turbulence coupling onto the dispersion process, three LPDM runs were made using the three interfacing methods described in

Section 4.3.3. Modelled concentrations are compared to measurements using time series plots and objective verification scores.

After analyzing the concentration time series (Figure 4.5), it can be concluded that the magnitude of the measured tracer concentration peaks are seriously underestimated in the Leventina Valley and well predicted in the lower Blenio Valley. This means, that the tracer which is coming from the Riviera Valley is not accurately partitioned between the Leventina and Blenio Valleys by the COSMO–LPDM system. As it will be shown in Section 4.5.3, one possible cause for this could be the too coarse model orography of COSMO-2. In the upper Blenio Valley (northern part of Blenio) the tracer concentration peak is slightly underestimated and a considerable time shift is present, which means that the valley wind in the simulation was not strong enough to transport the tracer to the farther parts of the valley system. This problem is further investigated in Section 4.5.1.

Results of the concentration simulations were objectively verified with the statistical scores proposed by Hanna (1989). Next to the mean of the observed ($\overline{C_o}$) and predicted ($\overline{C_p}$) concentrations, the normalized mean square error (*NMSE*), fractional bias (*FB*) and factor of two values (*FAC2*) were calculated, as well as the correlation coefficient (*R*) and the ranked Spearman correlation coefficient (*R_Sp*). The fractional bias is computed as:

$$FB = \frac{(\overline{C_o} - \overline{C_p})}{0.5(\overline{C_o} + \overline{C_p})}. \quad (4.12)$$

The normalized mean square error is defined as:

$$NMSE = \frac{\overline{(C_o - C_p)^2}}{\overline{C_o C_p}}. \quad (4.13)$$

The factor of two value indicates the fraction of data for which

$$0.5 \leq C_p / C_o \leq 2. \quad (4.14)$$

For the objective verification, the location of the concentration measurement stations was also taken into account in the following way: a station on the valley floor was only considered in the verification if the corresponding model grid point was also a “valley grid point”, and a station on the slope was only considered if the corresponding grid point was a “non-valley

grid point.” This method in the objective verification was mainly applied in order to separate the impact of the “SIM-ct” approach on the concentration results.

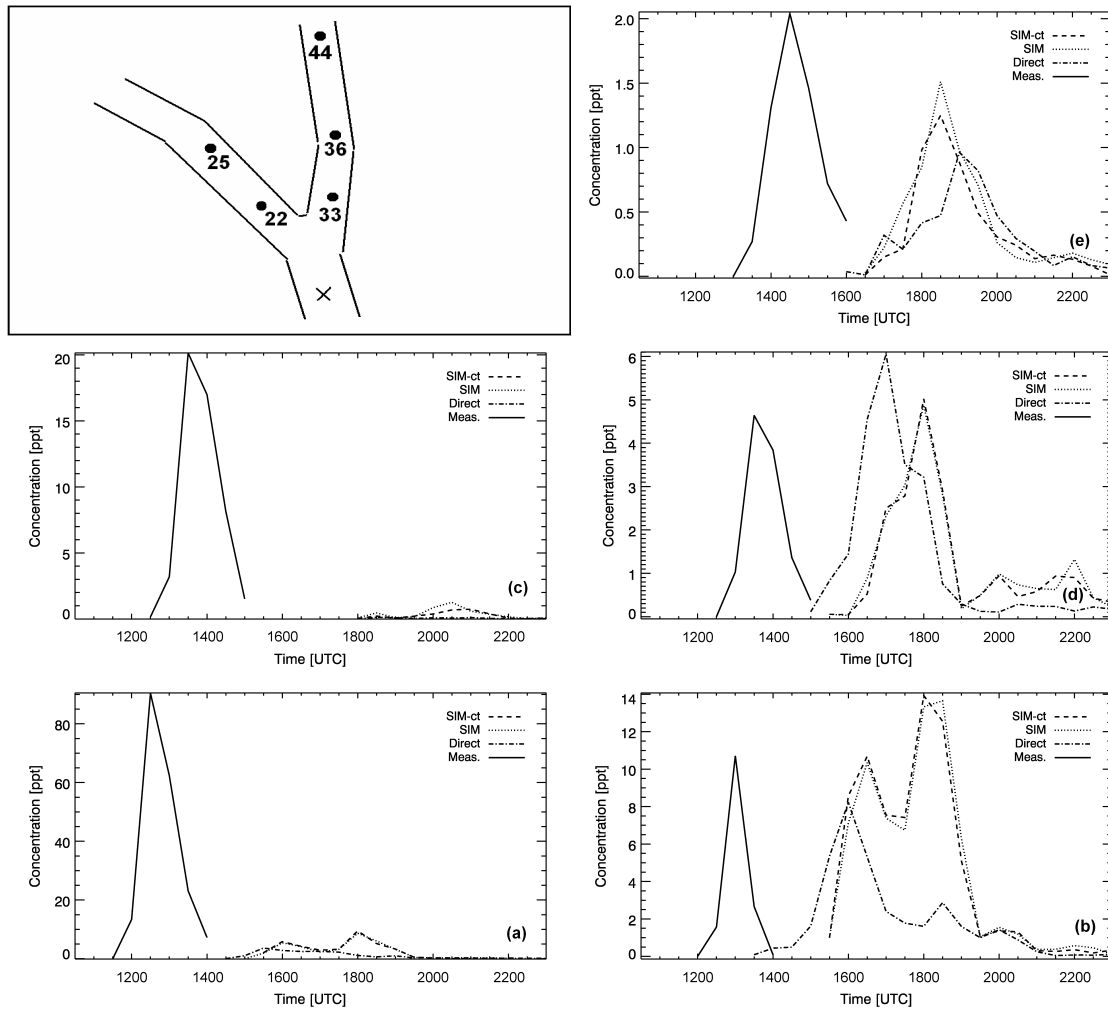


Figure 4.5: Simulated tracer concentrations on 19 October 1989 for five stations with different interfacing approaches: “Direct” (dash-dotted line), “SIM” (dotted line) and “SIM-ct” (dashed line) coupling methods, compared to tracer measurements (solid line). Station locations are indicated in the upper left corner and on Figure 4.1d: 22 (a), 33 (b), 25 (c), 36 (d) and 44 (e). For driving the dispersion model the COSMO-2 model was used with unmodified soil moisture from the ERA-Interim analysis (“control” run).

Table 4.1 presents the statistical scores for the three experiments with different interfacing approaches (Experiments 1, 2 and 3) based on both tracer experiment days. All the three interfacing methods considerably overestimate the measured concentrations and give rather poor correlations. The negative values of R_{Sp} indicate the late occurrence of the concentration peak in the simulations.

Table 4.1: Statistical scores for tracer concentration evaluation. Verification for both days and for all surface samplers, without subsequent shifting of the modelled time series. Number of verified samplers: 170 ('one sampler' corresponds to one half-hourly observation at a given location). Experiment number (see text), type of COSMO run, interfacing approach and PBL height determination method is indicated. \overline{C}_o : observed mean concentration; \overline{C}_p : predicted mean concentration; NMSE: normalized mean square error; FB: fractional bias; FAC2: factor of two; R: correlation coefficient; R_Sp: ranked Spearman correlation coefficient. The average time shift of the modelled concentration peak as compared to the measured peak is indicated as TS_ME (in hours, negative values indicate a late modelled peak).

Nr	COSMO run	Interface	PBL height	\overline{C}_o	\overline{C}_p	NMSE	FB	FAC2	R	R_Sp	TS_ME
1	COSMO-2 control	"SIM"	bulk_Ri	5.68	9.67	34.51	-0.52	0.04	0.03	-0.09	-2.11
2	COSMO-2 control	"SIM-ct"	bulk_Ri	5.68	10.76	42.11	-0.62	0.04	0.03	-0.05	-2.23
3	COSMO-2 control	"Direct"	implicit	5.68	7.53	16.70	-0.28	0.07	0.08	-0.01	-1.89
4	COSMO-2 "dry-soil"	"SIM"	bulk_Ri	5.68	7.90	31.51	-0.33	0.21	0.07	0.38	0.00
5	COSMO-2 "dry-soil"	"SIM-ct"	bulk_Ri	5.68	7.18	31.76	-0.23	0.21	0.07	0.40	0.05
6	COSMO-2 "dry-soil"	"Direct"	implicit	5.68	11.15	14.06	-0.65	0.16	0.10	0.24	0.05

Before analyzing the model results in more detail, the serious time shift of the modelled concentration peak had to be corrected. In the following the sensitivity of the modelling system towards the soil moisture, horizontal grid resolution, and boundary layer height determination approach is investigated.

4.5 Sensitivity experiments

In this section the sensitivity of the modelling system towards three different factors is investigated. First, the initial soil moisture is reduced. Secondly, a different method is applied for the determination of the PBL height in the turbulence coupling approach. Finally, a finer horizontal resolution is used in the COSMO model.

4.5.1 Initial soil moisture

In the previous section the late onset of the valley wind was identified as the main drawback of both the COSMO and LPDM simulations. As the timing of the valley wind could be highly sensitive to the soil moisture, in the following the sensitivity of both the atmospheric and dispersion simulations towards the soil moisture in the COSMO-2 model is investigated.

To analyse the problem, the initial soil moisture in the COSMO model was scaled with a constant factor on the whole COSMO-2 domain, and the simulation was repeated with the same lateral boundary conditions from the COSMO-7 model. After several experiments the factor of 0.5 (i.e., initial soil moisture is reduced by 50%) proved to be a reasonable choice for both days and consequently, results for this experiment are shown (further referred to as the “dry-soil” run).

Figure 4.6 shows again measured and modelled wind direction and speed for the two stations analysed in Section 4.4.1. Comparing Figure 4.3 to Figure 4.6 it can be noted that the onset of the valley wind is simulated with more accuracy in the “dry-soil” run.

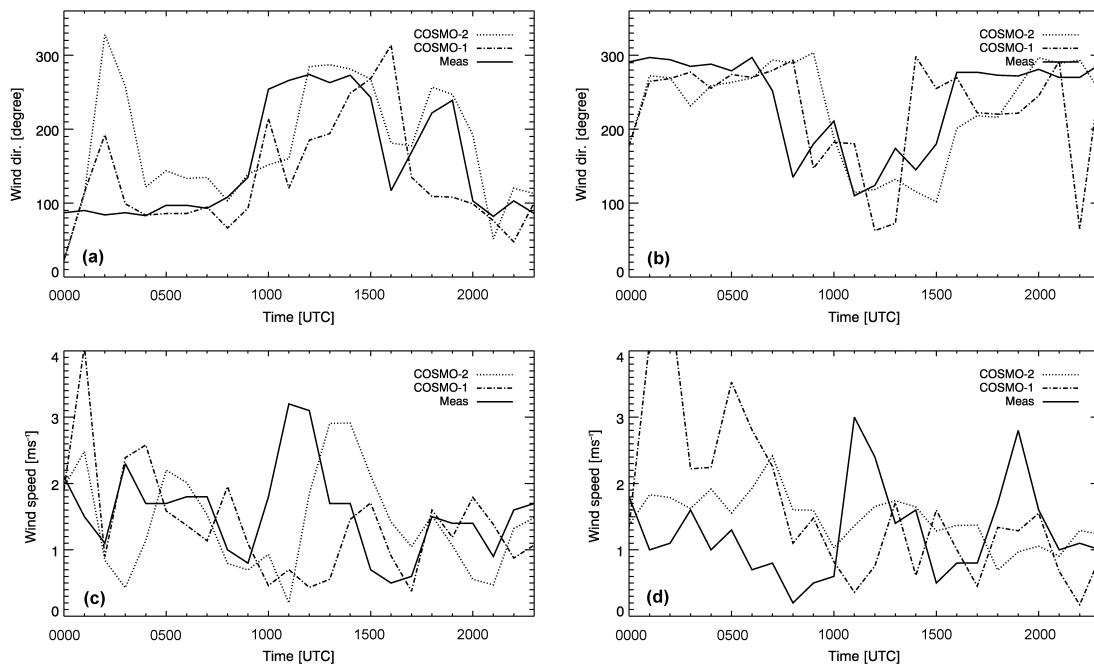


Figure 4.6: Measured (solid line) and modelled wind direction (a, b) and speed (c, d) for the Magadino (a, c) and Piotta (b, d) stations for 19 October 1989. COSMO-2 (dotted line) and COSMO-1 (dash-dotted line) model runs with reduced initial soil moisture (“dry-soil” runs).

In the “control” run (with unmodified soil moisture) the change of the wind direction from down-valley to up-valley wind occurred approximately 2-3 hours later in the model than in the measurements. This time shift is reduced in the “dry-soil” run, however, the daytime wind maximum is still missing for the Piotta station. In Figure 4.7, time series of 2–m temperature and relative humidity at the Piotta station are depicted for the “dry-soil” run. The important temperature underestimation of the “control” run around midday is considerably improved in the “dry-soil” run. The daytime values of relative humidity are much better reproduced, while night time values are still underestimated by the “dry-soil” run.

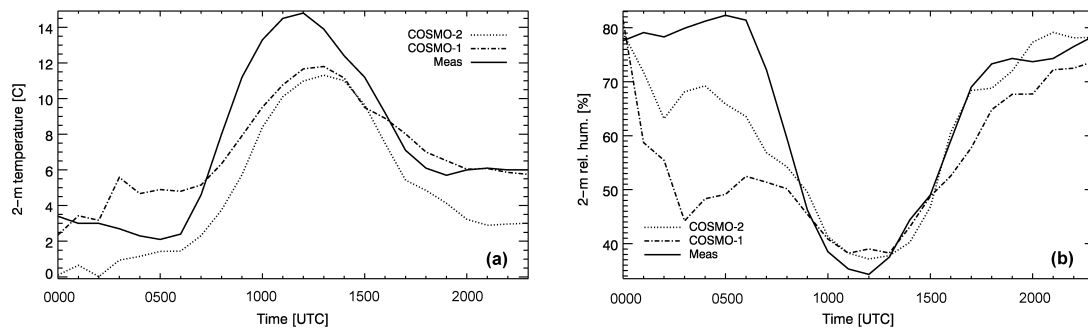


Figure 4.7: Measured (solid line) and modelled (dashed line) 2-m temperature (a) and relative humidity (b) for the Piotta station on 19 October 1989. COSMO-2 (dotted line) and COSMO-1 (dash-dotted line) model runs with reduced initial soil moisture (“dry-soil” runs).

The aim of the above experiment with reduced soil moisture was to obtain an adequate meteorological simulation which could serve as input for the dispersion runs. Using the output of the “dry-soil” COSMO-2 run, LPDM simulations with the different interfacing approaches were repeated (Figure 4.8) and compared to the “control” run (Figure 4.5). Due to a better simulation of the valley wind system the timing of the concentration peak is forecasted more accurately in the “dry-soil” run, and the time shift mentioned in Section 4.4.2 is mostly corrected. Considering the amplitude of the concentration peak, measured values are still underestimated in the Leventina Valley (Figure 4.8a and 4.8c) and overestimated in the Blenio Valley (Figure 4.8b and 4.8d). The serious underestimation of the “SIM” and “SIM-ct” approaches in the upper Blenio Valley is corrected using the modified soil moisture (Figure 4.8e). In the Leventina Valley the “Direct” approach gives the highest concentrations (while still underestimating) and there is no significant difference between the “SIM” and “SIM-ct” approaches. Furthermore, the curves of the “SIM” and “SIM-ct” approaches on Figure 4.8a and 4.8b are almost identical and therefore indistinguishable, which is caused by the small distance of these two stations from the emission source and thus the small travel time of the tracer. Time series in the Blenio Valley (Figure 4.8d and 4.8e) show a clear trend with the “Direct” approach giving the highest and the “SIM-ct” approach the lowest values, the latter being more accurate.

The higher predicted values of the “Direct” approach as compared to the similarity approaches can be understood by the investigation of the diagnosed turbulence characteristics, serving as input for LPDM. Figure 4.9 depicts the profiles of the vertical turbulent fluctuations for the three coupling methods over a selected grid point in the Blenio Valley (averaged profiles over the area show similar trends). It can be seen that the “Direct” approach predicts a much shallower PBL with weaker turbulence values as compared to the methods based on similarity relations.

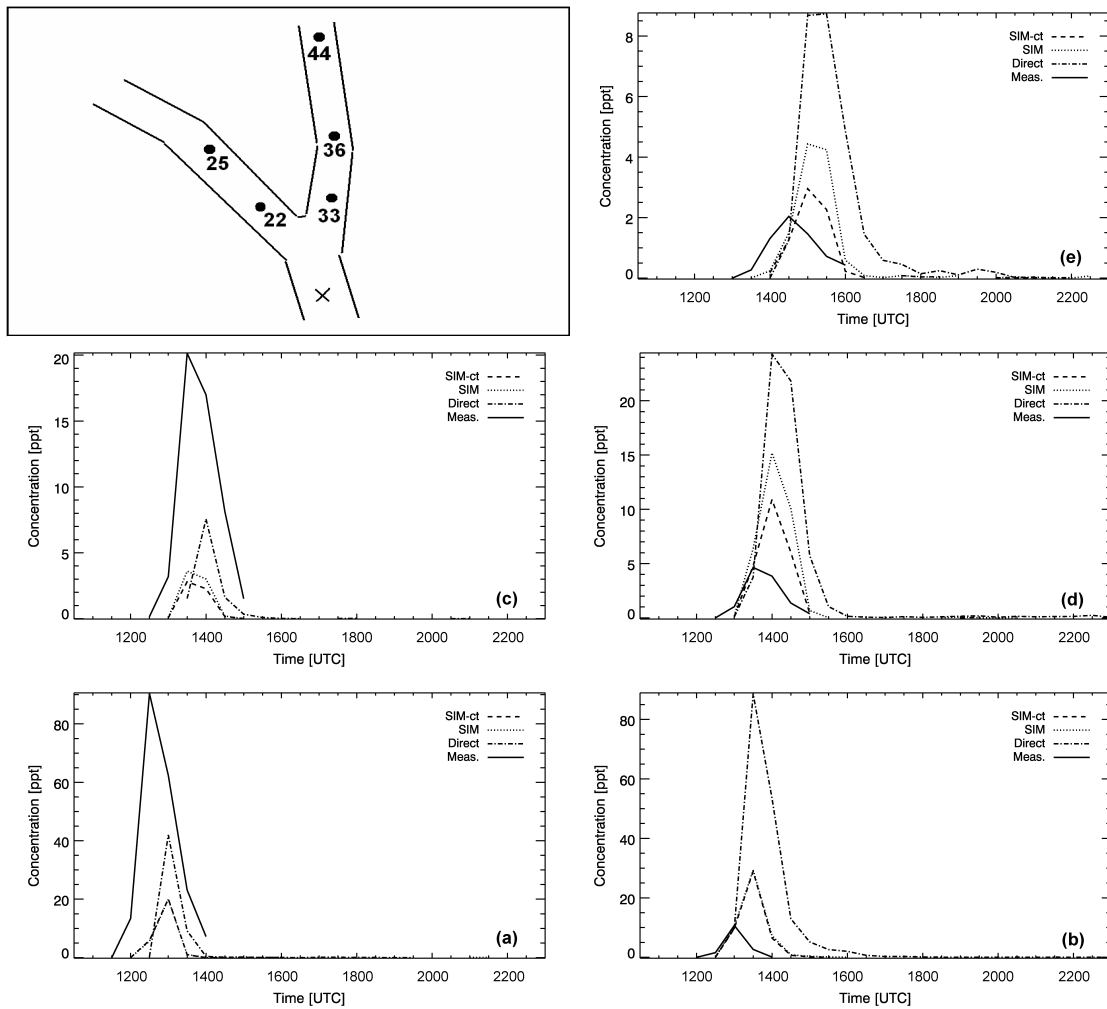


Figure 4.8: Same as Fig. 4.5 but for driving the dispersion model the COSMO-2 model with reduced soil moisture (“dry-soil” run) was used.

Consequently, the mixing of the tracer is much more effective in the case of the similarity approaches, which results in lower predicted concentrations. This relatively poor performance of the level 2.5 closure was also pointed out by Trini Castelli et al. (2006), who compared turbulence closure models for different stability conditions in complex terrain, and attributed the TKE underestimation of the level 2.5 closure to its one-dimensional approach. The PBL height difference is due to the fact that in the case of the “SIM” and “SIM-ct” methods the bulk Richardson number was used to determine the height of the PBL, while the “Direct” approach is inherently related to the TKE profile of the COSMO model itself. This sensitivity is further investigated in Section 4.5.2. Figure 4.9 also demonstrates the impact of soil moisture reduction onto the PBL height. With the “control” soil moisture the daytime PBL height diagnosed by the bulk Richardson number is around 200 m on 19 October 1989 (Figure 4.9a), while with the reduced soil moisture the PBL height is around 600 m (Figure 4.9b), which is closer to the observed value of 800 m, measured by a Sodar (Anfossi et al. 1998).

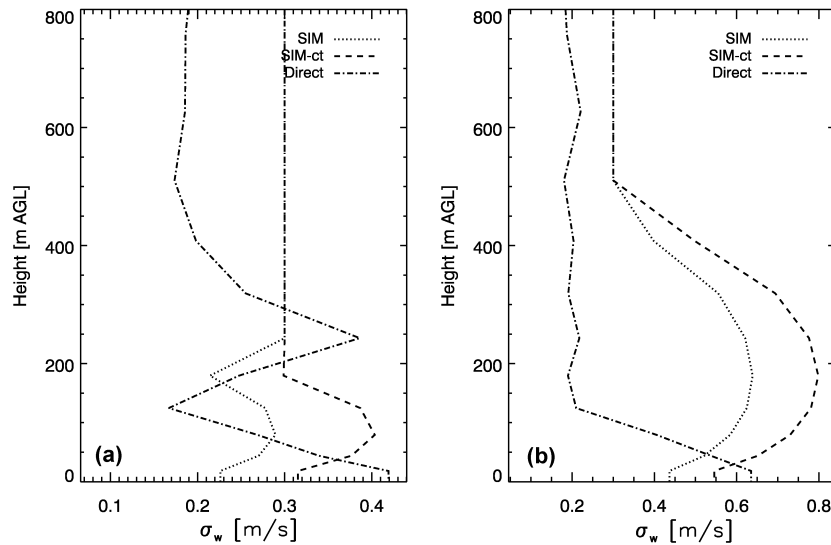


Figure 4.9: Profiles of vertical wind fluctuations (σ_w) for a selected grid point in the Blenio Valley diagnosed by the three interfacing approaches: “Direct” (dash-dotted line), “SIM” (dotted line) and “SIM-ct” (dashed line) methods. COSMO-2 model runs for 1200 UTC on 19 October 1989 with (a) unmodified soil moisture from the ERA-Interim analysis (“control” run) and with (b) reduced initial soil moisture (“dry-soil” run).

The improvement of the “dry-soil” run is also reflected in the statistical evaluation scores (Table 4.1, Experiments 4, 5 and 6). The overestimation of the system is reduced for the similarity approaches, while the “Direct” approach now gives a considerable overestimation. The improvement in the time shift is shown by the R_{Sp} score, which now has positive values as opposed to the negative values of the “control” run.

For a better understanding of the processes involved in the tracer dispersion, it is worth to perform the statistical evaluation also on different sub-domains of the valley system. During the tracer dispersion in the Riviera, Leventina, and Blenio Valleys, two main processes are involved. First, the partitioning of the tracer coming from the Riviera Valley between the Leventina and Blenio Valleys. Secondly, the strength and timing of the developing valley wind, which mainly determines the amount of tracer which is transported from the lower to the upper Blenio Valley. According to these two processes the statistical evaluation was performed on three sub-domains: the Leventina Valley, the lower and the upper Blenio Valley. The relatively large number of surface samplers and the two experimental days made it possible to analyze these sub-domains separately and at the same time preserve a sufficiently large sample. During the verification of sub-domains the possible small time shifts between measured and modelled concentration time series, which are present even after soil moisture reduction, are also removed by a subsequent shifting of the modelled values thus enforcing coinciding peak concentrations. The extent of this time

shift is an important verification parameter (further referred to as TS_{ME}), which indicates how accurately the timing of the tracer cloud was simulated.

Figure 4.10 presents scatter plot diagrams for the predicted concentrations of the COSMO-2 – LPDM system (“dry-soil” run with “SIM-ct” coupling) for both days of the tracer experiment and for the three sub-domains separately (the 1.1 km resolution and other coupling approaches show similar trends).

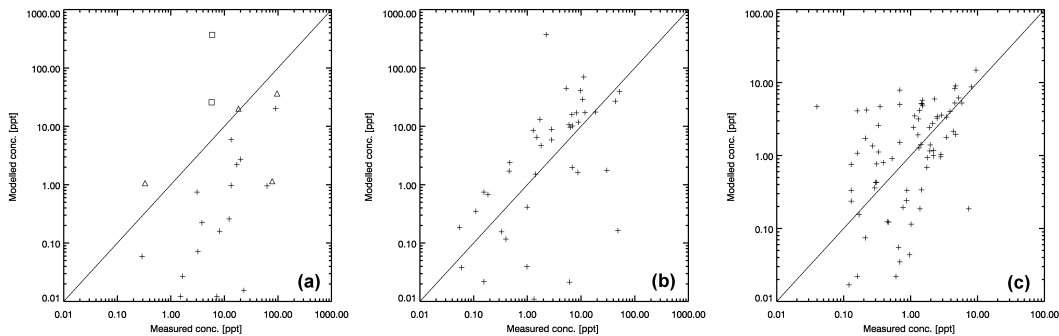


Figure 4.10: Scatter plots for the predicted concentrations of the COSMO-2 – LPDM system (“dry-soil” run with “SIM-ct” coupling) for both days of the tracer experiment for three sub-domains: Leventina Valley (a), lower Blenio Valley (b), and upper Blenio Valley (c). Sampler station nr. 21 in the Leventina Valley is indicated with squares (5 October) and triangles (19 October) (see text).

As discussed above, the Leventina Valley is characterized by a general underestimation while in the Blenio Valley concentrations are slightly overestimated. Sampler station No. 21 at the entrance of the Leventina Valley is a strong outlier, as concentrations are overestimated at this station as opposed to all other stations in the sub-domain. This overestimation is either caused by measurement error or by very small scale phenomena, which is still unresolved even with the 1.1 km orography.

Tables 4.2, 4.3, and 4.4 show verification scores for the three sub-domains (COSMO-2 – LPDM “dry-soil” runs are Experiments 1, 2, and 3). Predicted mean concentration in the Leventina Valley should be handled with certain care due to the strong outlier described above. In the lower and upper Blenio Valleys the similarity theory methods are performing better than the “Direct” approach for the 2.2 km resolution system, while in the Leventina Valley the situation is opposite. The “SIM” and “SIM-ct” methods are close to each other with the latter performing slightly better (mainly for the FB score). These scores will serve as a reference for two other sensitivity experiments, which are described in the next sub-section. It is also worth comparing these scores with other verification results of prognostic dispersion modelling systems presented in the literature. Carvalho et al. (2002) evaluated the RMS (i.e., RAMS-MIRS-SPRAY) system in the Rhine Valley and obtained scores between 0.04 and 1.41 for FB , and scores between 0.0 to 0.57 for $FAC2$.

Table 4.2: As Table 4.1, but for samplers only in the Leventina Valley and with subsequent shifting of the modelled time series. Number of verified samplers: 36.

Nr	COSMO run	Interface	PBL height	$\overline{C_o}$	$\overline{C_p}$	NMSE	FB	FAC2	R	R_Sp	TS_ME
1	COSMO-2 "dry-soil"	"SIM"	Ri bulk	13.81	14.07	21.95	-0.02	0.03	0.04	0.71	0.25
2	COSMO-2 "dry-soil"	"SIM-ct"	Ri bulk	13.81	13.56	22.50	0.02	0.03	0.03	0.76	0.33
3	COSMO-2 "dry-soil"	"Direct"	implicit	13.81	10.12	7.28	0.31	0.14	0.33	0.77	0.17
4	COSMO-2 "dry-soil"	"SIM"	TKE	13.81	13.68	22.03	0.01	0.08	0.03	0.71	0.25
5	COSMO-2 "dry-soil"	"SIM-ct"	TKE	13.81	13.40	22.27	0.03	0.06	0.03	0.65	0.25
6	COSMO-1 "dry-soil"	"SIM"	Ri bulk	13.81	31.99	8.54	-0.79	0.36	0.44	0.62	-0.25
7	COSMO-1 "dry-soil"	"SIM-ct"	Ri bulk	13.81	29.43	8.48	-0.72	0.36	0.40	0.62	-0.25
8	COSMO-1 "dry-soil"	"Direct"	implicit	13.81	20.22	5.80	-0.38	0.17	0.18	0.55	-0.08

Table 4.3: As Table 4.1, but for samplers only in the lower Blenio Valley and with subsequent shifting of the modelled time series. Number of verified samplers: 47.

Nr	COSMO run	Interface	PBL height	$\overline{C_o}$	$\overline{C_p}$	NMSE	FB	FAC2	R	R_Sp	TS_ME
1	COSMO-2 "dry-soil"	"SIM"	Ri bulk	7.04	17.81	27.49	-0.87	0.23	0.04	0.70	-0.12
2	COSMO-2 "dry-soil"	"SIM-ct"	Ri bulk	7.04	16.90	26.31	-0.82	0.21	0.05	0.71	-0.12
3	COSMO-2 "dry-soil"	"Direct"	implicit	7.04	25.06	9.87	-1.12	0.15	0.30	0.67	-0.19
4	COSMO-2 "dry-soil"	"SIM"	TKE	7.04	18.26	22.61	-0.89	0.30	0.06	0.66	0.00
5	COSMO-2 "dry-soil"	"SIM-ct"	TKE	7.04	17.74	20.86	-0.86	0.28	0.07	0.67	0.00
6	COSMO-1 "dry-soil"	"SIM"	Ri bulk	7.04	16.56	1.87	-0.81	0.23	0.87	0.68	-0.75
7	COSMO-1 "dry-soil"	"SIM-ct"	Ri bulk	7.04	14.87	1.65	-0.71	0.32	0.87	0.65	-0.81
8	COSMO-1 "dry-soil"	"Direct"	implicit	7.04	15.96	1.37	-0.78	0.21	0.82	0.75	-0.88

Table 4.4: As Table 4.1, but for samplers only in the upper Blenio Valley and with subsequent shifting of the modelled time series. Number of verified samplers: 87.

Nr	COSMO run	Interface	PBL height	$\overline{C_o}$	$\overline{C_p}$	NMSE	FB	FAC2	R	R_Sp	TS_ME
1	COSMO-2 "dry-soil"	"SIM"	Ri bulk	1.58	2.82	1.96	-0.56	0.38	0.64	0.59	-0.04
2	COSMO-2 "dry-soil"	"SIM-ct"	Ri bulk	1.58	2.14	1.34	-0.30	0.32	0.64	0.57	0.04
3	COSMO-2 "dry-soil"	"Direct"	implicit	1.58	5.67	6.65	-1.13	0.26	0.78	0.62	0.14
4	COSMO-2 "dry-soil"	"SIM"	TKE	1.58	3.08	1.76	-0.64	0.39	0.82	0.68	0.21
5	COSMO-2 "dry-soil"	"SIM-ct"	TKE	1.58	2.72	1.45	-0.53	0.37	0.80	0.64	0.21
6	COSMO-1 "dry-soil"	"SIM"	Ri bulk	1.58	1.75	1.56	-0.10	0.22	0.40	0.13	-1.50
7	COSMO-1 "dry-soil"	"SIM-ct"	Ri bulk	1.58	1.20	2.20	0.28	0.22	0.26	-0.01	-1.43
8	COSMO-1 "dry-soil"	"Direct"	implicit	1.58	3.32	2.17	-0.71	0.32	0.61	0.55	-1.54

In a more recent publication Hara et al. (2009) also used the RAMS model but with a much finer horizontal resolution in complex terrain. In this study the verification scores were between 0.32 and 0.36 for *FB*, and between -0.61 and 0.36 for *FAC2*. These scores are in the same order of magnitude as those presented in Tables 4.1–4.4.

4.5.2 PBL height determination

In the case of the “SIM” and “SIM-ct” approaches the bulk Richardson number method (in the following referred to as bulk_Ri method) was used to derive the height of the PBL from COSMO outputs. However, there are several other approaches for PBL height determination from NWP models. The sensitivity of the dispersion calculation towards this choice is discussed in the following.

As the “Direct” approach derives turbulence characteristics from the TKE of the COSMO model, it is interesting to determine the PBL height from predicted TKE profiles. When using TKE for PBL height determination, first the maximum value of TKE is searched in a predefined lower part of the atmosphere, and the critical TKE value is defined as a certain portion of the maximum value (Szintai and Kaufmann 2008). The PBL top is then given as the height where TKE first drops below this critical value (10% for unstable and 30% for stable stratification). Figure 4.11 shows fields of PBL height determined from outputs of the COSMO-2 model (“dry-soil” run) at 1200 UTC on 5 October 1989. In the case of the bulk_Ri method (Figure 4.11a), the PBL height field is quite smooth and certain features of the model orography can be recognized (i.e., the PBL is deeper in the valley than over the ridge). The PBL height field determined from TKE profiles (Figure 4.11b) is noisier and it is more difficult to correlate the PBL height with orography. On 5 October, in the morning hours until early afternoon (1300 UTC) the bulk_Ri method gives higher values for PBL height as compared to the TKE method, while in the late afternoon the situation is opposite. On 19 October, in the early afternoon the TKE method gives higher values for PBL height than the bulk_Ri method. However, comparison of the concentration time series of the bulk_Ri and TKE methods (not shown) does not reveal a clear relation between PBL height and the simulated concentration. This indicates that in the present case the PBL height is not the key factor that determines the modelled concentrations. This surprising conclusion might be related to two factors. First, unlike most of the Lagrangian Particle Dispersion Models, the LPDM used in this study does not apply a reflection of particles at the PBL top, thus the impact of PBL height on the predicted concentrations is less important. Secondly, due to the very complex topography and the relatively strong up-valley winds, the tracer can additionally be transported out of the PBL by the mean vertical wind.

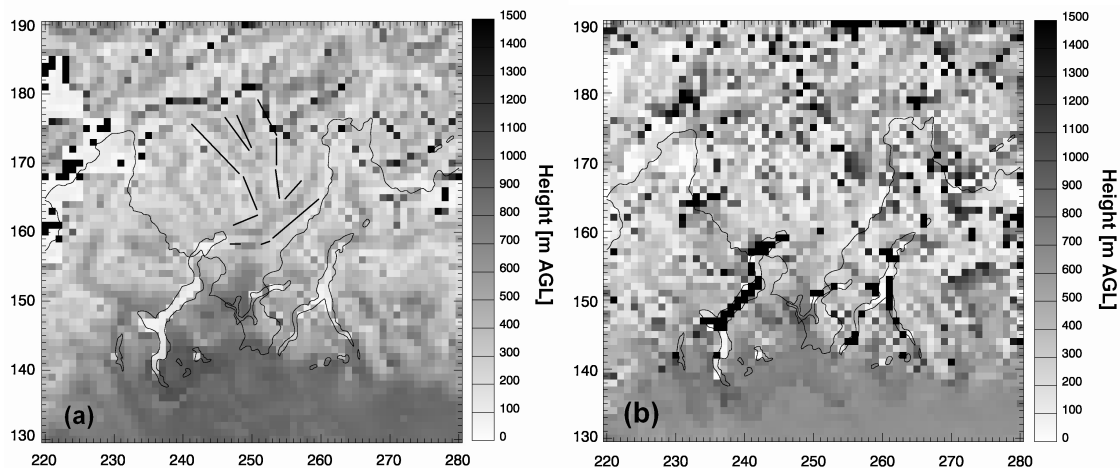


Figure 4.11: Fields of PBL height determined from outputs of the COSMO-2 model (“dry-soil” run) at 1200 UTC on 5 October 1989. (a) bulk Richardson number method, (b) TKE profile method. For the bulk Richardson method the contours of the main valleys of interest are indicated with solid black lines to show the correlation of PBL heights with model orography (see also Fig 4.2a). On the axes the grid point numbers are indicated.

The objective verification of the TKE method (Tables 4.2, 4.3, and 4.4; Experiments 4 and 5) generally shows similar skill as the bulk_Ri method for the 2.2 km resolution system. *FB* scores are slightly better for bulk_Ri, while other scores do not differ significantly. It is remarkable though, that all the similarity approaches perform better than the “Direct” approach irrespective of the PBL height method used (especially in the lower and upper Blenio Valleys). This implies that the COSMO model tends to underestimate the turbulence intensity in steep and narrow Alpine valleys, which might be explained by the inadequate simulation of the fine details of the valley wind system, and the fact that the one-dimensional turbulence scheme of COSMO is unable to generate TKE from horizontal wind shear.

4.5.3 Horizontal resolution

Due to the highly complex topography of the southern Alps with valleys as deep as 2 km with a crest-to-crest width of only 6 km, a grid resolution of 2.2 km can be considered as rather coarse. In the following, the sensitivity of the modelling results is investigated with respect to the horizontal resolution of the COSMO model.

Details of the COSMO simulations at 1.1 km resolution were previously described in Section 4.3.1. Considering the model numerics and physics, COSMO-1 uses the same methods and parameters as COSMO-2. External parameters (like soil and vegetation properties) are interpolated from COSMO-2 with the nearest neighbour method, except for model orography and subgrid-scale part of the roughness length, where the SRTM (NASA Shuttle Radar Topographic Mission) dataset is used instead of the GLOBE (Global Land

One-km Base Elevation) dataset, which is applied for COSMO-2. To avoid the time shift of the valley wind system, initial soil moisture was reduced by 50% also in the COSMO-1 simulation.

Figure 4.6 shows wind time series of COSMO-1 compared to COSMO-2 and measurements. For the Magadino station, COSMO-2 slightly outperforms COSMO-1, while for the Piotta station, which is in more complex terrain, the two models give similar results. Also for 2-m temperature and relative humidity time series no significant differences can be detected between COSMO-2 and COSMO-1 (Figure 4.7). This could imply that reducing the horizontal resolution only does not automatically lead to an improvement of the meteorological simulation for the cases investigated. External parameters at finer resolution, data assimilation at the high resolution, and better-suited physical parameterizations (e.g., three-dimensional turbulence) all may improve the COSMO-1 simulation. However, the study of these factors is beyond the scope of the present paper.

Tracer dispersion simulations are also made using output of COSMO-1. The main difference from the COSMO-2 – LPDM simulations is in the partitioning of the tracer between the Leventina and Blenio Valleys. To quantify this partitioning factor, three stations are selected in both the Leventina and Blenio Valleys at 6, 8 and 12 km distance from the valley bifurcation point (stations 22, 23 and 25 in Leventina; and 33, 34 and 41 in Blenio). The partitioning factor is determined as the average ratio between the concentrations at the corresponding stations (or grid points) in the two valleys. On 5 October this factor between the Leventina and Blenio Valleys is 1.2:1 in the measurements, thus nearly the same amount of tracer went into the two valleys. In COSMO-2 the factor is 1:15, so only a very small amount of the tracer is transported into the Leventina Valley. The partitioning is much better with COSMO-1; using the similarity approaches it is 1:5 and with the “Direct” approach 2:1. On 19 October the measured factor is 4:1, while with COSMO-2 it is simulated as 1:2, and with COSMO-1 as 1:1. The better partitioning of the tracer by using COSMO-1 simulations is attributed to the finer orography and thus a more accurate description of the wind field.

Tables 4.2, 4.3, and 4.4 show statistical scores for the 1.1 km simulations as well (Experiments 6, 7, and 8). To be comparable with the 2.2 km simulations, the 1.1 km simulations were up-scaled by averaging the concentration values of 2x2 grid boxes. It has to be noted though that scores computed on the original 1.1 km grid show similar trends with the up-scaled results. According to the verification scores, the 1.1 km resolution system performs better in all the three sub-domains (especially for the *NMSE* and *R* scores), which reflects the above described better tracer partitioning. The scores of the COSMO-1 – LPDM system indicate an improved performance of the “Direct” approach as compared to the similarity approaches. This could imply that the TKE values predicted by COSMO-1 are more accurate than those simulated by COSMO-2. It is remarkable, that the time shift of the fine resolution system (*TS_ME*) is significantly different from the coarse resolution one, which

indicates that the same soil moisture reduction has different impact on the valley wind simulated by the two systems.

It has to be mentioned that for all the scores presented in this study the special verification method presented in Section 4.4.2 is applied, which takes into account the location of the measurement stations. However, this only means a restriction in the case of the Leventina Valley and causes the decrease of the associated pairs by 50%. In the two other sub-domains no pairs are filtered out. For the Leventina Valley the filtering does not affect the mean measured concentrations, while predicted mean concentrations are increasing by 50% for all the coupling methods as a consequence of the filtering. Therefore, *FB* scores are improving for the 2.2 km resolution system and deteriorating for the 1.1 km system with the application of the station filtering method. For the other verification scores no significant difference can be detected.

4.6 Conclusions

The application of a new scaling approach for dispersion simulations is presented focusing on steep and narrow Alpine valleys. The modelling system used for this study consists of the non-hydrostatic NWP model COSMO and an LPDM. Results of two tracer simulations are evaluated on the TRANSALP-89 experiment, with 25 surface samplers on two measurement days.

Atmospheric conditions are simulated with the COSMO model at 2.2 and 1.1 km resolutions. It is found that the too high initial soil moisture deteriorates the COSMO forecast, causing a considerable time shift in the onset of the valley wind. After reducing the initial soil moisture by 50%, fairly accurate simulation of the valley wind can be achieved both with COSMO-2 and COSMO-1.

Both tracer experiments are modelled with LPDM using the forecasted fields of the COSMO model. Three different coupling approaches are applied between COSMO and LPDM using either the predicted TKE of the COSMO model directly or similarity theory approaches. Next to the classical Hanna (1982) method (“SIM”), a new coupling approach is introduced, where the scaling ideas of Weigel et al. (2007) are linked with the Hanna (1982) approach (“SIM-ct”). Comparing the different coupling methods in the case of the COSMO-2 – LPDM system, the best results are obtained with the “SIM-ct” approach. It has to be noted, that in most cases the partitioning into two different valley parts (the Leventina and Blenio Valleys) is not accurate in the 2.2 km simulation and more tracer is transported into the Blenio Valley than in reality. This general concentration overestimation in the Blenio Valley favours the “SIM-ct” approach which tends to give the lowest values among the three

coupling methods. It also has to be noted that the “SIM-ct” approach is based on measurements and simulation data from a single measurement campaign in Southern Switzerland. Applicability of the method for valleys with different orientation and geometry should be the subject of further studies.

Analyzing the impact of horizontal resolution to the concentration results, it can be concluded that next to the objective verification, which gives slightly better scores for the 1.1 km system, there are two other indications which could point towards the benefit of higher resolution. First, the partitioning between the Leventina and Blenio Valleys is better with COSMO-1. Secondly, in the case of COSMO-1, the performance of the “Direct” approach considerably increases relative to the similarity methods, which might indicate that the finer resolution model predicts the intensity of atmospheric turbulence with more accuracy in complex terrain.

The presented verification scores can be compared to previous modelling studies of the TRANSALP-89 campaign. Results of the COSMO–LPDM system are somewhat worse than the scores of Anfossi et al. (1998). However, it has to be emphasized that in the simulations of Anfossi et al. a diagnostic wind field model was used, based on a large number of observations, which produced a highly accurate input for the dispersion models. Consequently, such systems can only be applied for a given situation retrospectively, after the measurement campaign is finished. The main advantage of the modelling system presented in this study is thus that it is a prognostic system, which requires only initial and boundary conditions for the prediction of the pollutant concentrations. This property enables its application in real-time emergency problems, as it is done operationally at MeteoSwiss. It has to be noted, however, that the statistical scores for such prognostic dispersion simulations in real-world cases are still not optimal and considerable efforts will have to be made in improving these systems especially for application in complex terrain.

To conclude the main findings from the simulation of the TRANSALP-89 campaign we can highlight three main factors which determine the transport and diffusion of pollutants in Alpine valleys:

- 1) Most importantly, the *large-scale* features have to be simulated accurately. This includes the large-scale synoptical forcing and also the horizontal distribution and magnitude of soil moisture (or, more generally, the slowly changing surface characteristics).
- 2) Accurate simulation of *mesoscale* flow features is also of great importance. In the case of the TRANSALP-89 experiment this means the correct representation of the flow splitting between the two side valleys, which determines tracer concentrations to a great extent.

- 3) Finally, it is shown that *microscale* phenomena, such as turbulent diffusion in the Planetary Boundary Layer, can considerably influence the simulation results.

To achieve a correct simulation of pollutant dispersion in complex terrain, all the above mentioned three components have to be modelled accurately. In this paper a new approach is introduced, which can result in a better simulation of microscale phenomena in dispersion modelling systems.

Acknowledgements

The authors would like to thank Matteo Buzzi for useful discussions and for providing the high-resolution model orography based on the SRTM dataset. Detailed and constructive reviews from two anonymous reviewers, which lead to a significant improvement of the text are also appreciated.

5 Conclusions and outlook

5.1 Conclusions

In this thesis the main challenges in connection with the off-line coupling of NWP and Lagrangian particle dispersion models have been investigated. All the three main components of an emergency response system have been validated, namely, the NWP model, the meteorological pre-processor and the dispersion model. Based on the validation results, several recommendations for the improvement of the system have been proposed. In the following these findings are summarized, similarly to the structure of the thesis.

- 1) The performance of the COSMO model in the Planetary Boundary Layer was evaluated for different conditions. An ideal dry convective case (Mironov et al., 2000), a measurement campaign for the diurnal cycle of the convective PBL (LITFASS-2003; Beyrich and Mengelkamp, 2006) and a stable night (GABLS3; Bosveld, 2010) was investigated. Apart from the mean prognostic variables, the turbulence characteristics of the model were also verified. The following conclusions can be drawn from the experiments:
 - i) It has been shown that the COSMO model is able to reproduce the main evolution of the boundary layer in dry convective situations with the operational parameter setting if the external parameters are realistic and if the initial conditions are adequate. However, it has been found that the COSMO model tends to simulate a too moist and too cold convective PBL, with shallower PBL heights than observed. During stable conditions the operational parameter setting has to be modified significantly to obtain a good model performance. The findings of Buzzi (2008) could be confirmed that the minimum diffusion coefficient has to be reduced by two orders of magnitude to correctly simulate the main features of the stable boundary layer.
 - ii) The reasons for the inadequate temperature and humidity profiles in convective conditions have been investigated with the component testing approach. The budget terms in the TKE equation have been validated separately against LES

data and turbulence measurements. The turbulent transport term (third order moment) has been found to be significantly underestimated by the COSMO model. This results in inaccurate TKE profiles and thus missing entrainment fluxes at the top of the PBL. A solution to increase the TKE transport in the PBL was proposed, which consists of the enhancement of the diffusion coefficient for TKE by a factor of 50 below the level of the diagnosed PBL top. This modification results in a more realistic TKE profile and higher entrainment fluxes. This modification of the turbulence scheme has also been tested in a parallel experiment on a one-month period. Results show only minor impacts on the operationally verified fields.

- iii) The impact of the horizontal resolution on the simulation results has also been studied. It was shown that the three-dimensional structure of the PBL is significantly different in the 1 km simulation from that in the 2.2 km run, and the former shows great sensitivity towards the horizontal diffusion. The standard isotropic three-dimensional turbulence scheme was compared to the fourth-order numerical diffusion and to the newly implemented first-order Smagorinsky closure. It can be concluded that without horizontal diffusion the 1 km simulation exhibits unrealistically strong waves in the PBL. Based on these findings, it is recommended to use the three-dimensional turbulent diffusion scheme with horizontal mesh sizes on the order of 1 km, because it is more physically based than the fourth-order numerical filter. For flat convective conditions with very low horizontal wind field deformation the Smagorinsky closure in its classical formulation generates too low mixing, however, the extension of the scheme to include the horizontal shear of vertical wind might be beneficial for these cases.
- 2) The second component of the emergency response system, namely, the meteorological pre-processor has also been validated on selected case studies and continuous periods. The main findings are as follows:
- i) PBL height, which has not been implemented in the COSMO model so far, is an important parameter for certain turbulence post-diagnosis methods, thus several approaches have been tested for this variable. Results suggest that the bulk Richardson number and the momentum flux profile are the most reliable indicators of the PBL height. As the bulk Richardson number is more robust and easier to implement, this method was included in the official COSMO code.

- ii) Validation results of post-diagnosed turbulence characteristics have shown that during convective situations the similarity approach tends to overestimate the turbulence intensity, while the approaches based on the direct usage of TKE give more accurate results. For stable conditions the different approaches are closer to each other and both give reasonable predictions.
 - iii) Based on the validation results it is rather difficult to decide between the two main coupling methods for operational applications, as different verification exercises gave different results. As the present work is the first validation study for different meteorological pre-processors for the COSMO model, in the author's opinion, more weight should be given to the selected case studies than the continuous period. For the case studies investigated in this work the prognostic TKE of the COSMO model performs reasonably well. This is in contrast with the findings of Buzzi (2008), however, in that study an idealized stable boundary layer was studied, while here the focus was on real-world cases. Based on the good validation results, the direct usage of TKE is recommended for operational applications, and it should be investigated whether an anisotropic parameterization for the horizontal direction would improve the results.
- 3) The emergency response system of MeteoSwiss was validated on a real tracer experiment in very complex terrain with a prevailing valley wind system. From this case study the following conclusions can be drawn:
- i) COSMO simulations of the valley wind system have shown great sensitivity towards the initial soil moisture. With correct initialization of the soil parameters a fairly accurate simulation of the valley wind system could be achieved both with 2.2 and 1.1 km horizontal resolution. The criteria for assessing the quality of the simulation were the timing of the onset of the valley wind and the timing of the concentration peak in the dispersion simulation. With original soil moisture, which is assumed to be too high, the valley wind was late in the simulation by 2-3 hours, while a soil moisture reduction of 50% resulted in timing errors less than 1 hour.
 - ii) A new turbulence coupling approach which links the new findings of Weigel et al. (2007) with classical similarity approaches has been implemented and tested for convective conditions. It has been found that the classical flat-terrain coupling methods tend to overestimate the measured tracer concentrations.

The new coupling approach predicts stronger turbulence and thus lower and more accurate concentrations for the selected case.

Generally, it can be concluded that the COSMO numerical weather prediction model at 2–7 km horizontal resolution is capable of providing forecasts of both the mean (e.g. wind and temperature profiles) and subgrid scale variables (e.g. TKE) with acceptable accuracy for the application in Lagrangian Particle Dispersion Models. This allows the integration of the modelling system, which means that as far as possible all the necessary input variables for the dispersion model are taken directly from the NWP model. A further step in this process might be the full online coupling of NWP and dispersion models as it is done in the case of certain online coupled Eulerian chemistry transport modelling systems (Baklanov et al., 2007; Korsholm, 2009). In these systems the NWP and air quality models are interacting every time step thus bringing the role of the meteorological pre-processor to a minimum. The results of the present study might give a first positive sign that the online coupling could be a beneficial strategy for emergency response systems as well.

5.2 Outlook

The work presented in this thesis has pointed out some current issues in connection with the off-line coupling of NWP and Lagrangian dispersion models. Solutions for certain problems have been proposed in the framework of this thesis. However, several open questions remain, which have to be subject to further research. In the following these challenges are summarized.

- The modification proposed for the turbulence scheme of COSMO, namely the increase of the turbulent transport term, should be further evaluated. First of all, it has to be clearly understood, why the significant changes of the simulated TKE profile and diffusion coefficients do not lead to a modified temperature and humidity profile in the PBL.
- The presented COSMO simulations at 1 km horizontal resolution indicated that in highly convective conditions the assumptions in the current turbulence scheme might not be valid anymore, as a certain part of the large eddies in the PBL are explicitly resolved by the dynamics of the model. To validate this hypothesis, further evaluation of the COSMO simulations in the PBL is necessary, with special attention to the simulated three-dimensional PBL structures. This can only be achieved with the use

of reliable three-dimensional Large Eddy Simulation data. Consequently, a closer cooperation between the NWP and LES communities is desired.

- The review and evaluation of different turbulence post-diagnosis methods have shown that the PBL height is an important output variable of the COSMO model with respect to dispersion applications. Therefore, an operational verification of the PBL height is recommended at national weather services. As the PBL height diagnosis from radio sounding measurements is not reliable during stable conditions, it is recommended to use remote sensing instruments for this purpose. MeteoSwiss is routinely operating a Lidar in Payerne, Switzerland since 2008, which also measures the aerosol content of the atmosphere. These measurements could be used to implement automated algorithms for PBL height diagnosis, which could be compared to predictions of the COSMO model.
- The verification exercise of turbulence characteristics indicated that it is rather difficult to obtain the Lagrangian integral timescales from Eulerian turbulence measurements. Current state-of-the-art dispersion models apply a different form of the Langevin equation, which uses the dissipation rate instead of the Lagrangian timescale (e.g., van Dop et al., 1985; Thomson, 1987). As the dissipation rate can be obtained from measured turbulence spectra and thus is easier to use for validation, it might be beneficial to use such kind of a dispersion model in the emergency response system of MeteoSwiss.
- The new turbulence coupling approach suited for steep and narrow Alpine valleys should be evaluated for valleys with other location and orientation, before considering an operational application of this approach.
- Recently, the urban effect parameterization of Martilli et al. (2002) has been implemented in the COSMO model, and is planned to be applied operationally in future. Therefore, it would be necessary to evaluate the impact of this urban parameterization on the dispersion process in an operational setting.

Bibliography

- Albertson JD, Parlange MB (1999) Surface length-scales and shear stress: Implications for land-atmosphere interaction over complex terrain. *Water Resour Res* 35:2121–2132
- Ament F (2006) Energy and moisture exchange processes over heterogeneous land-surfaces in a weather prediction model. PhD thesis. University of Bonn.
- Ament F, Simmer C (2006) Improved representation of land-surface heterogeneity in a non-hydrostatic numerical weather prediction model. *Bound Layer Meteorol* 121:153-174
- Ambrosetti P, Anfossi D, Cieslik S, Graziani G, Lamprecht R, Marzorati A, Nodop K, Sandroni S, Stinglele A, Zimmermann H (1998) Mesoscale transport of atmospheric trace constituents across the central Alps: TRANSALP tracer experiments. *Atmos Environ* 32:1257-1272
- Anfossi D, Desiato F, Tinarelli G, Brusasca G, Ferrero E, Sacchetti D (1998) TRANSALP 1989 experimental campaign - II. Simulation of a tracer experiment with Lagrangian particle models. *Atmos Environ* 32:1157-1166
- Arakawa A, Lamb VR (1977) Computational design of the basic dynamical processes of the UCLA general circulation model. *Methods in computational physics*, vol. 17, Academic Press, pp. 173–265.
- Arpagaus M (2005) Verification of vertical profiles: Operational verification at MeteoSwiss. *COSMO Newsl* 5:102-105 (available from <http://www.cosmo-model.org>).
- Astrup P, Mikkelsen T, Deme S (2001) METRODOS: Meteorological preprocessor chain. *Phys Chem Earth B* 26:105-110
- Avissar, R. and R. A. Pielke, A (1989) Parameterization of Heterogeneous Land Surfaces for Atmospheric Models and Its Impact on Regional Meteorology. *Mon Wea Rev* 117:2113–2134

- Baklanov A, Sørensen JH, Hoe S, Amstrup B (2006) Urban Meteorological Modelling for Nuclear Emergency Preparedness. *J. Environ Radioactivity*, 85:154-170
- Baklanov A, Fay B, Kaminski J, Sokhi R, (2007) Overview of existing integrated (off-line and on-line) meso-scale systems in Europe, Joint Report of COST728 and GURME, WMO-COST publication, GAW Report No. 177, available at: <http://www.cost728.org>.
- Baldauf M (2006) Implementation of the 3D-turbulence metric terms in LMK. *COSMO Newsl* 6:44-51
- Bange J, Spiess T, Herold M, Beyrich F, Hennemuth B (2006) Turbulent fluxes from Helipod flights above quasi-homogeneous pathes within the LITFASS area. *Boundary-Layer Meteorol* 121:127-151
- Basu S, Bosveld FC, Holtslag AAM (2010) Stable boundary layers with low-level jets: what did we learn from the LES intercomparison within GABLS? In: *Proceeding of the 5th International Symposium on Computational Wind Engineering*.
- Batchelor GK (1949) Diffusion in a field of homogeneous turbulence. I. Eulerian analysis. *Aust J Sci Res* 2:437-450
- Batchvarova E, Gryning SE (1991) Applied model for the growth of the daytime mixed layer. *Boundary-Layer Meteorol* 56:261-274
- Belusic D, Güttler I (2010) Can mesoscale models reproduce meandering motions? *Quart J Roy Meteorol Soc* 136:553-565
- Belusic D, Mahrt L (2008) Estimation of length scales from mesoscale networks. *Tellus* 60A:706–715
- Beyrich F, Richter SH, Weisensee U, Kohsiek W, Lohse H, de Bruin HAR, Foken T, Göckede M, Berger F, Vogt R, Batchvarova E (2002) Experimental determination of turbulent fluxes over the heterogeneous LITFASS area: Selected results from the LITFASS-98 experiment. *Theor Appl Climatol* 73:9–34
- Beyrich F, Mengelkamp HT (2006) Evaporation over a Heterogeneous Land Surface: EVA_GRIPS and the LITFASS-2003 Experiment - An Overview. *Bound Layer Meteorol* 121:5-32

- Blackadar AK (1962) The vertical distribution of wind and turbulence exchange in a neutral atmosphere. *J Geophys Res* 67:3095–3102
- Bosveld FC, De Bruijn C, Holtslag AAM (2008) Intercomparison of Single-column Models for GABLS3 preliminary Results. In: Proceedings of the 18th Symposium on Boundary Layers and Turbulence.
- Bou-Zeid E, Meneveau C, Parlange MB (2005) A scale-dependent Lagrangian dynamic model for large eddy simulation of complex turbulent flows. *Phys Fluids* 17(2):025105
- Buzzi M (2008) Challenges in Operational Numerical Weather Prediction at High Resolution in Complex Terrain. Dissertation No. 17714, ETH Zürich, 197 pp.
- Buzzi M, Rotach MW, Raschendorfer M, Holtslag AAM (2010) Evaluation of the COSMO-SC boundary layer scheme for stable conditions. *Meteorol Z*, accepted.
- Caporaso L, Di Giuseppe F, Bonafè G, Deserti M, Stortini M, Petitta M, Castelli M, Gobbi G, Angelini F, Riccio A (2010) The relevance of PBL mixing height prediction for the retrieval and modelling of PM10 concentration. In: Proceedings of the 15th International Symposium of Boundary Layer Remote Sensing.
- Carvalho JC, Anfossi D, Trini Castelli S, and Degrazia GA (2002) Application of a model system for the study of transport and diffusion in complex terrain to the TRACT experiment. *Atmos Environ* 36:1147-1161
- Chow FK, Weigel AP, Street RL, Rotach MW, Xue M (2006) High-resolution large-eddy simulations of flow in a steep Alpine valley. Part I: Methodology, verification, and sensitivity experiments. *J Appl Meteorol* 45:63-86
- Christen A, van Gorsel E, Vogt R, Andretta M, Rotach MW (2001) Ultrasonic Anemometer Instrumentation at Steep Slopes: Wind Tunnel Study - Field Intercomparison - Measurements. *MAP NewsI* 15:164-167
- Christen A, Vogt A, Rotach MW (2009) The budget of turbulent kinetic energy in the urban roughness sublayer. *Boundary-Layer Meteorol* 131:193-223

- Culf AD, Foken T, Gash JHC (2004) The energy balance closure problem. In *Vegetation, Water, Humans and the Climate*, edited by Kabat and Claussen, p 159–166, Springer.
- Cuxart J, et al., (2006) Single-column model intercomparison for a stably stratified atmospheric boundary layer. *Boundary-Layer Meteorol* 118:273–303
- Deardorff JW (1966) The counter-gradient heat flux in the lower atmosphere and in the laboratory. *J Atmos Sci* 23:503-506
- Deardorff JW (1972) Numerical investigation of neutral and unstable planetary boundary layers. *J Atmos Sci* 29:91–115
- Desiato F, Finardi S, Brusasca G, and Morselli MG (1998) TRANSALP 1989 experimental campaign - I. Simulation of 3D flow with diagnostic wind field models. *Atmos Environ* 32:1141-1156
- De Wekker SFJ, Steyn DG, Fast JD, Rotach MW, Zhong S (2005) The performance of RAMS in representing the convective boundary layer structure in a very steep valley. *Environ Fluid Mech* 5:35-62
- Doms G, Schaettler U (2002) The nonhydrostatic limited-area model LM - Part I: Dynamics and Numerics. Scientific Documentation, Deutscher Wetterdienst, Offenbach, Germany, 140 pp. (available from <http://www.cosmo-model.org>).
- Enger L, Koracin D (1995) Simulations of dispersion in complex terrain using a higher order closure model. *Atmos Environ* 29:2449-2456
- Enger L, Koracin D, Yang X (1993) A numerical study of boundary-layer dynamics in a mountain valley. Part 1: Model validation and sensitivity experiments. *Boundary-Layer Meteorol* 66:357-394
- Fiedler F (1989) EUREKA Environmental Project - EUROTRAC, Proposal of a Subproject, Transport of Air Pollutants over Complex Terrain (TRACT), Karlsruhe.
- Foken T, Oncley SP (1995) Workshop on instrumental and methodical problems of land-surface flux measurements. *B Am Meteorol Soc* 76:1191–1193

- Folini D, Ubl S, Kaufmann P (2008) Lagrangian particle dispersion modeling for the high Alpine site Jungfraujoch, *J Geophys Res* 113:D18111
- Gal-Ghen T, Sommerville CJ (1975) On the use of a coordinate transformation for the solution of the Navier-Stokes equations. *J Comput Phys* 209-228
- Gantner L, Kalthoff N (2009) Sensitivity of a modelled life cycle of a mesoscale convective system to soil conditions over West Africa. *Quart J Roy Meteorol Soc* 136:471-482
- Glaab H, Fay B, Jacobsen I (1998) Evaluation of the emergency dispersion model at the Deutscher Wetterdienst using ETEX data, *Atmos Environ* 32:4359-4366
- Gryning SE, Holtslag AAM, Irwin JS, Sivertsen B (1987) Applied dispersion modelling based on meteorological scaling parameters. *Atmos Environ* 21:79-89
- Gupta S, McNider RT, Trainer M, Zamora RJ, Knupp K, Singh MP (1997) Nocturnal wind structure and plume growth rates due to inertial oscillations. *J Appl Meteorol* 36:1050–1063
- Hanna SR (1982) Applications in air pollution modeling. In: Nieuwstadt F.T.M. and H. van Dop (ed.): *Atmospheric Turbulence and Air Pollution Modelling*. D. Reidel Publishing Company, Dordrecht, Holland, p. 275-310.
- Hanna SR (1989) Confidence limit for air quality models as estimated by bootstrap and jackknife resampling methods. *Atmos Environ* 23:1385-1395
- Hanna SR (1990) Lateral dispersion in light-wind stable conditions. *Il Nuovo Cimento* 13C:889–894
- Hara T, Trini Castelli S, Ohba R, Tremback CJ (2009) Validation studies of turbulence closure schemes for high resolutions in mesoscale meteorological models – A case of gas dispersion at the local scale. *Atmos Environ* 43:3745-3753
- Heimann D, de Franceschi M, Emeis S, Lercher P, Seibert P (Eds.) (2008): *Air Pollution, Traffic Noise and Related Health Effects in the Alpine Space: A Guide for Authorities and Consultants*, ALPNAP comprehensive report. Università degli Studi di Trento, Dipartimento di Ingegneria Civile e Ambientale, Trento, Italy, 335 pp.

- Herzog HJ, Vogel G, Schubert U (2002) LLM - a nonhydrostatic model applied to high-resolving simulations of turbulent fluxes over heterogeneous terrain. *Theor Appl Climatol* 73:67-86
- Holtslag AAM (2006) Gewex atmospheric-boundary layer study (gabls) on stable boundary layers. *Boundary-Layer Meteorol* 118:243–246
- Joffre SM, Kangas M, Heikinheimo M, Kitaigorodskii SA (2001) Variability of the stable and unstable atmospheric boundary-layer height and its scales over a boreal forest. *Boundary-Layer Meteorol* 99:429-450
- Kaufmann P (2005) Verification of aLMo with SYNOP and GPS data over Europe. *COSMO Newsl* 5:113-117 (available from <http://www.cosmo-model.org>).
- Kolmogorov AN (1941) The local structure of turbulence in incompressible viscous fluid for very large Reynolds numbers. *Doklady ANSSSR*, 30:301-304
- Korsholm U (2009) Integrated modeling of aerosol indirect effects - development and application of a chemical weather model. PhD thesis University of Copenhagen, Niels Bohr Institute and DMI, Research department.
- Kumar V, Kleissl J, Meneveau C, Parlange MB (2006) Large-eddy simulation of a diurnal cycle of the atmospheric boundary layer: Atmospheric stability and scaling issues. *Water Resour Res* 42:W06D09
- Laubach J, Teichmann U (1999) Surface energy budget variability: A case study over grass with special regard to minor inhomogeneities in the source area. *Theor Appl Climatol* 62:9-24
- Lean HW, Clark PA, Dixon M, Roberts NM, Fitch A, Forbes R, Halliwell C (2008) Characteristics of high-resolution versions of the Met Office Unified Model for forecasting convection over the United Kingdom. *Mon Weather Rev* 136:3408-3424
- Legg BJ, Raupach M (1982) Markov-chain simulation of particle dispersion in inhomogeneous flows: the mean drift velocity induced by a gradient in Eulerian velocity variance. *Boundary-Layer Meteorol* 24:3-13

- Leuenberger D, Rossa A (2007) Revisiting the latent heat nudging scheme for the rainfall assimilation of a simulated convective storm. *Meteor Atmos Phys* 98:195–215
- Mahrt L (2007) Weak-wind mesoscale meandering in the nocturnal boundary layer. *Env Fluid Mech* 7:331-347
- Mahrt L, Vickers D (2002) Contrasting vertical structures of nocturnal boundary layers. *Boundary-Layer Meteorol* 105:351-363
- Martilli A, Clappier A, Rotach MW (2002) An urban surface exchange parameterisation for mesoscale models. *Boundary-Layer Meteorol* 104:261–304
- Martilli A, Roulet Y-A, Junier M, Kirchner F, Rotach MW, Clappier A (2003) On the impact of urban surface exchange parameterisations on air quality simulations: the Athens case. *Atmos Environ* 37:4217-4231
- Maryon RH (1998) Determining cross-wind variance for low frequency wind meander. *Atmos Environ* 32:115–121
- Mauder M, Foken T (2004) Documentation and instruction manual of the eddy covariance software package TK2. *Arbeitsergebnisse von Universität Bayreuth, Nr. 26.*
- Mauder M, Liebethal C, Göckede M, Leps J-P, Beyrich F, Foken T (2006) Processing and quality control of flux data during LITFASS-2003, *Boundary-Layer Meteorol* 121:67–88
- Mellor GL, Yamada T (1974) A hierarchy of turbulence closure models for planetary boundary layers. *J Atmos Sci* 31:1791-1806
- Mellor GL, Yamada T (1982) Development of a turbulence closure model for geophysical flow problems. *Rev Geophys Space Phys* 20:851-875
- Michioka T, Chow FK (2008) High-resolution large-eddy simulations of scalar transport in atmospheric boundary layer flow over complex terrain. *J Appl Meteorol* 47:3150-3169
- Mironov DV, Gryanik VM, Moeng C-H, Olbers DJ, Warncke TH (2000) Vertical turbulence structure and second-moment budgets in convection with rotation: A large-eddy simulation study. *Quart J Roy Meteorol Soc* 126:477-515

- Mironov, D., 2008: Turbulence in the lower troposphere: second-order closure and mass-flux modelling frameworks. *Interdisciplinary Aspects of Turbulence*, Springer Lecture Notes in Physics, W. Hillebrandt and F. Kupka, Eds., Springer-Verlag, Berlin.
- Müller MD, Scherrer D (2005) A grid and subgrid scale radiation parameterization of topographic effects for mesoscale weather forecast models. *Mon Weather Rev* 133:1431-1442
- Mölders N, Raabe A (1996) Numerical Investigation on the Influence of Subgrid-Scale Surface Heterogeneity on Evaporation and Cloud Processes. *J Appl Meteorol* 35:782–795
- Porté-Agel F, Meneveau C, Parlange MB (2000) A scale-dependent dynamic model for large-eddy simulation: Application to a neutral atmospheric boundary layer. *J Fluid Mech* 415:261–284
- Raschendorfer M (2001) The new turbulence Parameterization of LM. *COSMO Newsl* 1:89-97
- Raschendorfer M (2007a) A new TKE-based scheme for vertical diffusion and surface-layer transfer, available at Deutscher Wetterdienst (DWD), Offenbach.
- Raschendorfer M (2007b) A single column (SC) framework applied to the COSMO local model (SCLM), available at Deutscher Wetterdienst (DWD), Offenbach.
- Readings CJ, Haugen DA, Kaimal JC (1974) The 1973 Minnesota Atmospheric Boundary Layer Experiment. *Weather* 29:309-312
- Reinhardt, T., and A. Seifert, 2006: A three-category ice scheme for LMK. *COSMO Newsl* 6:115-120 (available from <http://www.cosmo-model.org>).
- Riemer N, Vogel H, Vogel B, Fiedler F (2003) Modelling aerosols on the mesoscale- μ : Treatment of soot aerosol and its radiative effects, *J Geophys Res*, 109:4601
- Ritter B, Geleyn J-F (1992) A comprehensive radiation scheme for numerical weather prediction models with potential applications in climate simulations. *Mon Weather Rev* 120:303–325.
- Rotach MW (1999) On the influence of the urban roughness sublayer on turbulence and dispersion. *Atmos Environ* 33:4001-4008

- Rotach MW (2001) Simulation of urban-scale dispersion using a Lagrangian stochastic dispersion model. *Boundary-Layer Meteorol* 99:379-410
- Rotach MW, Calanca P, Graziani P, Gurtz J, Steyn DG, Vogt R, Andretta M, Christen A, Cieslik S, Connolly R, De Wekker SFJ, Galmarini S, Kadygrov EN, Kadygrov V, Miller E, Neininger B, Rucker M, van Gorsel E, Weber H, Weiss A, Zappa M (2004) Turbulence structure and exchange processes in an Alpine Valley: The Riviera project. *B Am Meteorol Soc* 85:1367-1385
- Rotta JC (1951a) Statistische Theorie nichthomogener Turbulenz. *Z Phys* 129:547-572
- Rotta JC (1951b) Statistische Theorie nichthomogener Turbulenz. *Z Phys* 131:51-77
- Schicker I, Seibert P, (2009) Simulation of the meteorological conditions during a winter smog episode in the Inn Valley. *Meteorol Atmos Phys* 103:211-222
- Schmid HP, Bünzli B (1995) The influence of surface texture on the effective roughness length. *Quart. J. Roy. Meteorol Soc* 121:1-21
- Schrodin R, Heise E (2001) The multi-layer version of the soil model TERRA_LM. Consortium for Small-Scale Modelling (COSMO), Technical Report 2, 17 pp. (available from <http://www.cosmo-model.org>).
- Schumann U (1987) The counter-gradient heat flux in turbulent stratified flows. *Nuclear Engineering and Design* 100:255-262
- Seibert P, Beyrich F, Gryning SE, Joffre S, Rasmussen A, Tercier P (2000) Review and intercomparison of operational methods for the determination of the mixing height. *Atmos Environ* 34:1001-1027
- Seth A, Giorgi F, Dickinson RE (1994) Simulating fluxes from heterogeneous land surface: Explicit subgrid method employing the biosphere-atmosphere transfer scheme (BATS). *J Geophys Res* 99:18651–18667
- Skamarock WC, Klemp JB, Dudhia J, Gill DO, Barker DM, Wang W, Powers JG (2005) A description of the Advanced Research WRF Version 2. NCAR Technical Note.

- Smagorinsky J (1963) General circulation experiments with the primitive equations: I. The basic experiment. *Mon Weather Rev* 91:99-164
- Someria G, Deardoff JW (1976) Subgrid-scale condensation in models of non-precipitating clouds. *J Atmos Sci* 34:344–355
- Sørensen JH, Rasmussen A, Svensmark H (1996) Forecast of atmospheric boundary-layer height utilised for ETEX real-time dispersion modeling. *Phys Chem Earth* 21:435-439
- Stohl A, Forster C, Frank A, Seibert P, Wotawa G (2005) Technical note: The Lagrangian particle dispersion model FLEXPART version 6.2, *Atmos Chem Phys* 5:2461-2474
- Svensson G, Holtslag AAM (2007) The diurnal cycle - GABLS second Intercomparison Project. *GEWEX News*, *GEWEX Newsl* 17:9–10
- Szintai B, Kaufmann P (2008) TKE as a measure of turbulence. *COSMO Newsl* 8:2-10. (available from <http://www.cosmo-model.org>).
- Szintai B, Kaufmann P, Rotach MW (2009) Deriving turbulence characteristics from the COSMO numerical weather prediction model for dispersion applications. *Adv Sci Res* 3:79-84
- Thomson DJ (1987) Criteria for the selection of stochastic models of particle trajectories in turbulent flows. *J Fluid Mech* 180:529-556
- Tiedtke M (1989) A Comprehensive Mass Flux Scheme for Cumulus Parameterization in Large-Scale Models. *Mon Weather Rev* 117:1779-1800
- Tomas S, Masson V (2006) A parameterization of third-order moments for the dry convective boundary layer. *Boundary-Layer Meteorol* 120:437-454
- Trini Castelli S, Anfossi D (1997) Intercomparison of 3-D turbulence parameterizations for dispersion models in complex terrain derived from a circulation model. *Il Nuovo Cimento* 20C:287-313
- Trini Castelli S, Hara T, Ohba R, Tremback CJ (2006) Validation studies of turbulence closure schemes for high resolutions in mesoscale meteorological models. *Atmos Environ* 40:2510-2523

- Trini Castelli S, Belfiore G, Anfossi D, Elampe E, Clemente M (2007) Modelling the meteorology and traffic pollutant dispersion in highly complex terrain: the ALPNAP Alpine Space Project. Proceedings of the 11th International Conference on Harmonisation within Atmospheric Dispersion Modelling for Regulatory Purposes; Cambridge (UK) 2-5 July 2007, 1:225-229
- Uhlenbrock J (2006) Numerische Untersuchung der konvektiven Grenzschicht über realen heterogenen Landoberflächen mit einem Grobstruktursimulationsmodell. PhD thesis University of Hannover.
- Uppala S, Dee D, Kobayashi S, Berrisford P, Simmons A (2008) Towards a climate data assimilation system: Status update of ERA-Interim. ECMWF Newsl 115:12-18
- Van Dop H, Nieuwstadt FTM, Hunt JCR (1985) Random walk models for particle displacements in inhomogeneous unsteady turbulent flows. Phys Fluids 28:1639–1653
- Vickers D, Mahrt L. (2007) Observations of the cross-wind velocity variance in the stable boundary layer. Environ Fluid Mech 7:55–71
- Vickers D, Mahrt L, Belusic D. (2008) Particle simulations of dispersion using observed meandering and turbulence. Acta Geophys 56:234–256
- Vogelzang DHP, Holtslag AAM (1996) Evolution and model impacts of alternative boundary layer formulations. Boundary-Layer Meteorol 81:245-269
- Weigel AP, Chow FK, Rotach MW (2007) On the nature of turbulent kinetic energy in a steep and narrow Alpine valley. Boundary-Layer Meteorol 123:177-199
- Weigel AP, Rotach MW (2004) Flow structure and turbulence characteristics of the daytime atmosphere in a steep and narrow Alpine valley. Quart J Roy Meteorol Soc 130:2605-2627
- Wetzel PJ (1982) Toward parametrization of the stable boundary layer. J Appl Meteorol 21:7-13

Weusthoff T, Ament F, Arpagaus M, Rotach MW (2010) Assessing the benefits of convection permitting models by Neighborhood Verification - examples from MAP D-PHASE. *Mon Wea Rev* early online release, doi: 10.1175/2010MWR3380.1.

Wicker L, Skamarock W (2002) Time-splitting methods for elastic models using forward time schemes. *Mon Weather Rev* 130:1857–1875

Zängl G, Chimani B, Häberli C (2004) Numerical simulations of the foehn in the Rhine Valley on 24 October 1999 (MAP IOP 10). *Mon Weather Rev* 132:368-389

Zilitinkevich S, Esau I, Baklanov A (2007) Further comments on the equilibrium height of neutral and stable planetary boundary layers. *Quart J Roy Meteorol Soc* 133:265-271

List of acronyms and abbreviations

ALADIN	Aire Limitée Adaptation Dynamique Développement International
BOLCHEM	Bologna limited area model for meteorology and chemistry
CALPUFF	Air quality dispersion model
CAMx	Comprehensive Air quality Model with extensions
CBL	Convective Boundary Layer
CHIMERE	Eulerian chemistry transport model
CMAQ	Community Multiscale Air Quality Modeling System
COSMO	COnsortium for Small-scale MOdelling
COSMO-ART	COSMO model with aerosols and reactive trace gases
COSMO-SC	COSMO Single Column Model
DWD	Deutscher Wetterdienst
ECMWF	European Centre for Medium-Range Weather Forecasts
EFLUM	Laboratory of Environmental Fluid Mechanics and Hydrology
ENVIRO-HIRLAM	Online integrated NWP—chemistry transport system
EPFL	Swiss Federal Institute of Technology Lausanne
EVA_GRIPS	Evaporation at Grid / Pixel Scale Project
FAC2	Factor of two score
FB	Fractional bias
FLEXPART	Community particle dispersion model
GABLS	GEWEX Atmospheric Boundary layer Study
GEWEX	Global Energy and Water Cycle Experiment
HIRLAM	High resolution limited area model
LES	Large Eddy Simulation
LIDAR	Light Detection And Ranging
LITFASS	Lindenberg Inhomogeneous Terrain - Fluxes between Atmosphere and Surface: a Long-term Study
LLJ	Low-level jet
LPDM	Lagrangian particle dispersion model
NWP	Numerical weather prediction
MC2	Mesoscale Compressible Community Model
MM5	Fifth generation mesoscale model from PSU/NCAR
NMSE	Normalized mean square error

PBL	Planetary Boundary Layer
RAMS	Regional Atmospheric Modelling System
RMSE	Root mean square error
SBL	Stable Boundary Layer
SODAR	SOnic Detection And Ranging
STDEV	Standard deviation of errors
TKE	Turbulent Kinetic Energy
TRANSALP	Mesoscale transport of atmospheric pollutants across the Alps
WRF	Weather Research and Forecasting Model
WRF-Chem	Online integrated NWP—chemistry transport system

List of symbols

A_{Θ_t}	coefficient of liquid water potential temperature
A_{Q_w}	coefficient of total water content
c_p	specific heat of air
$\overline{C_o}$	mean of the observed concentrations
$\overline{C_p}$	mean of the predicted concentrations
C_s	Smagorinsky coefficient
e	Turbulent Kinetic Energy
f	Coriolis parameter
g	acceleration due to gravity
G_o	ground heat flux
G_M	dimensionless vertical gradient for momentum
G_H	dimensionless vertical gradient for heat
H_o	surface sensible heat flux
h	height of the Planetary Boundary Layer
K_M	vertical turbulent diffusion coefficient for momentum
K_H	vertical turbulent diffusion coefficient for heat
K_{Mh}	horizontal turbulent diffusion coefficient for momentum
K_{Hh}	horizontal turbulent diffusion coefficient for heat
k	von Karman constant
L_{pat}	horizontal length scale of surface inhomogeneities
LW_{up}	longwave upwelling radiation
LW_{down}	longwave downwelling radiation
L	Obukhov length
l	turbulent length scale for horizontal direction
m_i	portion of TKE for the i -th coordinate direction

N	Brunt-Väisälä frequency
P_r	Prandtl number
Q	Net radiation
q	turbulent velocity scale
Q_w	total water content
R	correlation coefficient
R_{Sp}	Spearman correlation coefficient
R_f	flux Richardson number
Ri	gradient Richardson number
Ri_b	bulk Richardson number
S_M	stability function for momentum
S_H	stability function for heat
SW_{up}	shortwave upwelling radiation
SW_{down}	shortwave downwelling radiation
T_L	Lagrangian integral timescale of turbulence
U	mean zonal wind speed
u'_i	velocity fluctuation (i-th component)
$\overline{u'_i u'_j}$	Reynolds stress
$\overline{u'_i \theta'}$	kinematic heat flux
u_*	friction velocity
V	mean meridional wind speed
w_*	convective velocity scale
z	height above surface
z_0	roughness length
α	diffusion coefficient for TKE
β	buoyancy parameter
γ_θ	background stratification above the PBL
λ	master length scale in the one-dimensional turbulence scheme
λE_0	surface latent heat flux
ρ	density of air
σ_i	standard deviation of the i-th component of the wind fluctuation

σ_{θ}	standard deviation of wind direction
Θ	mean potential temperature
Θ_v	mean virtual potential temperature
Θ_l	liquid water potential temperature
θ'	potential temperature fluctuation
$\overline{w'\theta'_{vs}}$	kinematic heat flux at the surface

Acknowledgements

There are numerous people who helped me throughout the three and a half years to complete my thesis, in the following I would like to thank all of you. First of all, I would like to thank Prof. Marc Parlange for kindly accepting me as his PhD student and always taking the time to discuss with me in Lausanne. I would also like to thank my two advisors, Prof. Mathias Rotach and Dr. Pirmin Kaufmann for helping to complete my PhD work. Mathias, with his broad scientific knowledge helped me to look into the depth of the problems, and Pirmin was the one who always assisted me with both scientific and technical challenges.

The help of my direct colleagues at MeteoSwiss, the members of the Numerical Modelling Group, is also highly appreciated. First, I would like to thank Philippe Steiner for giving me the possibility to work at MeteoSwiss, and for always paying attention to my private life as well. Great thanks go to Matteo Buzzi and Oliver Fuhrer my two colleagues who helped me the most, both from scientific and personal side. Also thanks to my other MO-colleagues (Jean-Marie, Guy, Francis, Marco, Christophe, Anne, Marie, Stephanie, Vanessa, Tanja, Felix Fundel, Felix Ament, Silke, Petra, Philipp, Dani, André, Emanuele) for always assisting me with my technical questions in connection with the COSMO model and for providing a good working atmosphere. Special thanks go to Anne and Oli for the French translation of the Abstract, and to Vanessa for printing and binding the thesis. I would also like to thank Andreas Weigel for interesting discussions and his valuable work in connection with turbulence in steep valleys, which represented the basis for my studies related to dispersion modelling in complex terrain.

I would also like to thank Dmitrii Mironov for making it possible to work in the UTCS Project and assisting me throughout my whole work. The help of Matthias Raschendorfer in connection with the scientific and technical aspects of the turbulence scheme of COSMO is also acknowledged. I would also like to thank the many experts (mentioned at the end of each chapter) for helping me to conduct my investigations by providing either measurements or LES data.

Finally, I would like to thank my family for supporting me in these years in Switzerland. I am indebted to my parents, who always helped me throughout my studies and work with love and understanding. And I am mentioning last the one who I should have written first, Ágnes, my wife and the mother of my soon to be born daughter. I am dedicating this work to you for always believing in me and standing by my side.

Curriculum Vitae

Balázs Szintai, Kis Rákos utca 48/D, Budapest, Hungary
born on 28 January 1983 in Budapest, Hungary, Hungarian citizen.

Education

- 09/2007 – 06/2010 **Swiss Federal Institute of Technology, Lausanne (EPFL)**
Environmental Engineering Doctoral School
Laboratory of Environmental Fluid Mechanics and Hydrology
External PhD student in the group of Prof. Marc Parlange
- 09/2001 – 06/2006 **Eötvös Loránd University, Budapest, Hungary**
Faculty of Science, Meteorologist (Master degree)
- 09/2003 – 06/2006 **Eötvös Loránd University, Budapest, Hungary**
Centre for Foreign Languages, English translator

Professional experience

- 07/2010 – today **Hungarian Meteorological Service**
Numerical Modelling Division
- 02/2007 – 06/2010 **Federal Office of Meteorology and Climatology MeteoSwiss**
Numerical Modelling Division
PhD student under the supervision of Prof. M. W. Rotach and
Dr. P. Kaufmann
- 09/2006 – 01/2007 **Hungarian Meteorological Service**
Remote Sensing Division
- 01/2005 – 08/2006 Fellowship at the Hungarian Meteorological Service
Numerical Modelling Division

International conferences

COST-728 Final Conference, Geneva, Switzerland, 2010
EGU General Assembly, Vienna, Austria, 2009
EMS Annual Meeting, Amsterdam, The Netherlands, 2008